Appendix H

List of Tables

Table 1. Cox PH parameter estimates for model 1 (base model) 31
Table 2. Cox PH parameter estimates for model 2 31
Table 3. Cox PH parameter estimates for model 3 32
Table 4. Cox PH parameter estimates for model 4 32
Table 5. Cox PH parameter estimates for model 5 32
Table 6. Cox PH parameter estimates for model 7 32
Table 7. Cox PH parameter estimates for model 8 33
Table 8. AFT model (Weibull distribution) parameter estimates - model 1 (base model) 41
Table 9. AFT model (Weibull distribution) parameter estimates - model 2 41
Table 10. AFT model (Weibull distribution) parameter estimates - model 3 41
Table 11. AFT model (Weibull distribution) parameter estimates - model 4 42
Table 12. AFT model (Weibull distribution) parameter estimates - model 5 42
Table 13. AFT model (Weibull distribution) parameter estimates - model 7 42
Table 14. AFT model (Weibull distribution) parameter estimates - model 8 43

List of Figures

Figure 1. Risk of T1D diagnosis stratified by using only the number of islet AAs present at the first patient record (including zero) 4
Figure 2. Survival plot, number of subjects at risk and distribution of censoring events stratified by GAD65_IAA 5
Figure 3. Survival plot, number of subjects at risk and distribution of censoring events stratified by GAD65_IA-2 6
Figure 4. Survival plot, number of subjects at risk and distribution of censoring events stratified by GAD65_ZnT8 7
Figure 5. Survival plot, number of subjects at risk and distribution of censoring events stratified by IA-2_IAA 8
Figure 6. Survival plot, number of subjects at risk and distribution of censoring events stratified by IA-2_ZnT8 9
Figure 7. Survival plot, number of subjects at risk and distribution of censoring events stratified by IAA_ZnT8 10
Figure 8. Survival plot, number of subjects at risk and distribution of censoring events stratified by GAD65_IAA_ZnT8 11
Figure 9. Survival plot, number of subjects at risk and distribution of censoring events stratified by GAD65_IA-2_IAA 12
Figure 10. Survival plot, number of subjects at risk and distribution of censoring events stratified by GAD65_IA-2_ZnT8 13
Figure 11. Survival plot, number of subjects at risk and distribution of censoring events stratified by IA-2_IAA_ZnT8 14
Figure 12. Survival plot, number of subjects at risk and distribution of censoring events stratified by GAD65_IA-2_IAA_ZnT8 15
Figure 13. Survival plot, number of subjects at risk and distribution of censoring events stratified by TEDDY_Trial 16
Figure 14. Survival plot, number of subjects at risk and distribution of censoring events stratified by High Risk HLA (HRHLA). High risk is defined in Section 4.3.1. 17

Figure 15. Survival plot, number of subjects at risk and distribution of censoring events stratified by FDR with T1D 18
Figure 16. Survival plot, number of subjects at risk and distribution of censoring events stratified by SEX (Male =1 and Female = 0) 19
Figure 17. Survival plot, number of subjects at risk and distribution of censoring events stratified by AGE_binary 20
Figure 18. Survival plot, number of subjects at risk and distribution of censoring events stratified by HbA1c_binary 21
Figure 19. Survival plot, number of subjects at risk and distribution of censoring events stratified by GLU0_binary 22
Figure 20. Survival plot, number of subjects at risk and distribution of censoring events stratified by GLU120_binary 23
Figure 21. Survival plot, number of subjects at risk and distribution of censoring events stratified by BMI_binary 24
Figure 22. Distribution of baseline age by AA combinations 26
Figure 23. Distribution of BMI by AA combinations 27
Figure 24. Distribution of HbA1c % by AA combinations 28
Figure 25. Distribution of 0-minute OGTT by AA combinations 29
Figure 26. Distribution of 120-minute OGTT by AA combinations 30
Figure 27. Graphical diagnostics with Scaled Schoenfeld residuals (Beta(t)) against survival time – final Cox PH model GAD65_IAA 33
Figure 28. Graphical diagnostics with Scaled Schoenfeld residuals (Beta(t)) against survival time – final Cox PH model GAD65_ZnT8 34
Figure 29. Graphical diagnostics with Scaled Schoenfeld residuals (Beta(t)) against survival time – final Cox PH model IA-2_ZnT8 34
Figure 30. Graphical diagnostics with Scaled Schoenfeld residuals (Beta(t)) against survival time – final Cox PH model IA-2_IAA_ZnT8 35
Figure 31. Graphical diagnostics with Scaled Schoenfeld residuals (Beta(t)) against survival time – final Cox PH model GAD65_IA-2_IAA_ZnT8 36
Figure 32. The survival and hazard function plots for exponential distributions 37
Figure 33. The survival and hazard function plots for gamma distributions 37
Figure 34. The survival and hazard function plots for generalized gamma distributions 38
Figure 35. The survival and hazard function plots for generalized F distributions 38
Figure 36. The survival and hazard function plots for log logistic distributions 39
Figure 37. The survival and hazard function plots for gompertz distributions 39
Figure 38. The survival and hazard function plots for log normal distributions 40
Figure 39. k-fold cross validation analysis stratified by HbA1c_binary threshold of 5.25%– Fold 1 42
Figure 40. k-fold cross validation analysis stratified by HbA1c_binary threshold of 5.25% – Fold 2 44
Figure 41. k-fold cross validation analysis stratified by HbA1c_binary threshold of 5.25% – Fold 3 45
Figure 42. k-fold cross validation analysis stratified by HbA1c_binary threshold of 5.25% – Fold 4 45
Figure 43. k-fold cross validation analysis stratified by HbA1c_binary threshold of 5.25%– Fold 5 46
Figure 44. k-fold cross validation analysis stratified by GAD65_IA-2_IAA_ZnT8 – Fold 1 ... 46
Figure 45. k-fold cross validation analysis stratified by GAD65_IA-2_IAA_ZnT8 – Fold 2 ... 47
Figure 46. k-fold cross validation analysis stratified by GAD65_IA-2_IAA_ZnT8 – Fold 3 ... 47

Figure 47. k-fold cross validation analysis stratified by GAD65_IA-2_IAA_ZnT8 – Fold 4 ... 48
Figure 48. k-fold cross validation analysis stratified by GAD65_IA-2_IAA_ZnT8 – Fold 5 ... 48
Figure 49. k-fold cross validation analysis stratified by GAD65_IAA – Fold 1 ... 49
Figure 50. k-fold cross validation analysis stratified by GAD65_IAA – Fold 2 ... 49
Figure 51. k-fold cross validation analysis stratified by GAD65_IAA – Fold 3 ... 50
Figure 52. k-fold cross validation analysis stratified by GAD65_IAA – Fold 4 ... 50
Figure 53. k-fold cross validation analysis stratified by GAD65_IAA – Fold 5 ... 51
Figure 54. k-fold cross validation analysis stratified by GAD65_ZnT8 – Fold 1 ... 51
Figure 55. k-fold cross validation analysis stratified by GAD65_ZnT8 – Fold 2 ... 52
Figure 56. k-fold cross validation analysis stratified by GAD65_ZnT8 – Fold 3 ... 52
Figure 57. k-fold cross validation analysis stratified by GAD65_ZnT8 – Fold 4 ... 53
Figure 58. k-fold cross validation analysis stratified by GAD65_ZnT8 – Fold 5 ... 53
Figure 59. k-fold cross validation analysis stratified by GLU120_binary threshold of 100 mg/dl – Fold 1 ... 54
Figure 60. k-fold cross validation analysis stratified by GLU120_binary threshold of 100 mg/dl – Fold 2 ... 55
Figure 61. k-fold cross validation analysis stratified by GLU120_binary threshold of 100 mg/dl – Fold 3 ... 55
Figure 62. k-fold cross validation analysis stratified by GLU120_binary threshold of 100 mg/dl – Fold 4 ... 56
Figure 63. k-fold cross validation analysis stratified by GLU120_binary threshold of 100 mg/dl – Fold 5 ... 56
Figure 64. k-fold cross validation analysis stratified by IA-2_IAA_ZnT8 – Fold 1 ... 57
Figure 65. k-fold cross validation analysis stratified by IA-2_IAA_ZnT8 – Fold 2 ... 57
Figure 66. k-fold cross validation analysis stratified by IA-2_IAA_ZnT8 – Fold 3 ... 58
Figure 67. k-fold cross validation analysis stratified by IA-2_IAA_ZnT8 – Fold 4 ... 58
Figure 68. k-fold cross validation analysis stratified by IA-2_IAA_ZnT8 – Fold 5 ... 59
Figure 69. k-fold cross validation analysis stratified by IA-2_ZnT8 – Fold 1 ... 59
Figure 70. k-fold cross validation analysis stratified by IA-2_ZnT8 – Fold 2 ... 60
Figure 71. k-fold cross validation analysis stratified by IA-2_ZnT8 – Fold 3 ... 60
Figure 72. k-fold cross validation analysis stratified by IA-2_ZnT8 – Fold 4 ... 61
Figure 73. k-fold cross validation analysis stratified by IA-2_ZnT8 – Fold 5 ... 61

APPENDIX H

As discussed in section 4.3.2.1 the risk of T1D diagnosis is significantly lower for subjects with zero or one AA compared to subjects with multiple AAs at baseline (Figure 1). The incidence of T1D diagnosis for subjects with multiple AA at baseline supports the time frame over which clinical trials of reasonable duration would be conducted.

Figure 1. Risk of T1D diagnosis stratified by using only the number of islet AAs present at the first patient record (including zero)

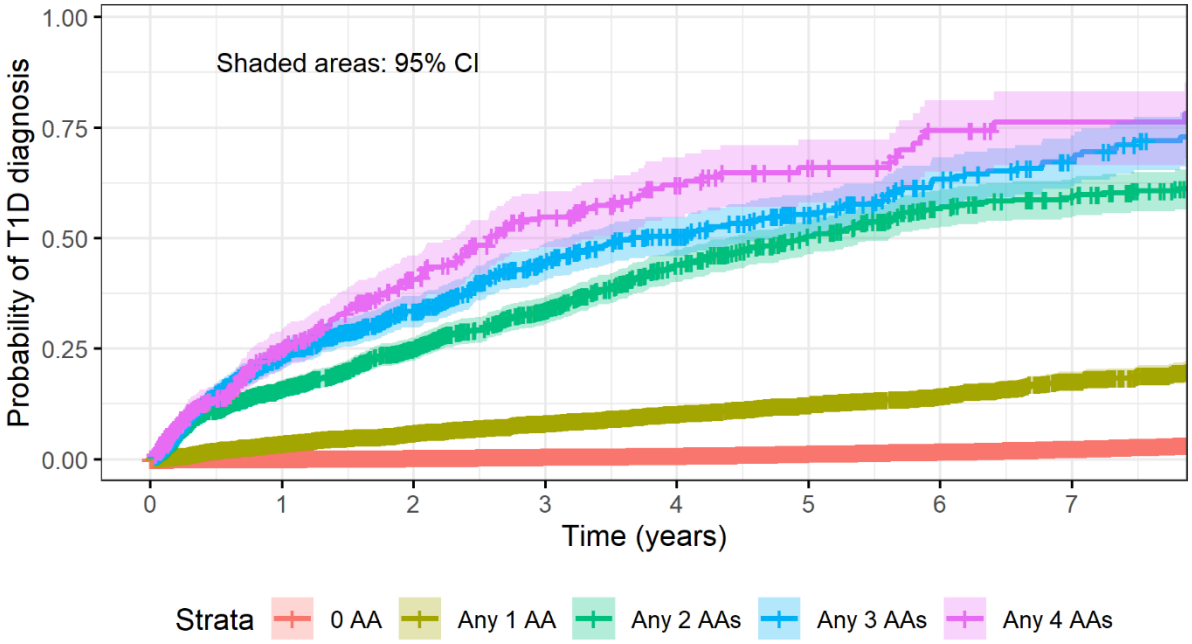

A comprehensive data tabulation and visualization of probability of diagnosis and distribution of censoring event stratified by binary covariates was conducted (Figure 2-21). Specifically the Kaplan-Meier curves, number of subjects at risk and number of subject censored over time were obtain for AA combinations including GAD65_IAA (Figure 2), GAD65_IA-2 (Figure 3), GAD65_ZnT8 (Figure 4), IA-2_IAA (Figure 5), IA-2_ZnT8 (Figure 6), IAA_ZnT8 (Figure 7), GAD65_IAA_ZnT8 (Figure 8), GAD65_IA-2_IAA (Figure 9), GAD65_IA-2_ZnT8 (Figure 10), IA-2_IAA_ZnT8 (Figure 11), GAD65_IA2A_IAA_ZnT8 (Figure 12). A clear stratification can be seen with AA combination GAD65_IAA, GAD65_ZnT8, IA-2_IAA_ZnT8, GAD65_IA2A_IAA_ZnT8 and IA-2_ZnT8. The number of censoring events were evenly distribution for all the AA combination with minor spike in the first two years. Other binary covariates that were analyzed included TEDDY_Trial (Figure 13), HRHLA (Figure 14), FDR (Figure 15), SEX (Figure 16), among which only SEX showed clear separation between male and female Kaplan-Meier curves. The continuous covariates were also analyzed by creating a binary covariate using a threshold value. These include AGE_binary with a threshold of 12 years (Figure 17), HbA1c_binary with a threshold of 5.25% (Figure 18), GLU0_binary with a threshold of 95 mg/dl (Figure 19), GLU120_binary with a threshold of 100 mg/dl (Figure 20), and BMI_binary with a threshold of 19.4 (Figure 21), among which AGE_binary, HbA1c_binary, and GLU120_binary showed clear separation between the two Kaplan-Meier curves.

Figure 2. Survival plot, number of subjects at risk and distribution of censoring events stratified by GAD65_IAA

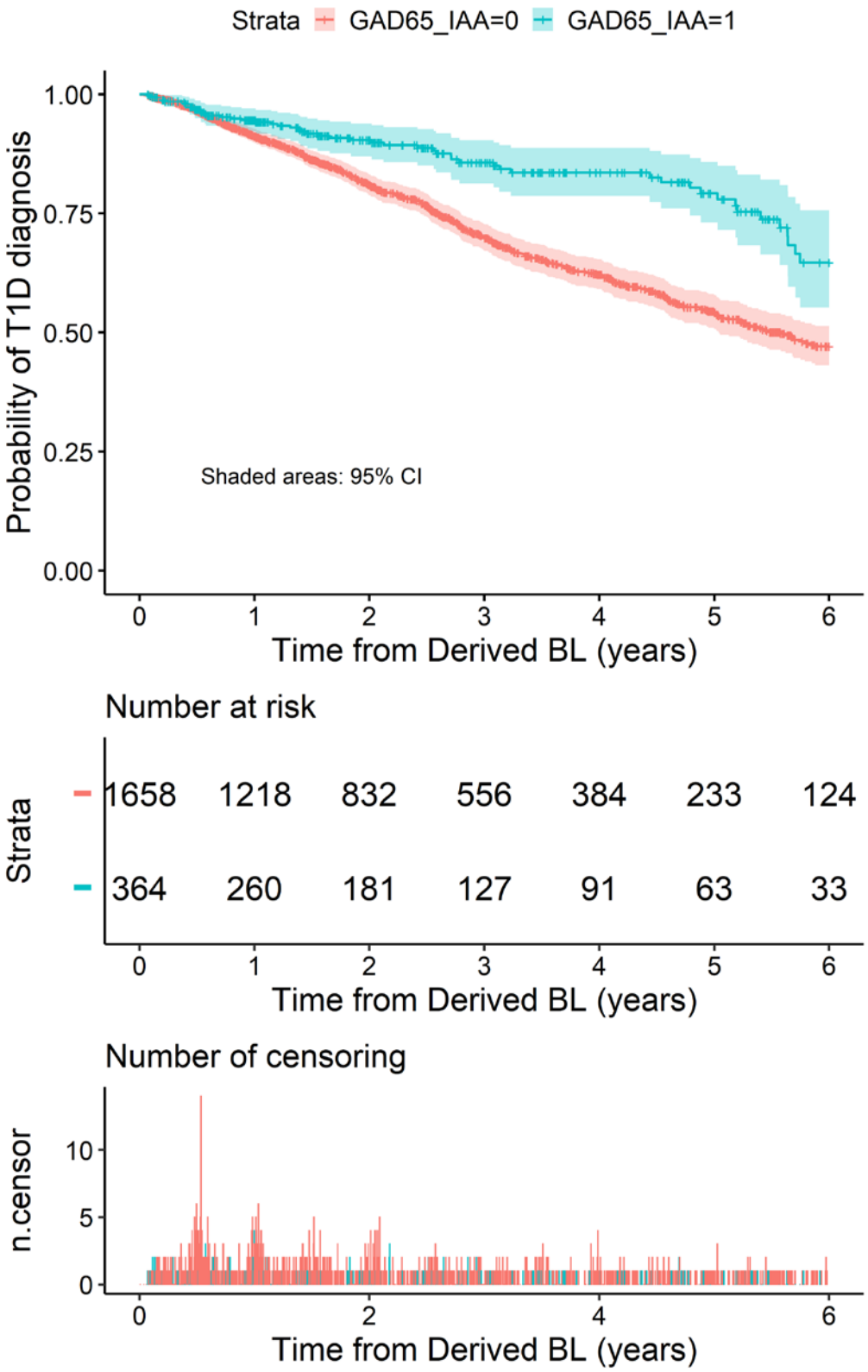

Figure 3. Survival plot, number of subjects at risk and distribution of censoring events stratified by GAD65_IA-2

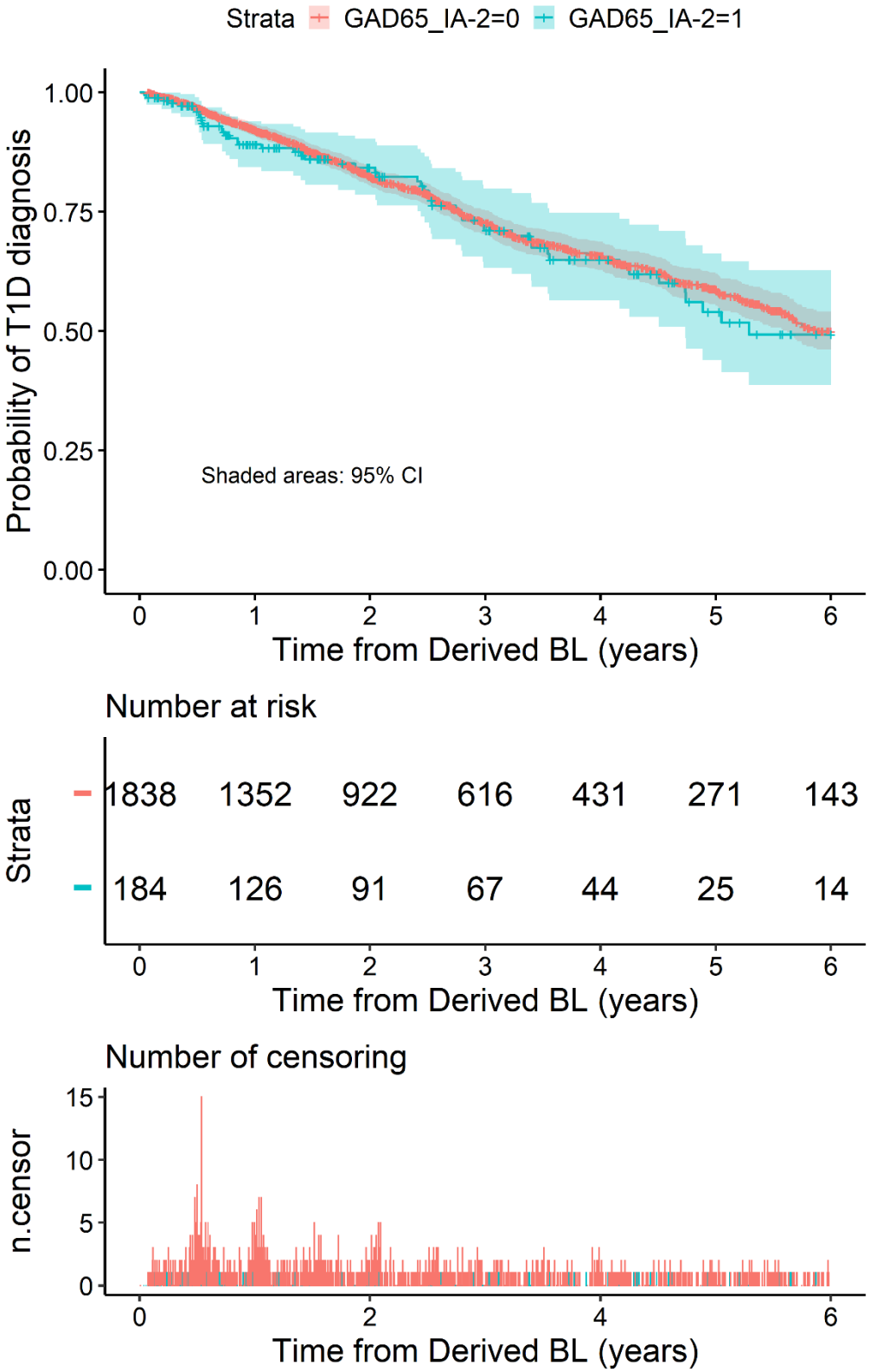

Figure 4. Survival plot, number of subjects at risk and distribution of censoring events stratified by GAD65_ZnT8

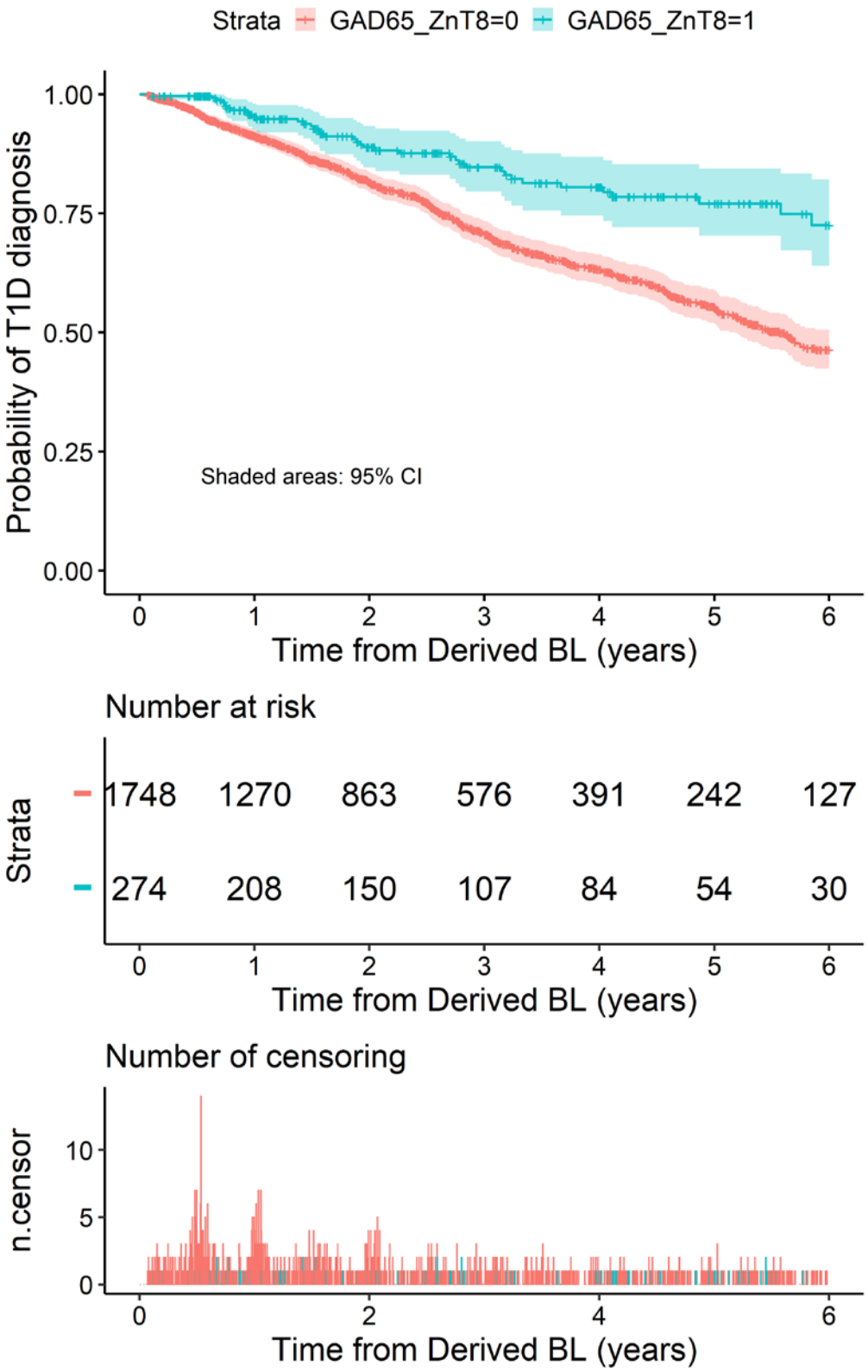

Figure 5. Survival plot, number of subjects at risk and distribution of censoring events stratified by IA-2_IAA

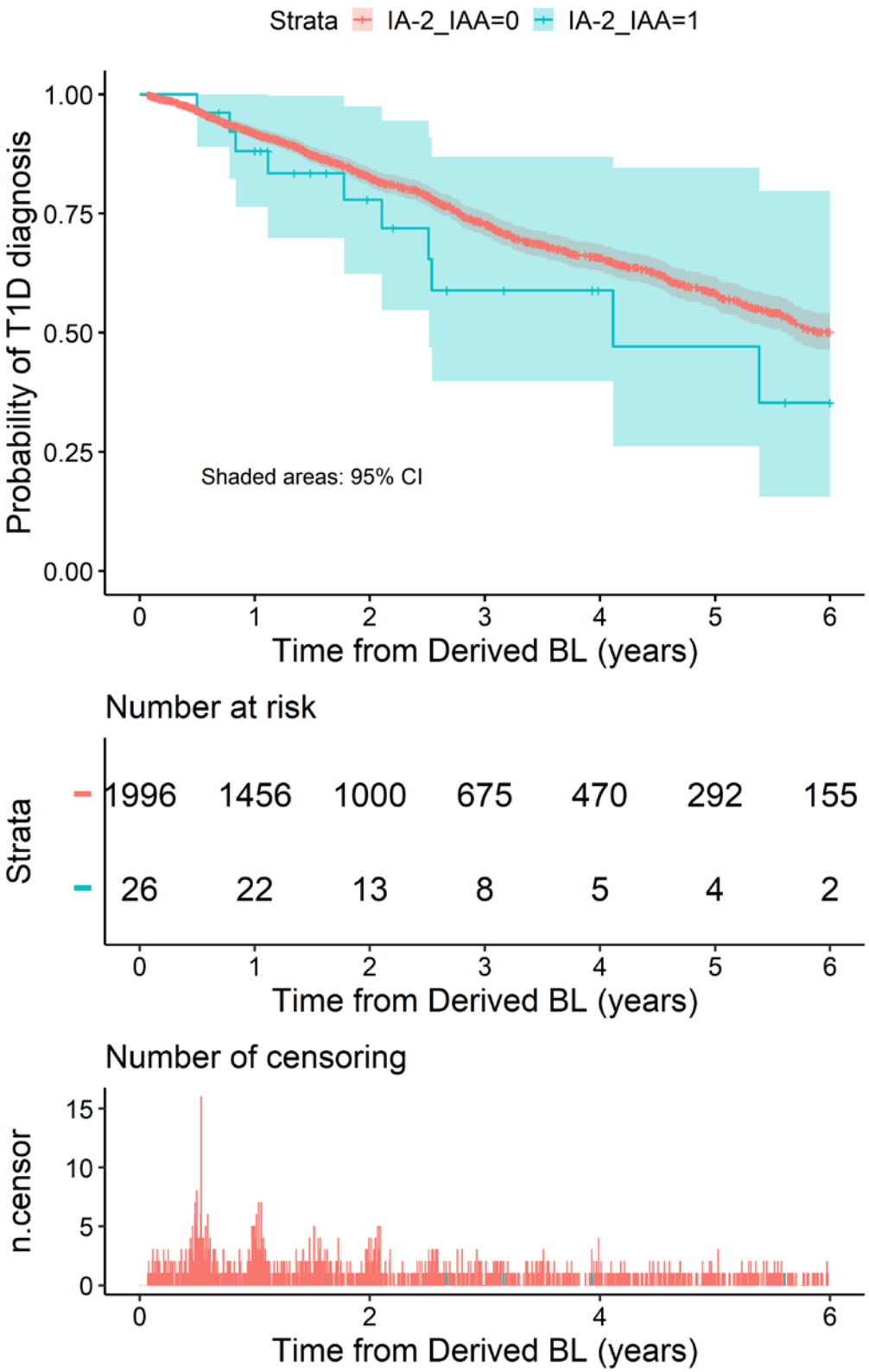

Figure 6. Survival plot, number of subjects at risk and distribution of censoring events stratified by IA-2_ZnT8

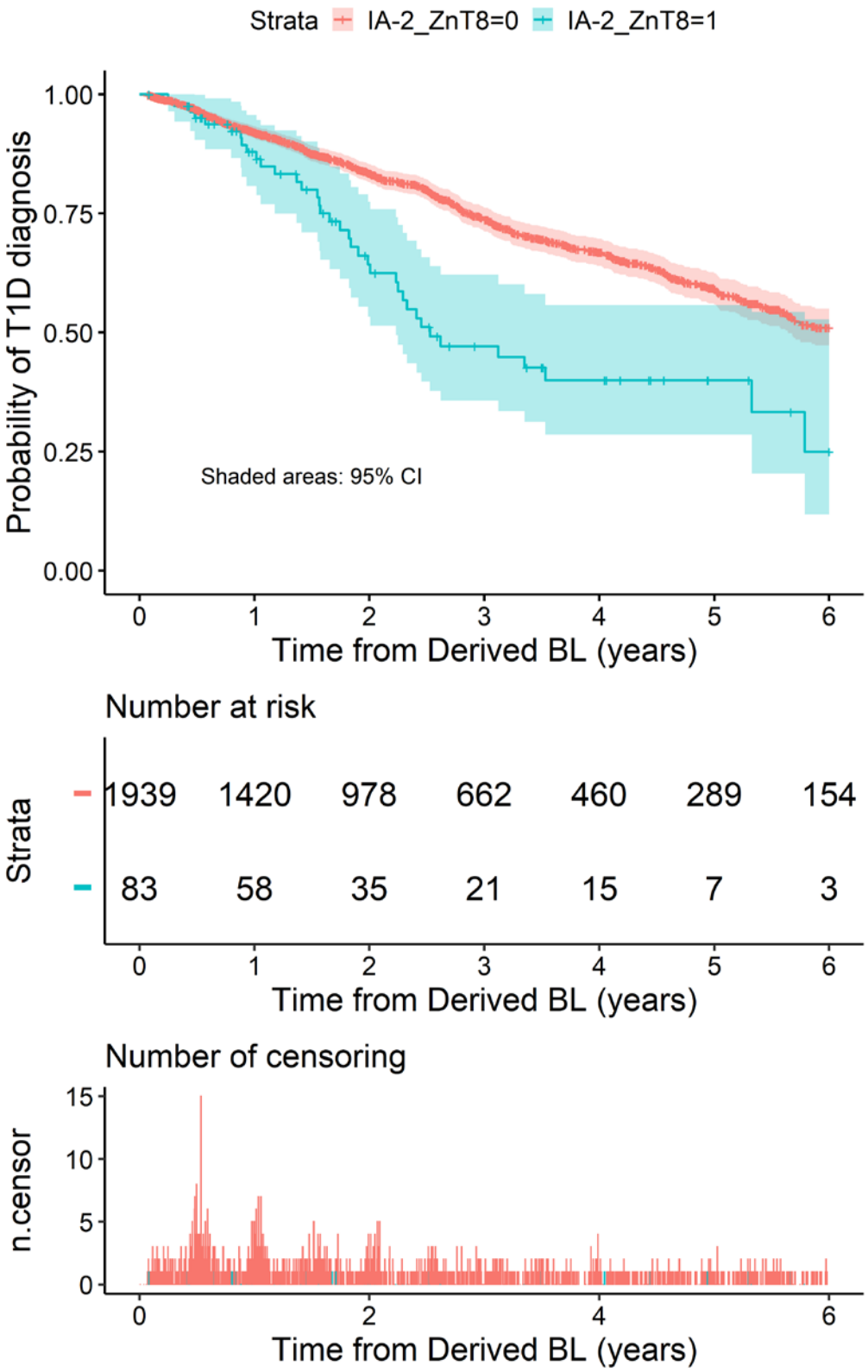

Figure 7. Survival plot, number of subjects at risk and distribution of censoring events stratified by IAA_ZnT8

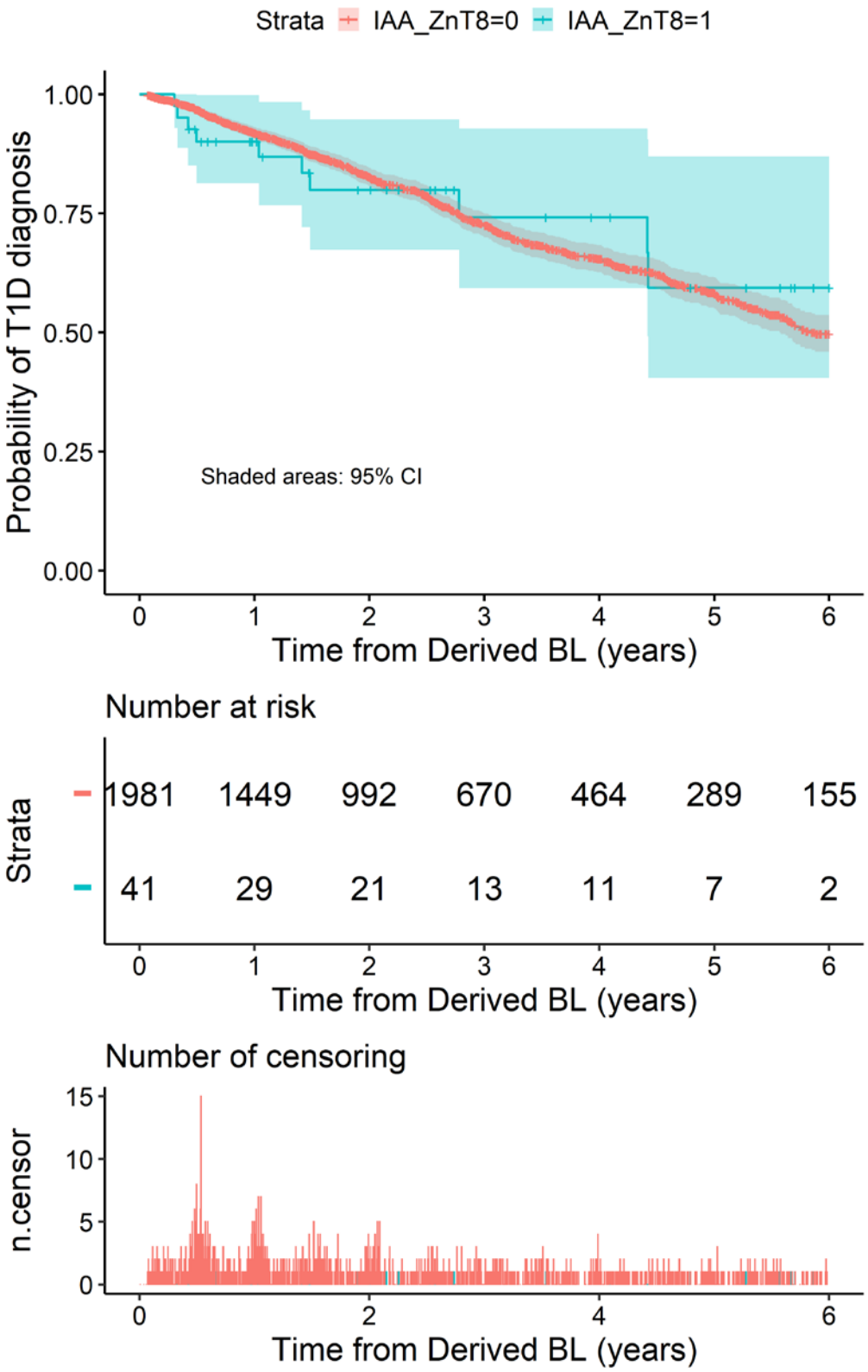

Figure 8. Survival plot, number of subjects at risk and distribution of censoring events stratified by GAD65_IAA_ZnT8

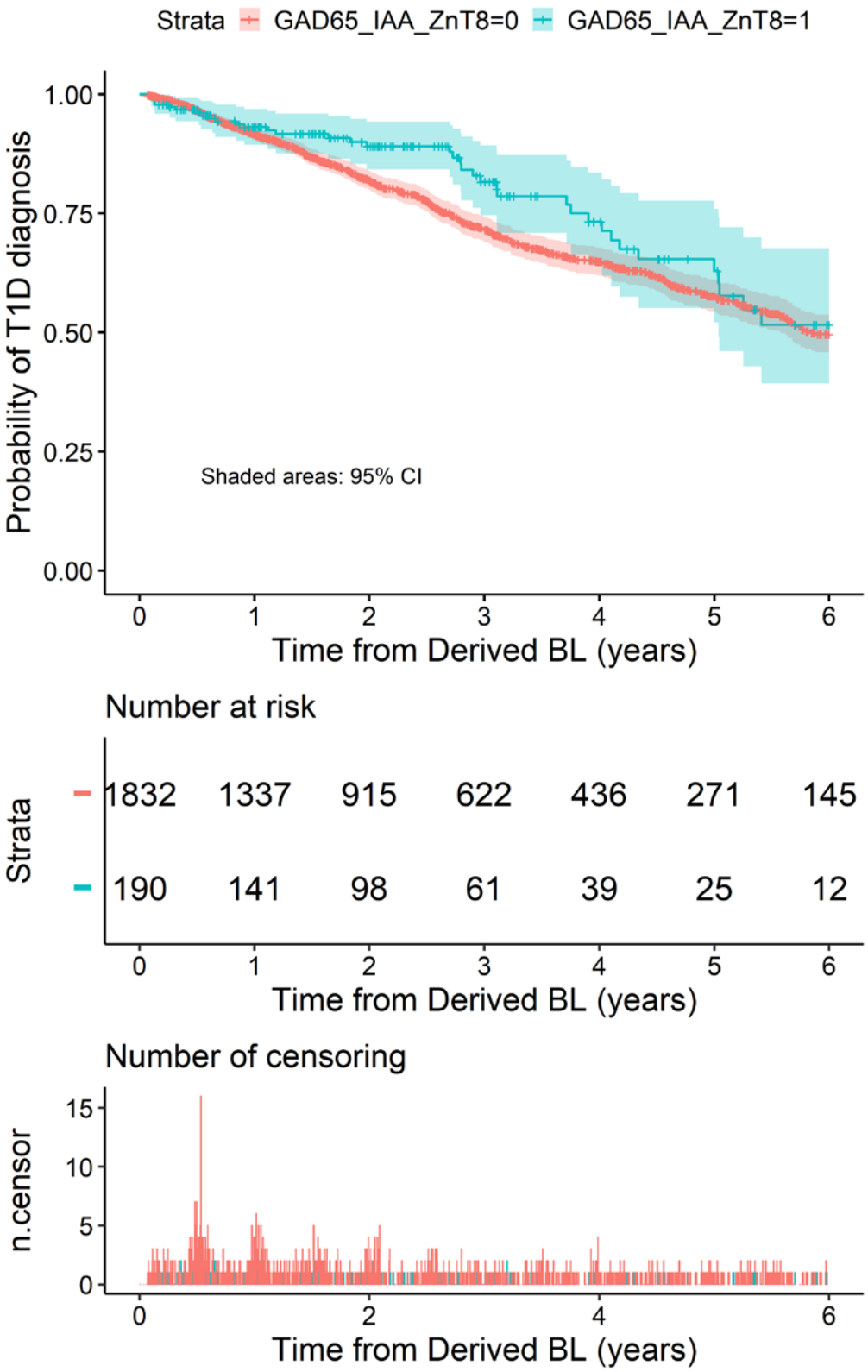

Figure 9. Survival plot, number of subjects at risk and distribution of censoring events stratified by GAD65_IA-2_IAA

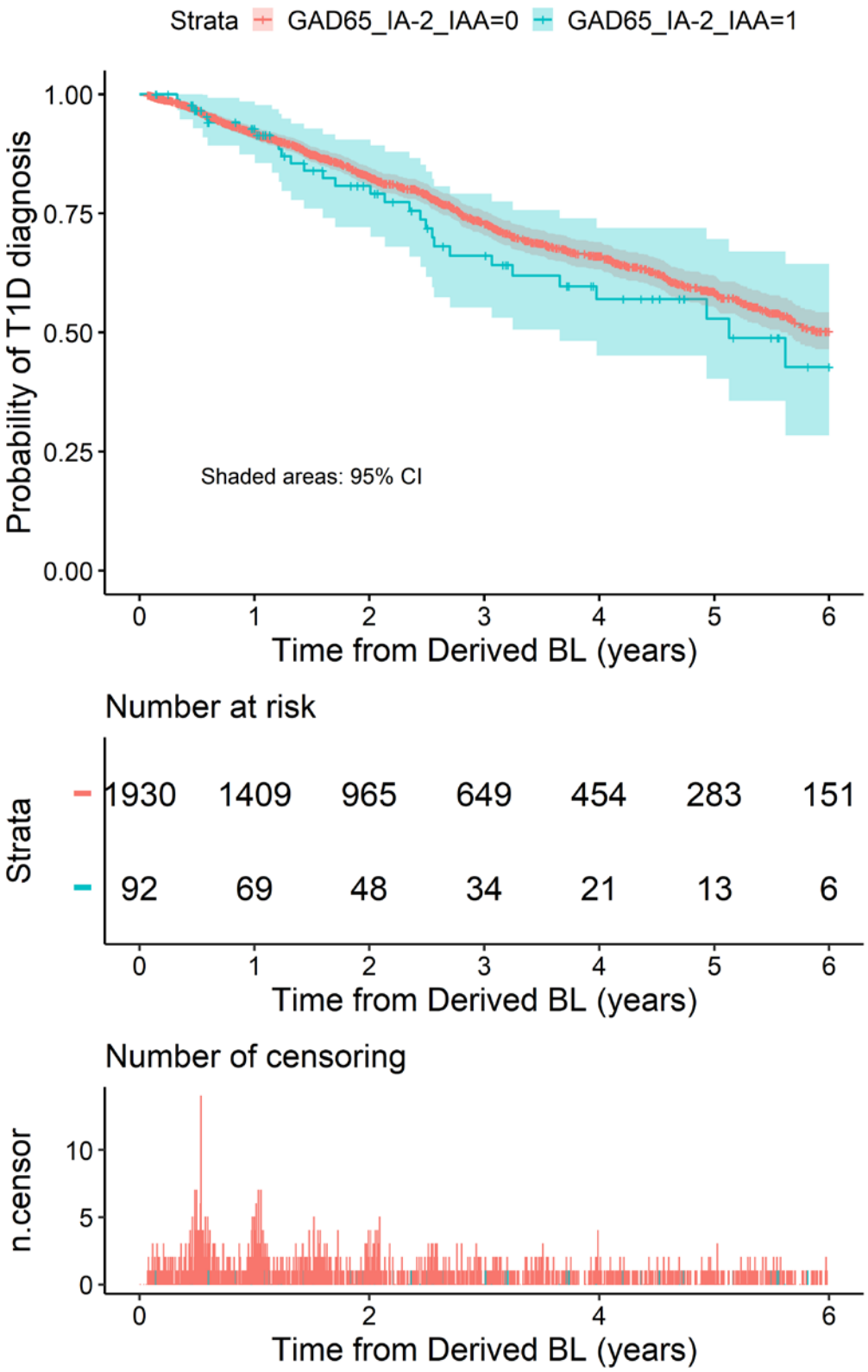

Figure 10. Survival plot, number of subjects at risk and distribution of censoring events stratified by GAD65_IA-2_ZnT8

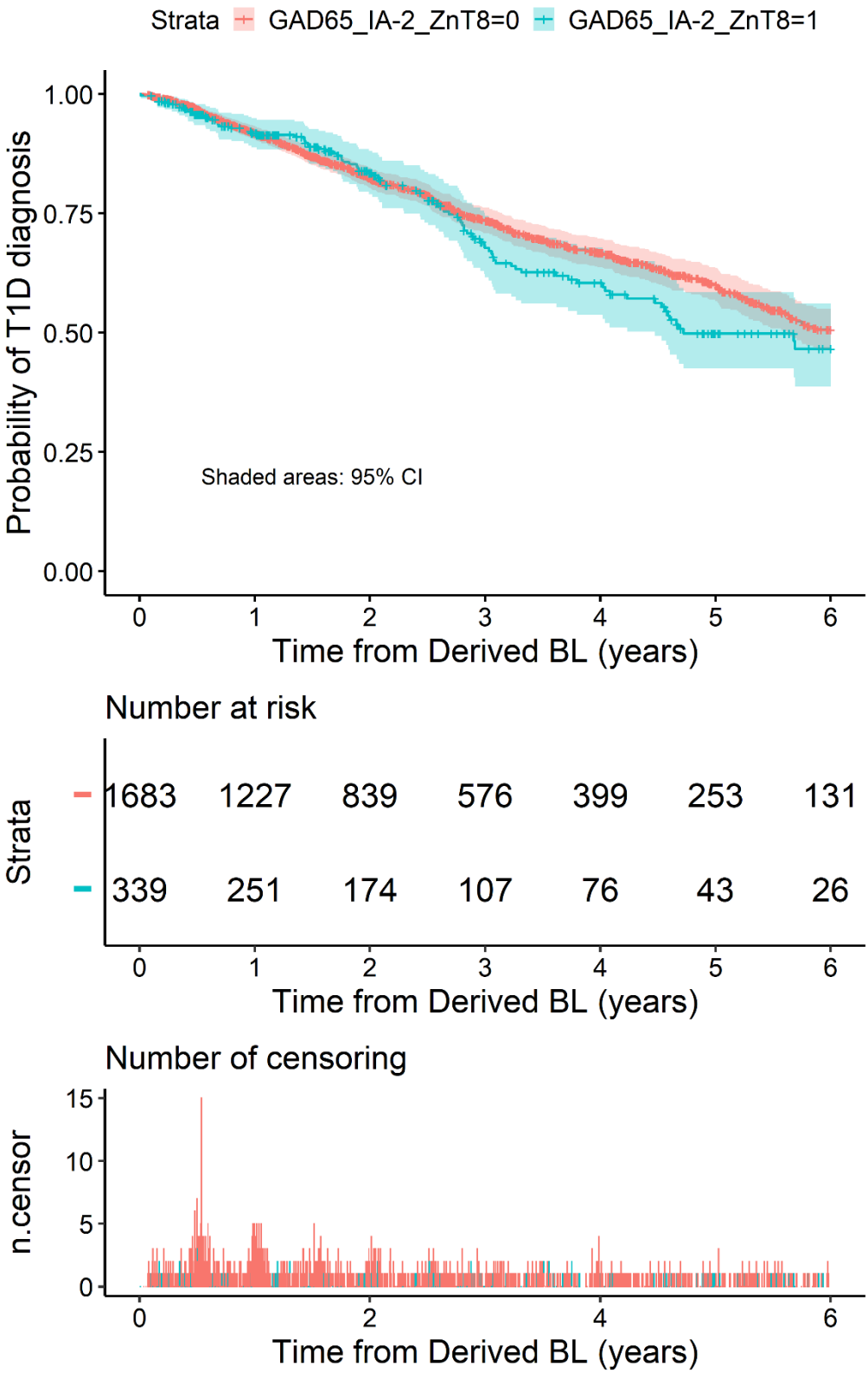

Figure 11. Survival plot, number of subjects at risk and distribution of censoring events stratified by IA-2_IAA_ZnT8

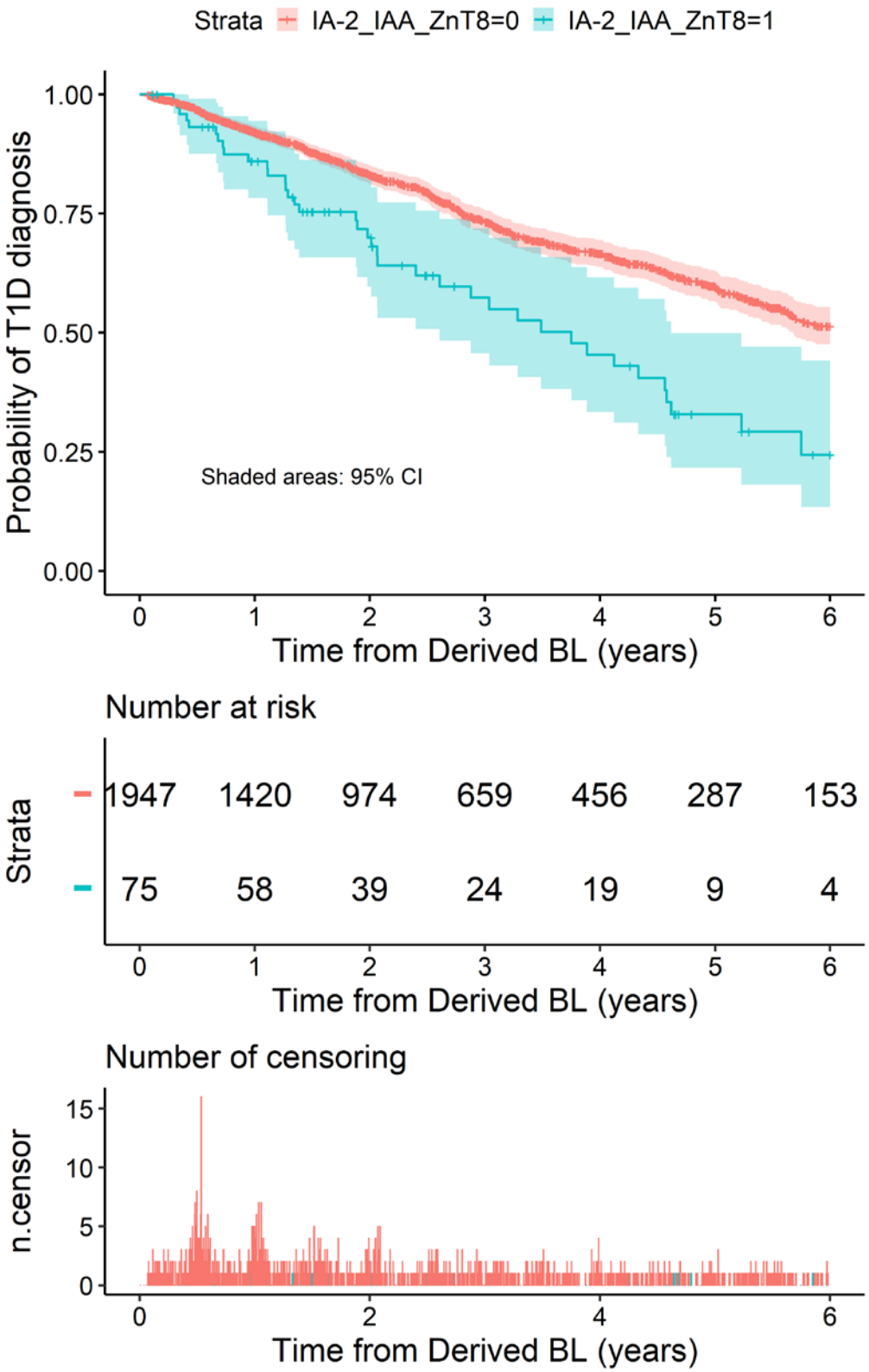

Figure 12. Survival plot, number of subjects at risk and distribution of censoring events stratified by GAD65_IA-2_IAA_ZnT8

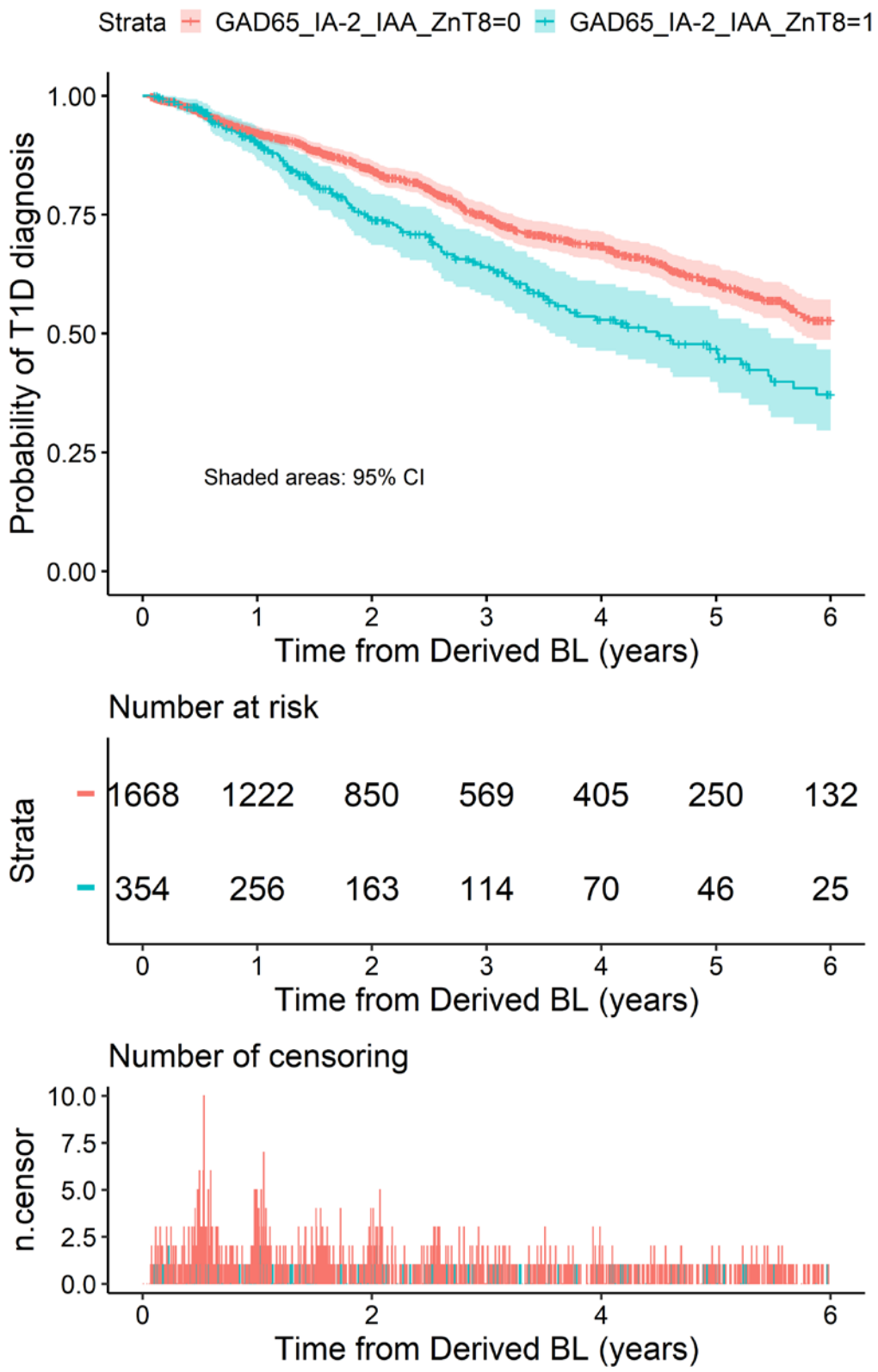

Figure 13. Survival plot, number of subjects at risk and distribution of censoring events stratified by TEDDY_Trial

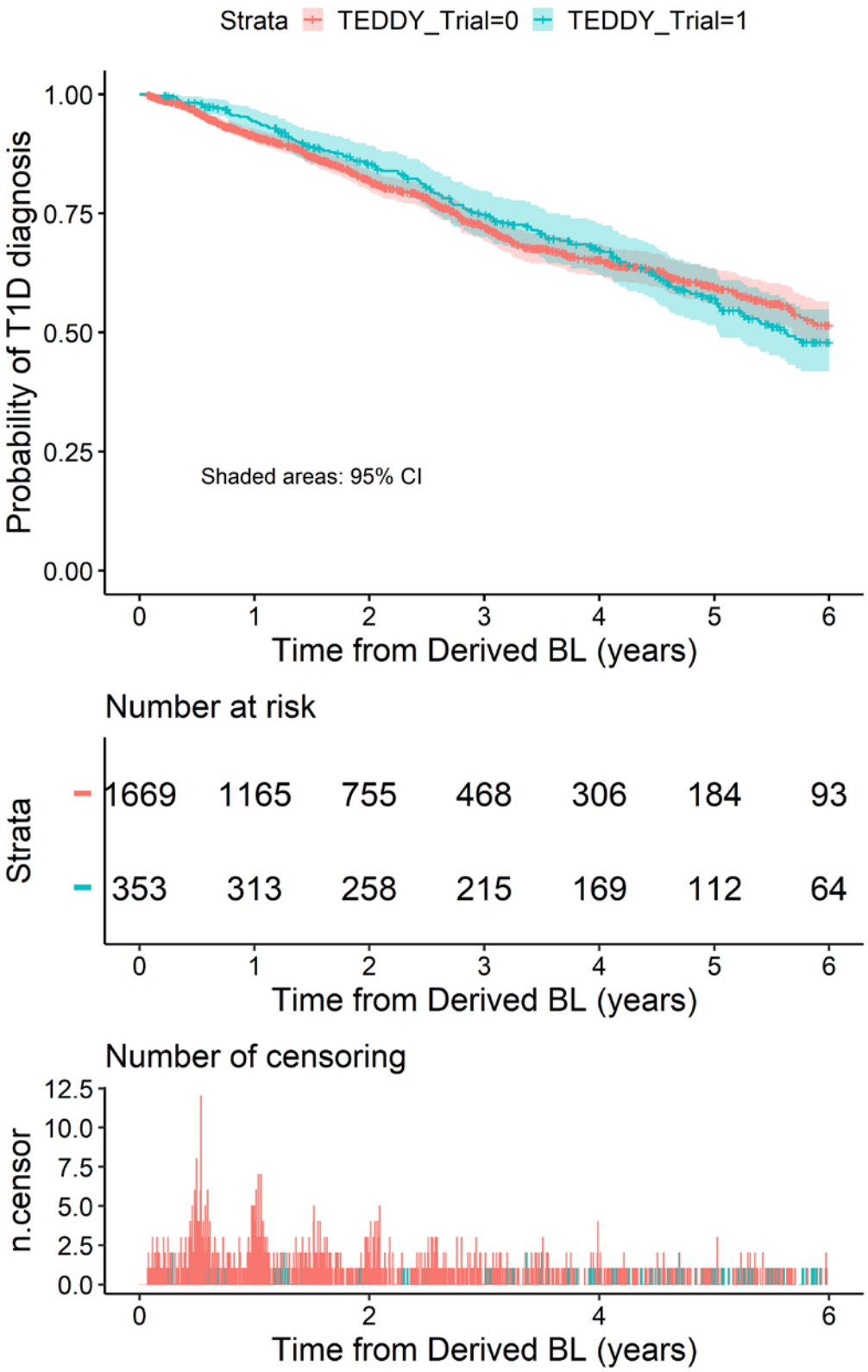

Figure 14. Survival plot, number of subjects at risk and distribution of censoring events stratified by High Risk HLA (HRHLA). High risk is defined in Section 4.3.1.

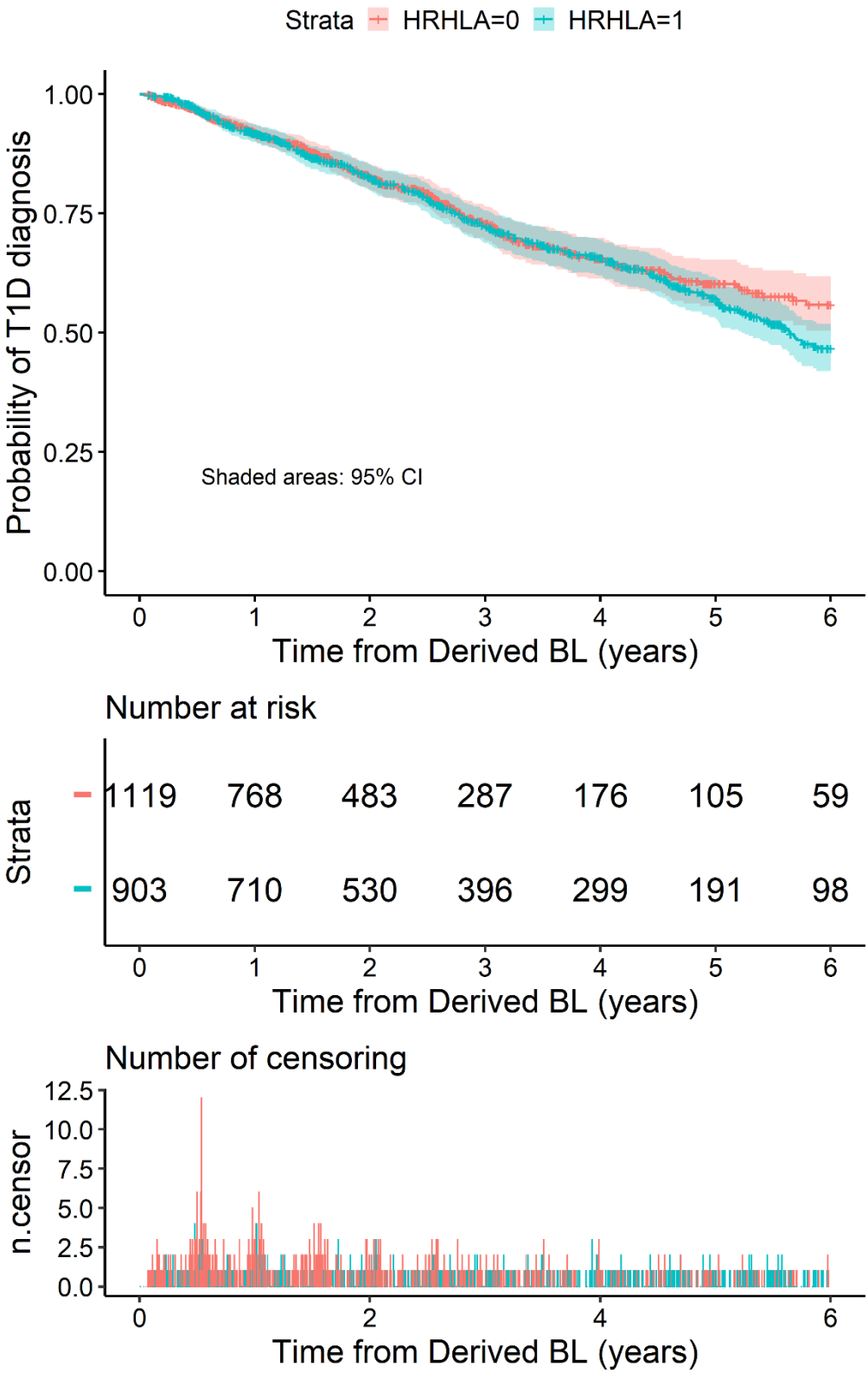

Figure 15. Survival plot, number of subjects at risk and distribution of censoring events stratified by FDR with T1D

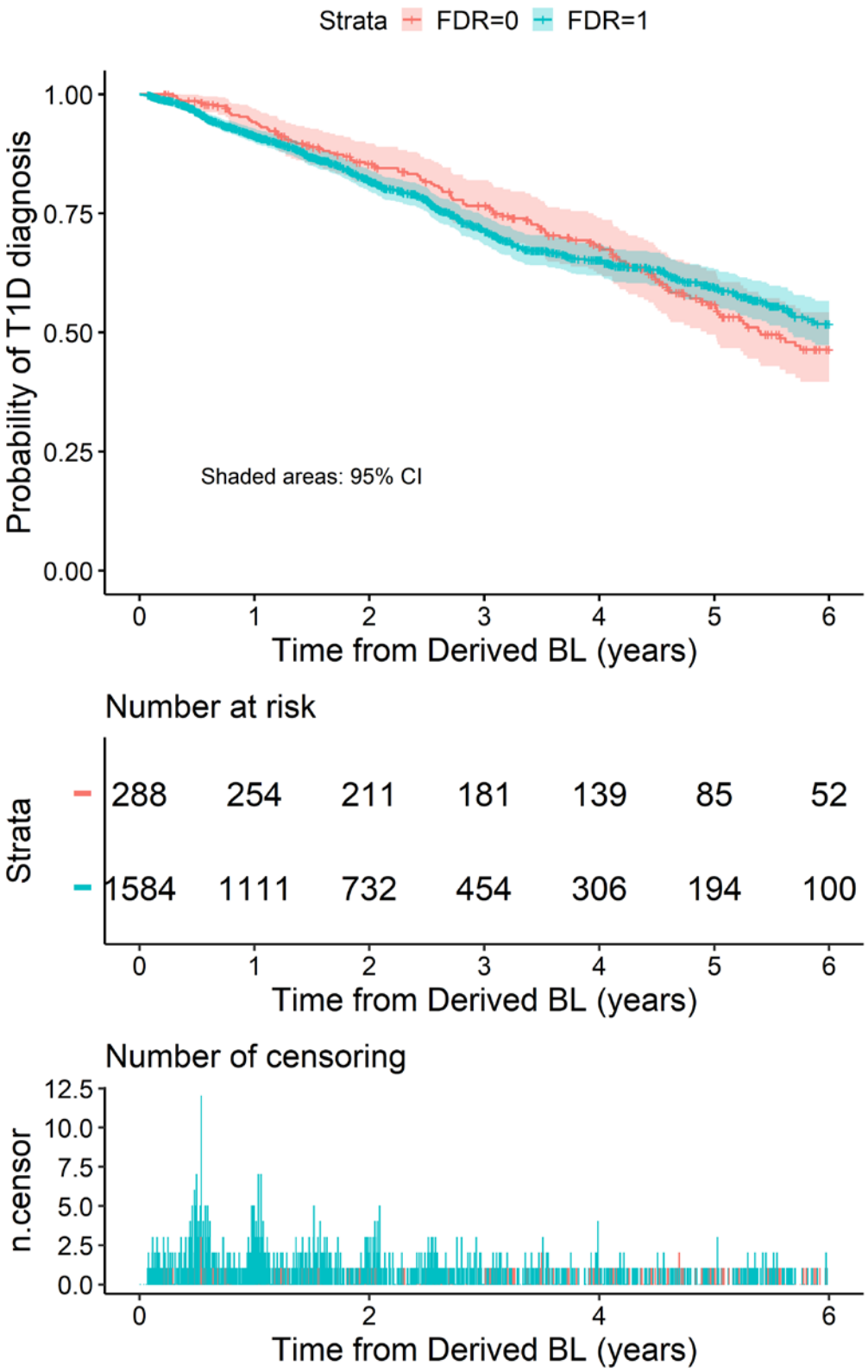

Figure 16. Survival plot, number of subjects at risk and distribution of censoring events stratified by SEX (Male =1 and Female = 0)

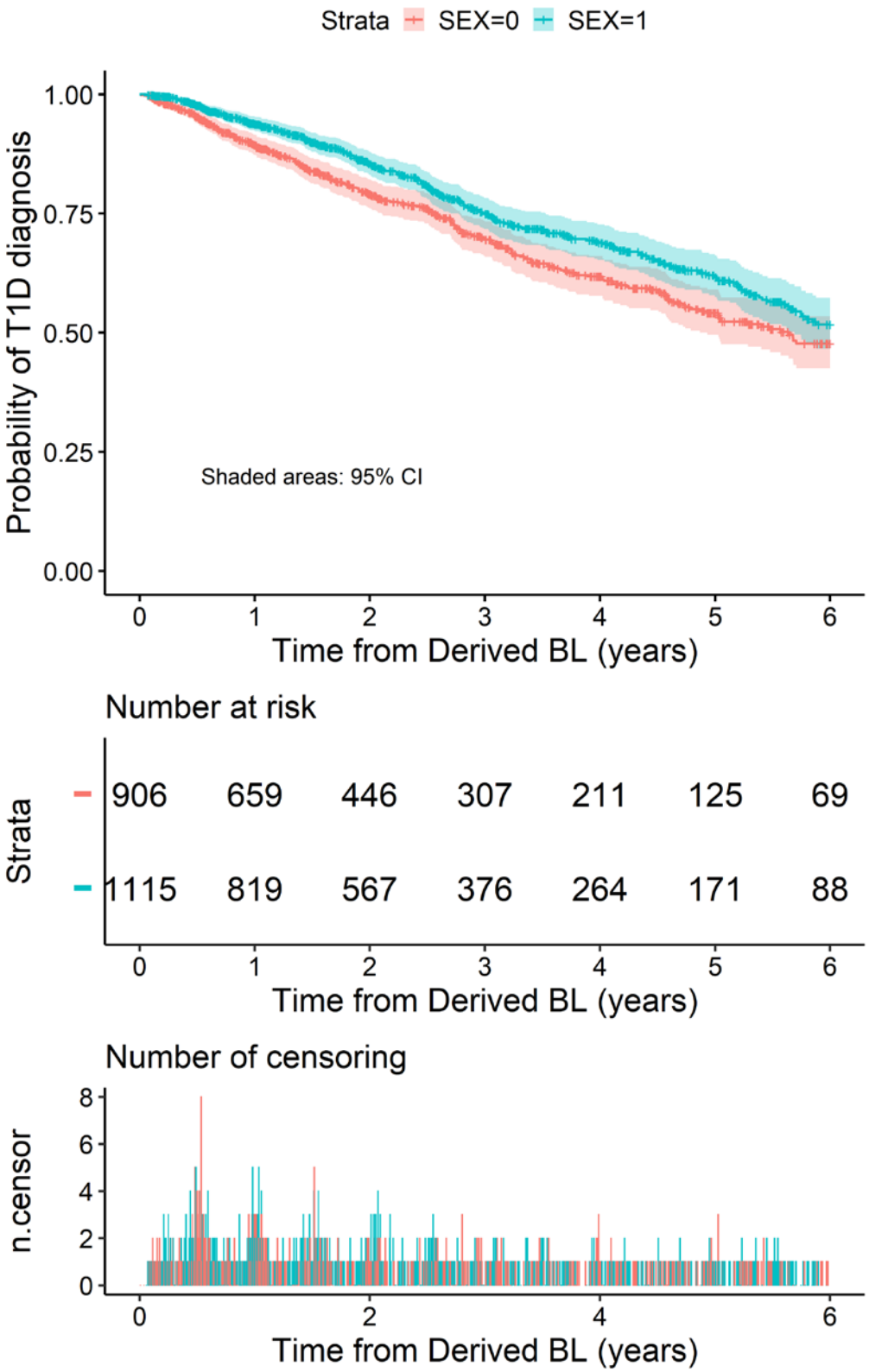

Figure 17. Survival plot, number of subjects at risk and distribution of censoring events stratified by AGE_binary

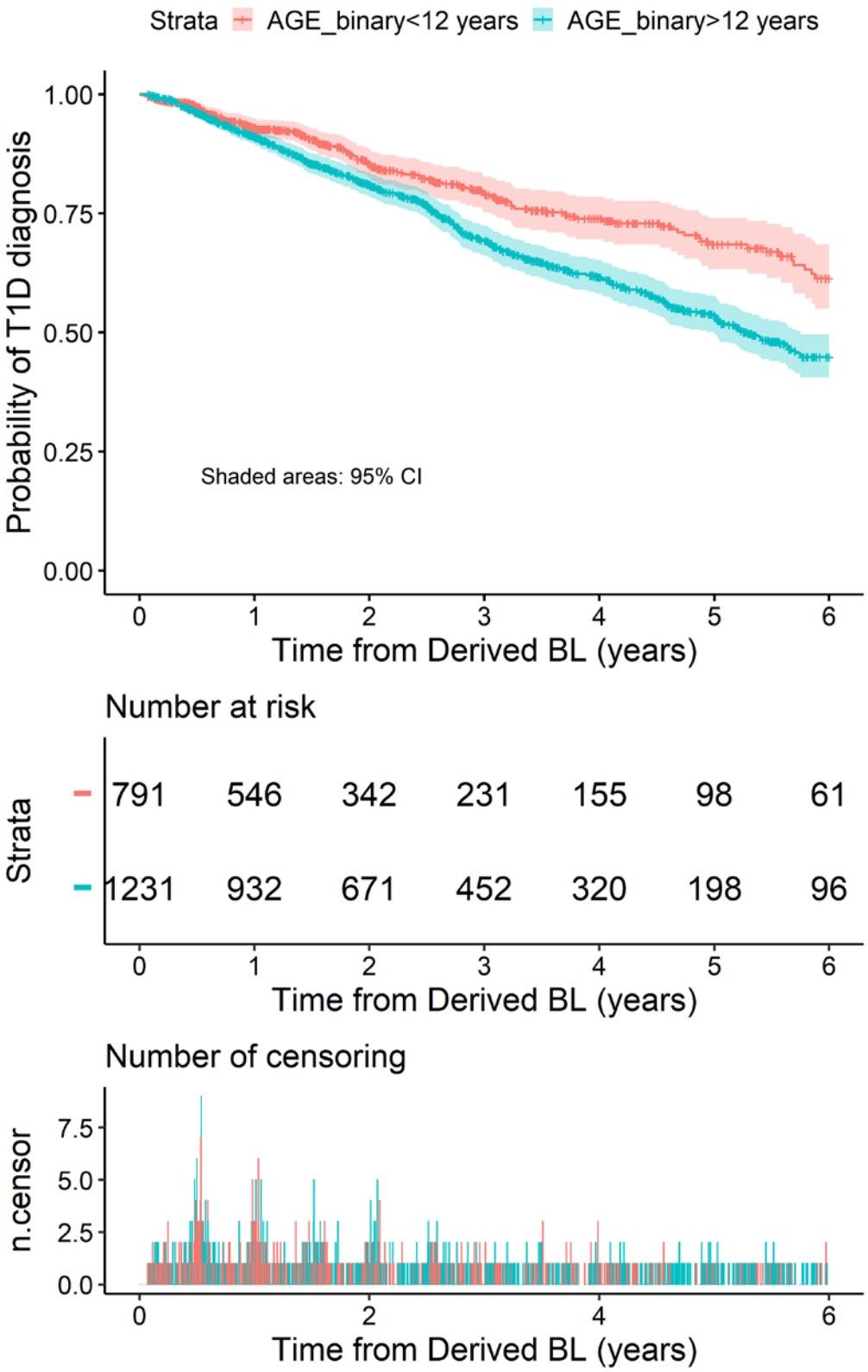

Figure 18. Survival plot, number of subjects at risk and distribution of censoring events stratified by HbA1c_binary

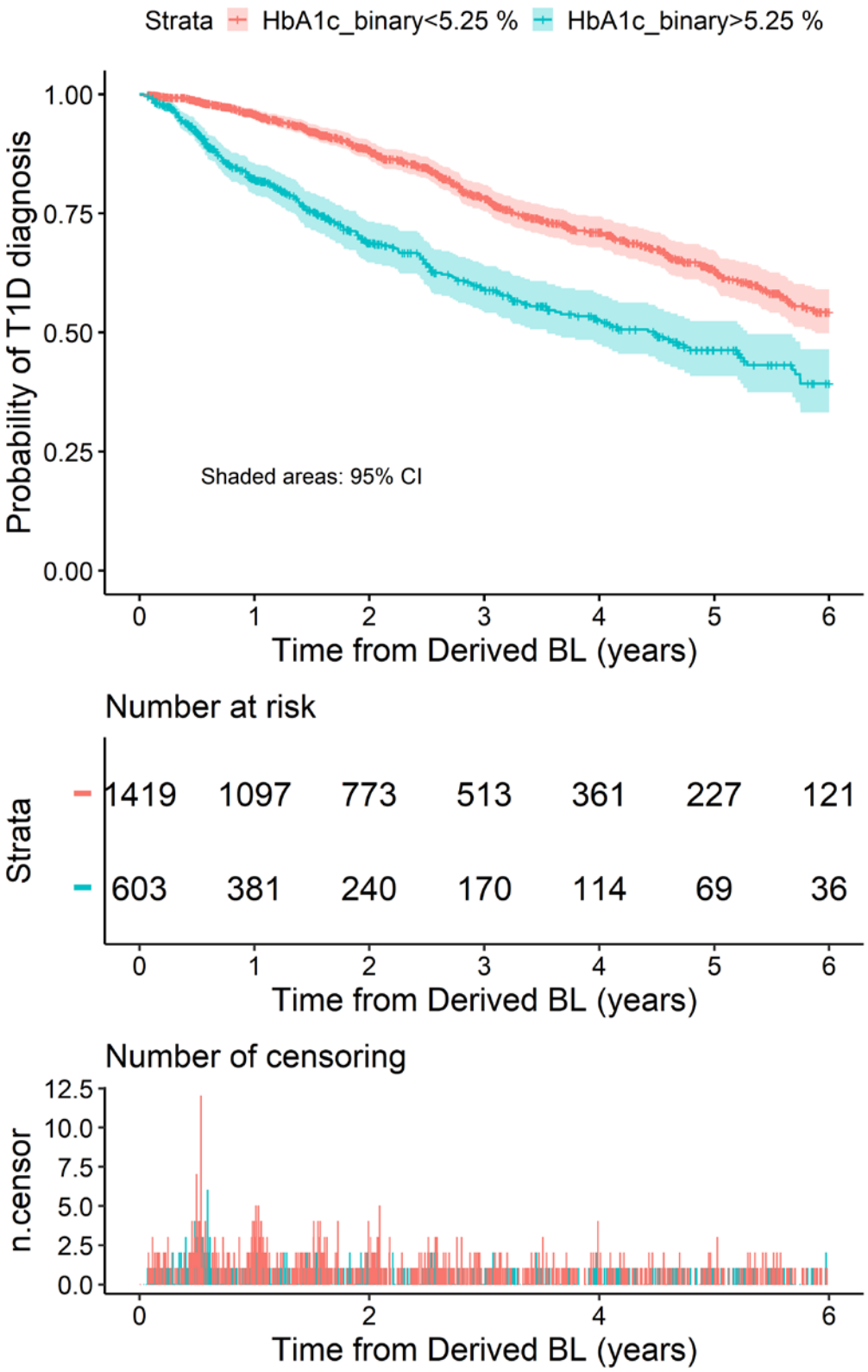

Figure 19. Survival plot, number of subjects at risk and distribution of censoring events stratified by GLU0_binary

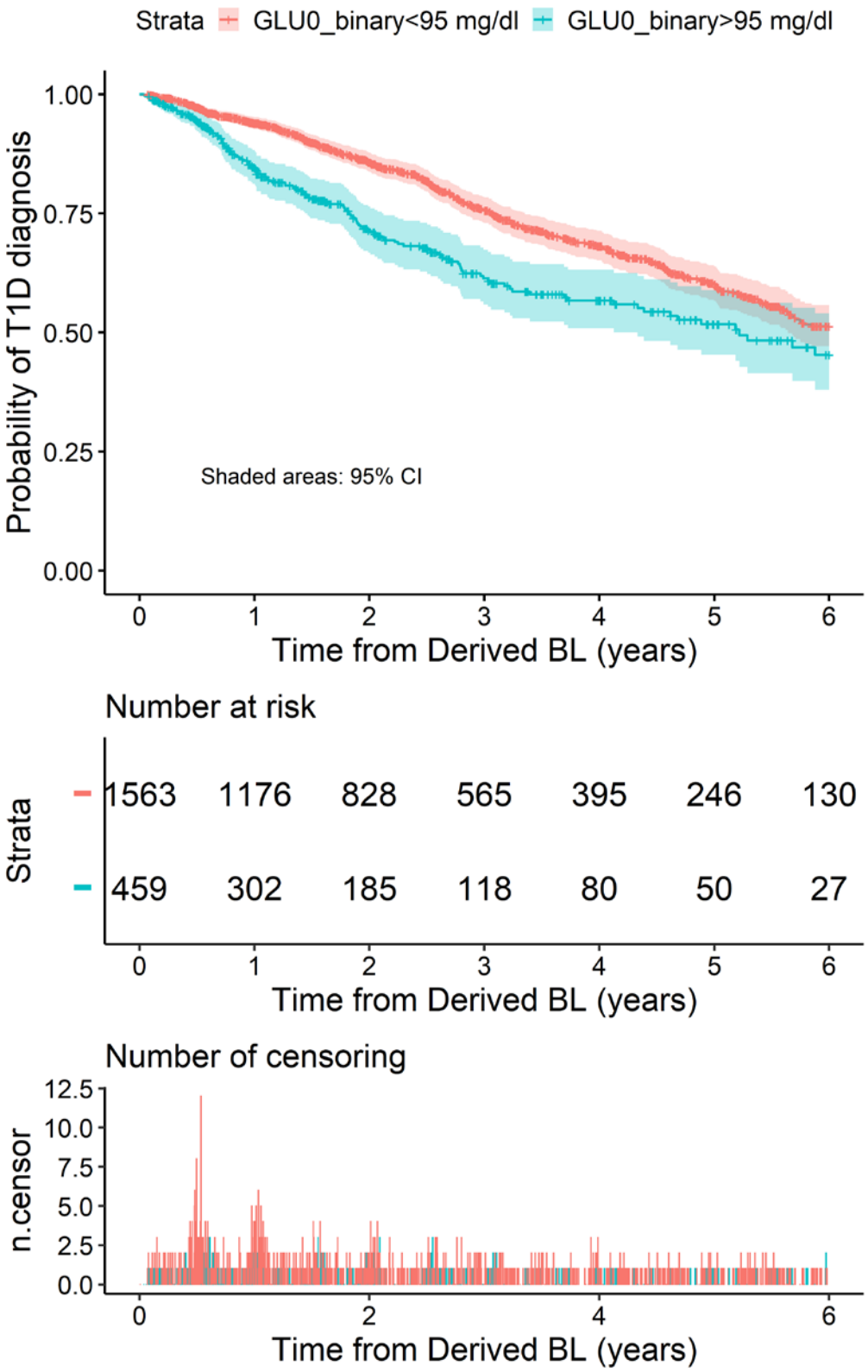

Figure 20. Survival plot, number of subjects at risk and distribution of censoring events stratified by GLU120_binary

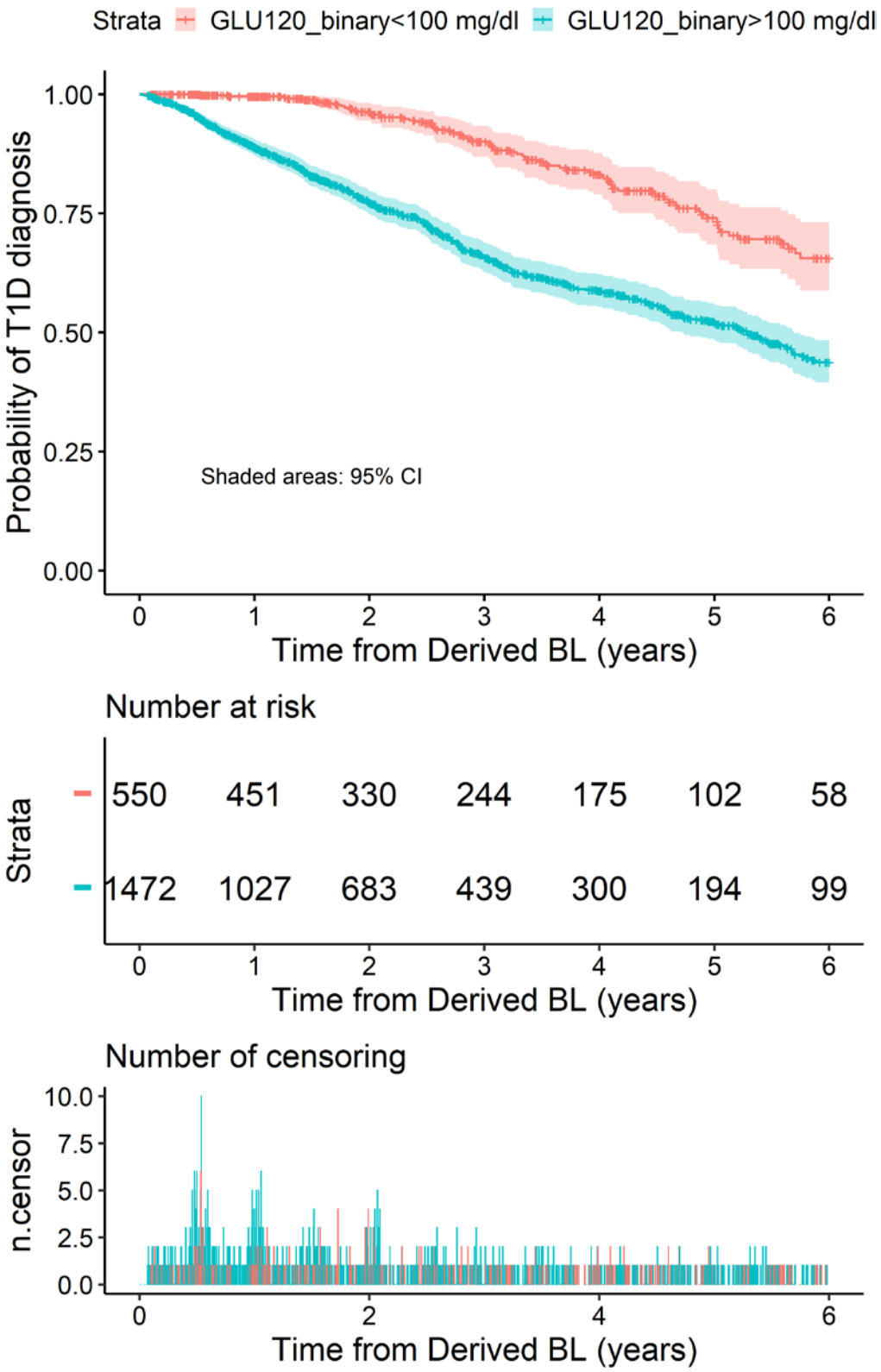

Figure 21. Survival plot, number of subjects at risk and distribution of censoring events stratified by BMI_binary

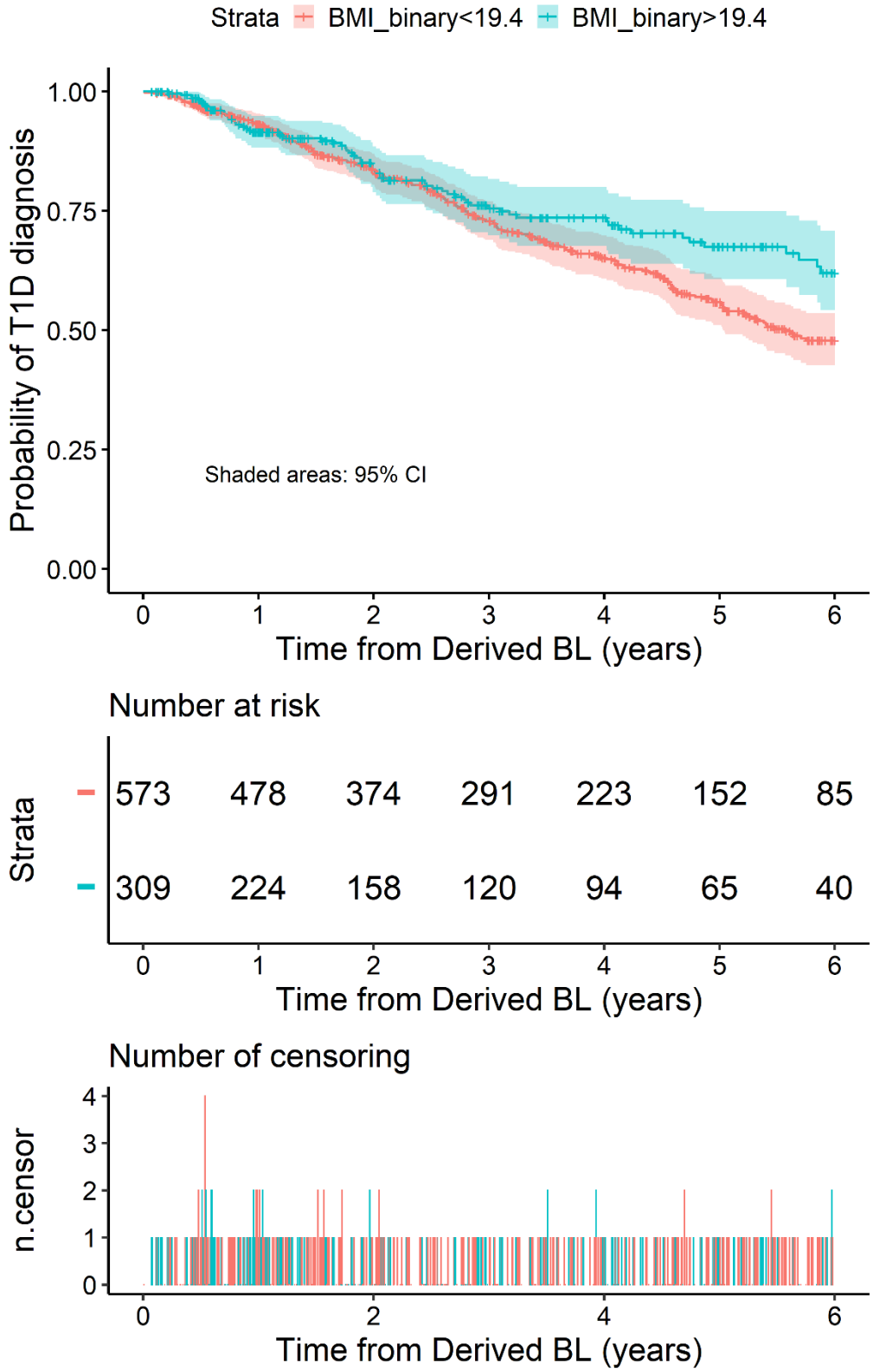

Section 4.3.3.1 provides summary statistics for the 2,022 subjects available in the analysis set and visualization of continuous covariates stratified by diagnosis. Additional visualization was performed to understand the distribution of continuous covariates across different AA combinations (Figure 22-26). These continuous covariates include baseline age (Figure 22), BMI (Figure 23), HbA1C % (Figure 24), 0-minute OGTT (Figure 25), and 120-minute OGTT (Figure 26). The distributions were obtain for 11 AA combinations, GAD65_IA-2, GAD65_IAA, GAD65_ZnT8, IA-2_IAA, IA-2_ZnT8, IAA_ZnT8, GAD65_IA-2_IAA, GAD65_IA-2_ZnT8, GAD65_IAA_ZnT8, IA-2_IAA_ZnT8, and GAD65_IA-2_IAA_ZnT8, across each continuous covariate. Majority of subjects were below 20 year of age for all AA combinations with GAD65_IAA and GAD65_IA-2_IAA_ZnT8 being the most prominent (Figure 22). The HbA1c %, 0-minute OGTT, and 120-minute OGTT were mostly normally distribution across different AA combinations.

Figure 22. Distribution of baseline age by AA combinations

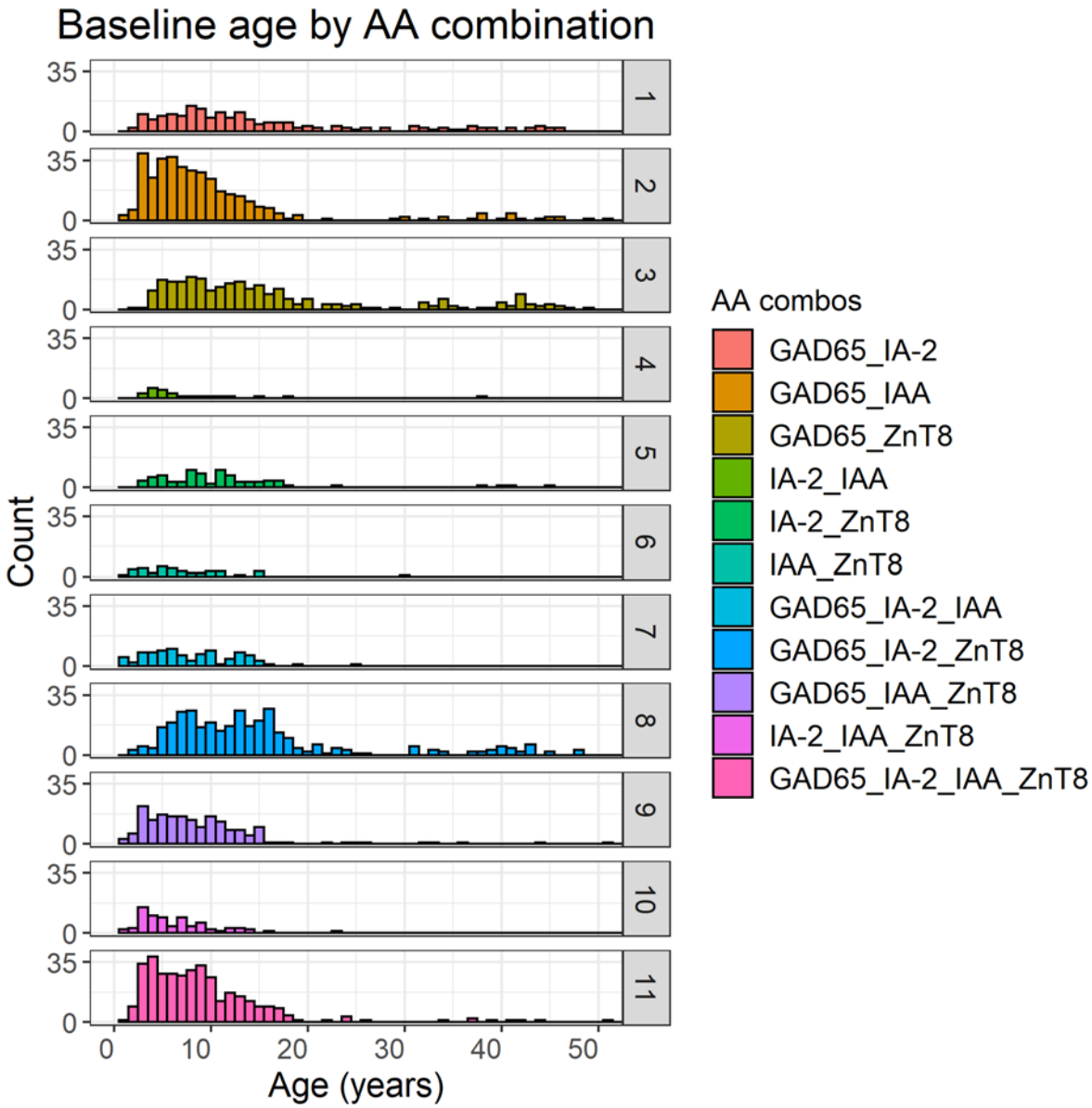

Figure 23. Distribution of BMI by AA combinations

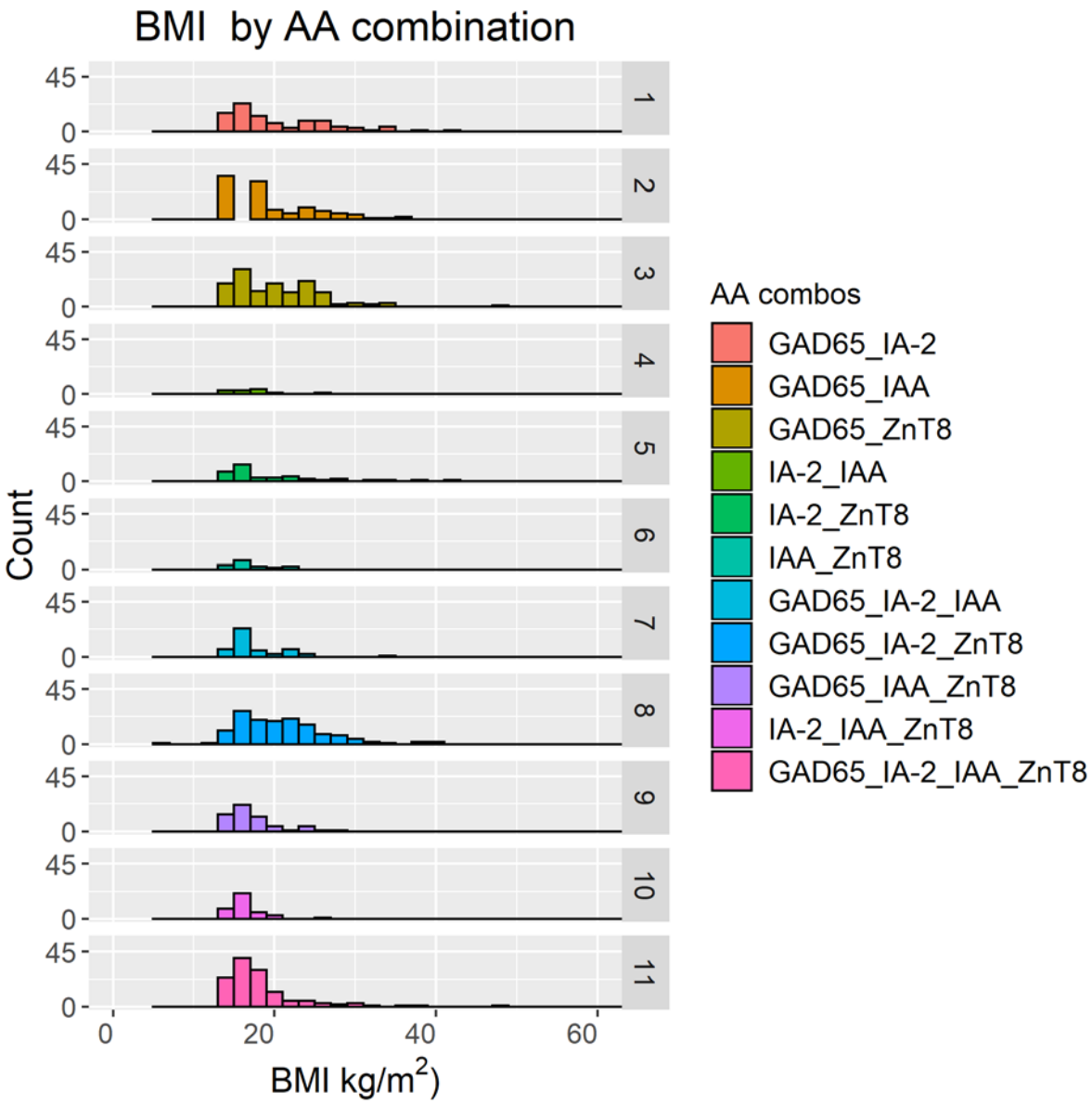

Figure 24. Distribution of HbA1c % by AA combinations

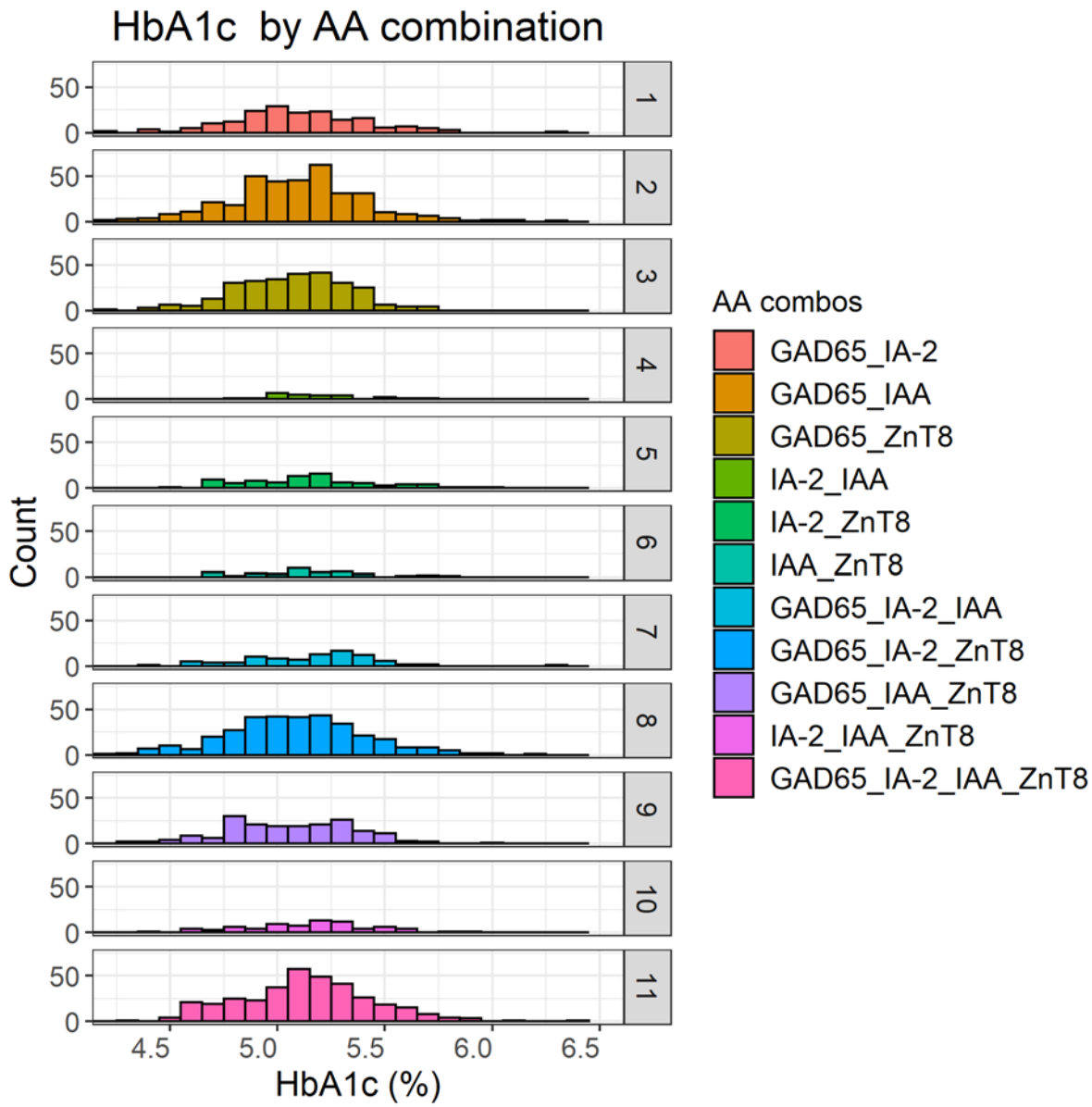

Figure 25. Distribution of 0-minute OGTT by AA combinations

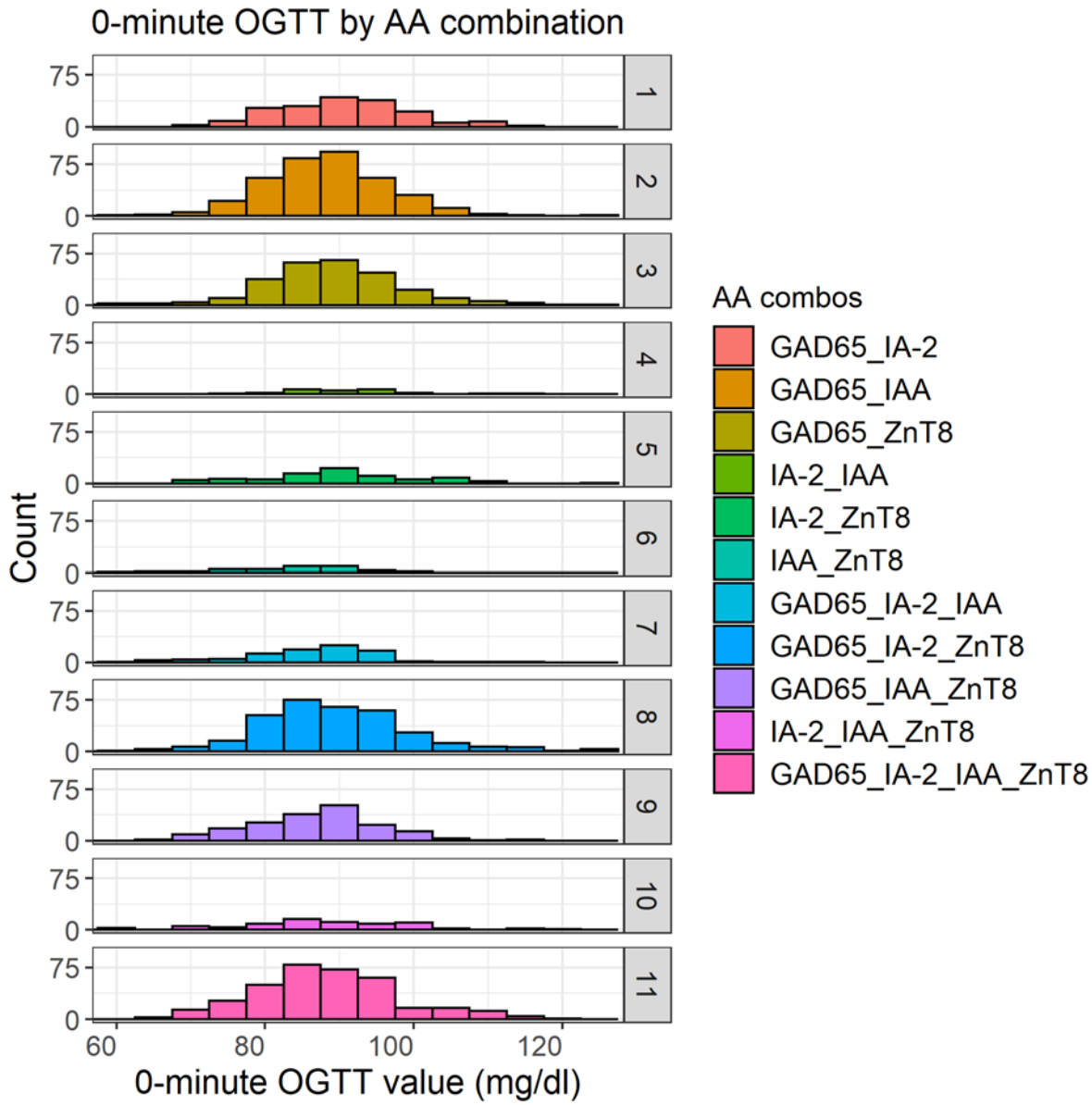

Figure 26. Distribution of 120-minute OGTT by AA combinations

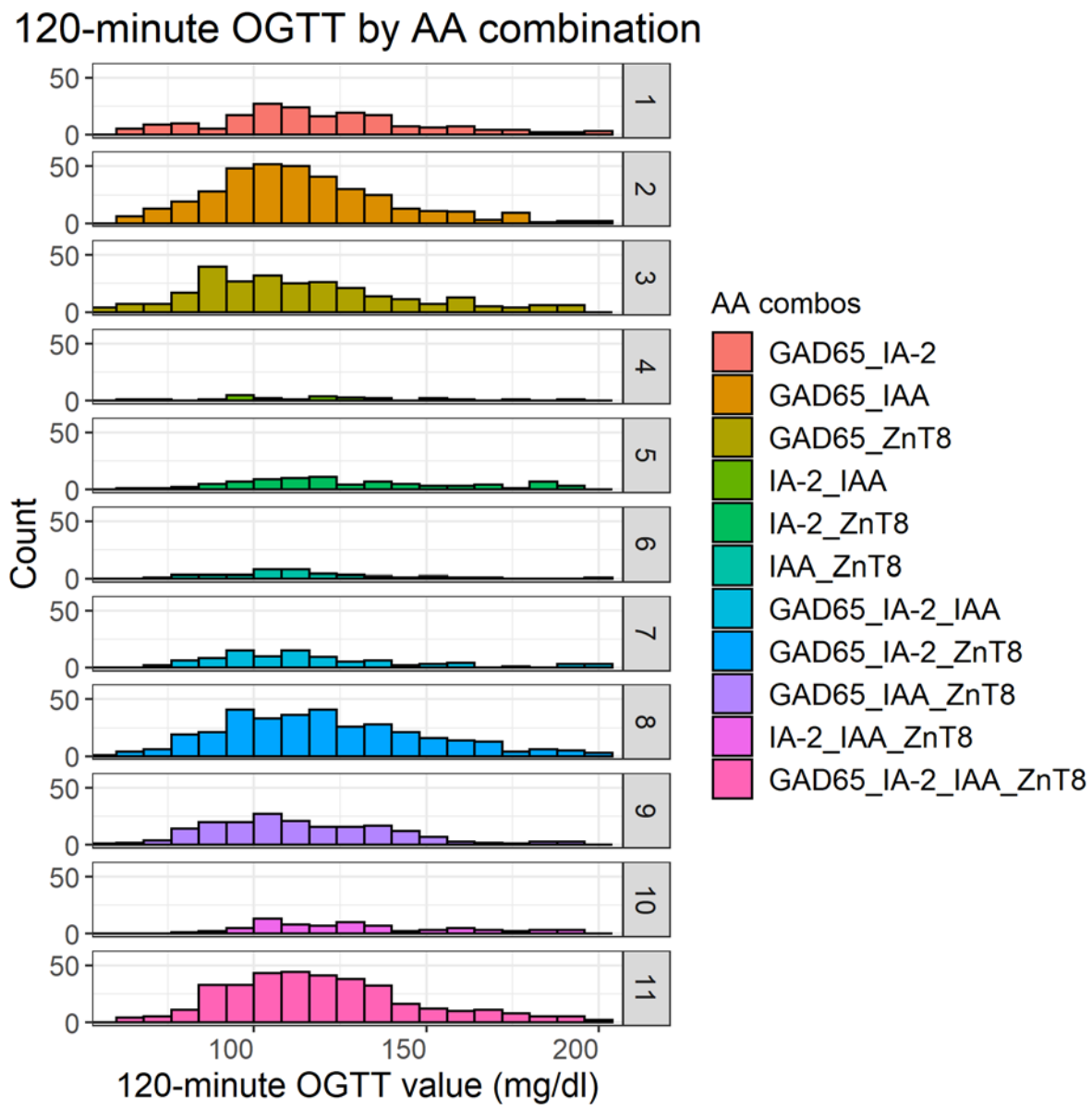

The Cox PH multivariate analysis produced 8 possible models as discussed in Section 4.4.1.3. The parameter estimates and hazard ratio for the base model, comprised of AA combinations GAD65_ZnT8, IA-2_ZnT8, IA-2_IAA_ZnT8, and GAD65_IA-2_IAA_ZnT8, as shown in Table 1. The IA-2_ZnT8 AA combination had the highest relative hazard ratio of 1.94 in the multivariate base model. Model 2 included Log_GLU0_s covariate with AA combinations from the base model. Similar to the base model IA-2_ZnT8 AA combination had the high relative hazard ratio (Table 2). Model 3 comprised on AA combinations from the base model and HbA1c_s covariate. Among the 6 covariates IA-2_IAA_ZnT8 had the highest relative hazard ratio (Table 3). Model 4 had Log_GLU120_s covariate along with AA combinations from the base model, with highest relative hazard ratio of 2.14 for Log_GLU120_s (Table 4). Model 5 had both OGTT covariates, Log_GLU120_s and Log_GLU0_s, along with AA combination from base model. Log_GLU120_s had the highest relative hazard ratio among the 7 covariates (Table 5). The parameter estimates and hazard ratios for Model 6 is provided in Section 4.4.1.3 Table 13, which

was selected as the selected Cox PH model. Model 7 included Log_GLU0_s and HbA1c_s covariates along with AA combinations from the base model. IA-2_IAA_ZnT8 had the highest relative hazard ratio among the 7 covariates (Table 6). Model 8 had all 8 covariates, GAD65_IAA, GAD65_ZnT8, IA-2_ZnT8, IA-2_IAA_ZnT8, GAD65_IA-2_IAA_ZnT8, Log_GLU0_s, Log_GLU120_s, and HbA1c_s, that were chosen for multivariate analysis based on univariate analysis (Section 4.4.1.1) and analysis of correlation and association between covariates (Section 4.4.1.2). Among the 8 covariates in model 8, Log_GLU120_s had the highest relative hazard ratio (Table 7).

Table 1. Cox PH parameter estimates for model 1 (base model)

Covariate	beta	Std Error (beta)	HR	Wald Statistic	p-value
GAD65_ZnT8	-0.7635	0.1731	0.466	-4.412	1.03E-05
IA-2_ZnT8	0.6624	0.1771	1.9394	3.74	0.000184
IA-2_IAA_ZnT8	0.6344	0.175	1.8859	3.625	0.000289
GAD65_IA-2_IAA_ZnT8	0.3079	0.1118	1.3606	2.755	0.005875

Table 2. Cox PH parameter estimates for model 2

Covariate	beta	Std Error (beta)	HR	Wald Statistic	p-value
GAD65_IAA	-0.64128	0.15351	0.52662	-4.177	2.95E-05
GAD65_ZnT8	-0.76004	0.17307	0.46765	-4.392	1.13E-05
IA-2_ZnT8	0.65326	0.17718	1.9218	3.687	0.000227
IA-2_IAA_ZnT8	0.64281	0.175	1.90182	3.673	0.000239
GAD65_IA-2_IAA_ZnT8	0.32811	0.11191	1.38834	2.932	0.003369
Log_GLU0_s	0.18156	0.04671	1.19908	3.887	0.000101

Table 3. Cox PH parameter estimates for model 3

Covariate	beta	Std Error (beta)	HR	Wald Statistic	p-value
GAD65_IAA	-0.66385	0.15344	0.51486	-4.327	1.51E-05
GAD65_ZnT8	-0.7305	0.17324	0.48167	-4.217	2.48E-05
IA-2_ZnT8	0.58937	0.17726	1.80285	3.325	0.000884
IA-2_IAA_ZnT8	0.61986	0.17502	1.85867	3.542	0.000398
GAD65_IA-2_IAA_ZnT8	0.21442	0.1121	1.23915	1.913	0.055779
HbA1c_s	0.52246	0.04764	1.68617	10.966	< 2e-16

Table 4. Cox PH parameter estimates for model 4

Covariate	beta	Std Error (beta)	HR	Wald Statistic	p-value
GAD65_IAA	-0.55215	0.15362	0.57571	-3.594	0.000325
GAD65_ZnT8	-0.7398	0.17323	0.47721	-4.271	1.95E-05
IA-2_ZnT8	0.53584	0.17771	1.70888	3.015	0.002567
IA-2_IAA_ZnT8	0.48627	0.17526	1.62624	2.775	0.005527
GAD65_IA-2_IAA_ZnT8	0.30239	0.11182	1.35309	2.704	0.006847

Log_GLU120_s	0.76391	0.05114	2.14664	14.938	< 2e-16

Table 5. Cox PH parameter estimates for model 5

Covariate	beta	Std Error (beta)	HR	Wald Statistic	p-value
GAD65_IAA	-0.54065	0.15367	0.58237	-3.518	0.000435
GAD65_ZnT8	-0.72493	0.17326	0.48436	-4.184	2.86E-05
IA-2_ZnT8	0.51182	0.17804	1.66833	2.875	0.004043
IA-2_IAA_ZnT8	0.51561	0.17546	1.67465	2.939	0.003296
GAD65_IA-2_IAA_ZnT8	0.31242	0.1119	1.36673	2.792	0.005239
Log_GLU120_s	0.75648	0.05137	2.13076	14.725	< 2e-16
Log_GLU0_s	0.11983	0.04208	1.1273	2.848	0.004403

Table 6. Cox PH parameter estimates for model 7

Covariate	beta	Std Error (beta)	HR	Wald Statistic	p-value
GAD65_IAA	-0.65337	0.15358	0.52029	-4.254	2.10E-05
GAD65_ZnT8	-0.72615	0.17327	0.48377	-4.191	2.78E-05
IA-2_ZnT8	0.58208	0.17735	1.78975	3.282	0.001031
IA-2_IAA_ZnT8	0.62355	0.17503	1.86555	3.563	0.000367
GAD65_IA-2_IAA_ZnT8	0.22756	0.11237	1.25554	2.025	0.042855
Log_GLU0_s	0.07712	0.04696	1.08017	1.642	0.100522
HbA1c_s	0.50424	0.04876	1.65572	10.342	< 2e-16

Table 7. Cox PH parameter estimates for model 8

Covariate	beta	Std Error (beta)	HR	Wald Statistic	p-value
GAD65_IAA	-0.57843	0.15367	0.56078	-3.764	0.000167
GAD65_ZnT8	-0.71996	0.17343	0.48677	-4.151	3.30E-05
IA-2_ZnT8	0.41199	0.17874	1.50982	2.305	0.021167
IA-2_IAA_ZnT8	0.47914	0.17571	1.61469	2.727	0.006393
GAD65_IA-2_IAA_ZnT8	0.19679	0.11279	1.21748	1.745	0.081048
Log_GLU0_s	0.02908	0.04339	1.02951	0.67	0.502695
Log_GLU120_s	0.69087	0.05157	1.99546	13.398	< 2e-16
HbA1c_s	0.40945	0.0486	1.50599	8.424	< 2e-16

The model diagnostics for the selected Cox PH model was performed using Schoenfeld residuals to test the PH assumption as discussed in Section 4.4.1.4. The Schoenfeld residual plot for AA combinations, GAD65_IAA, GAD65_ZnT8, IA-2_ZnT8, IA-2_IAA_ZnT8, and GAD65_IA-2_IAA_ZnT8, in the selected Cox PH model showed not systematic departure from a horizontal line (Figure 27-31). Additionally, the p-values (Section 4.4.1.4 Table 14) for these AA combinations were greater than 0.05 suggestion validity of PH assumption for these

combinations. However, the continuous covariate, Log_GLU_120s and HbA1c_s, violated the PH assumption, resulting in a global p-value less than 0.05.

Figure 27. Graphical diagnostics with Scaled Schoenfeld residuals (Beta(t)) against survival time – selected Cox PH model GAD65_IAA

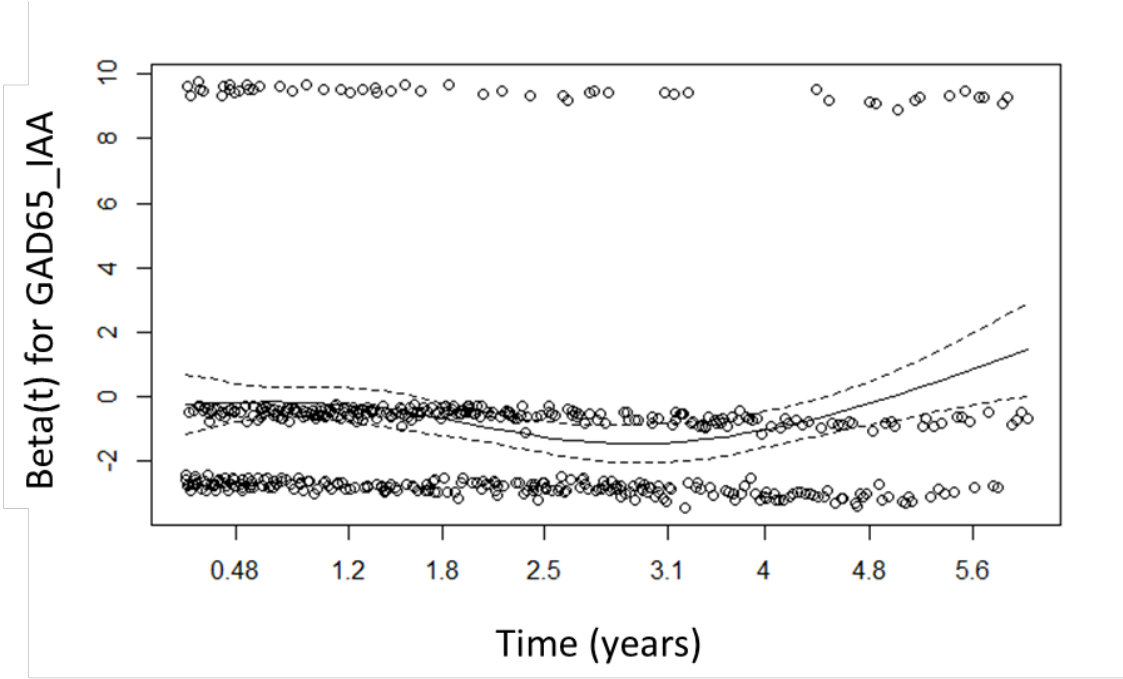

Figure 28. Graphical diagnostics with Scaled Schoenfeld residuals (Beta(t)) against survival time – selected Cox PH model GAD65_ZnT8

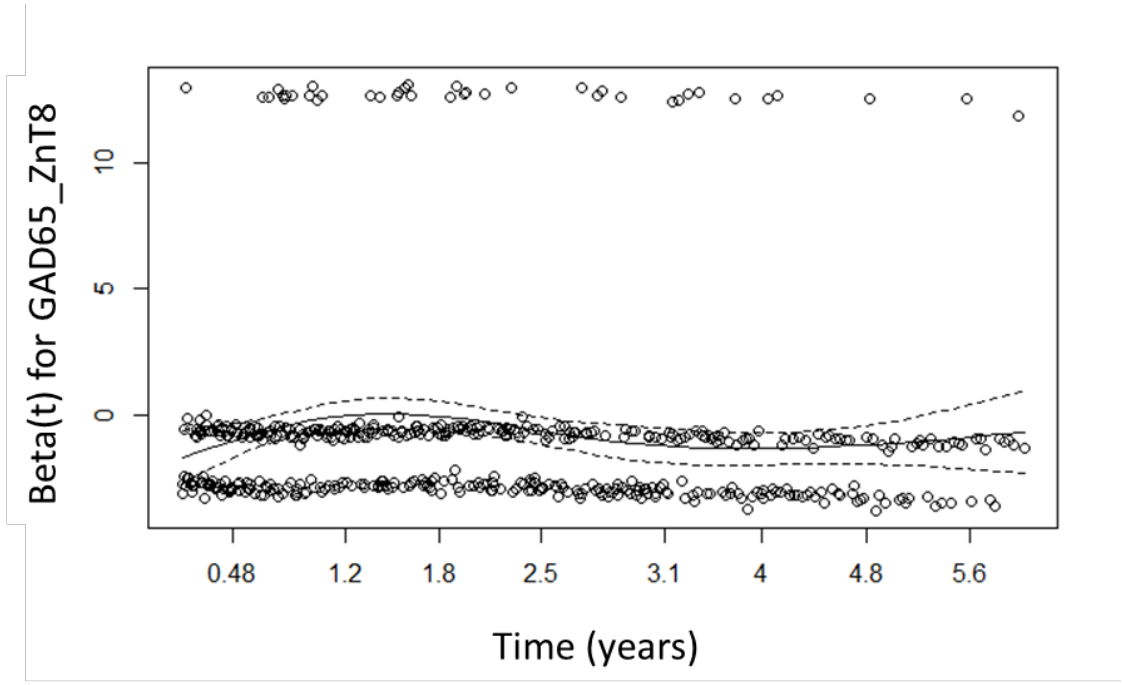

Figure 29. Graphical diagnostics with Scaled Schoenfeld residuals (Beta(t)) against survival time – selected Cox PH model IA-2_ZnT8

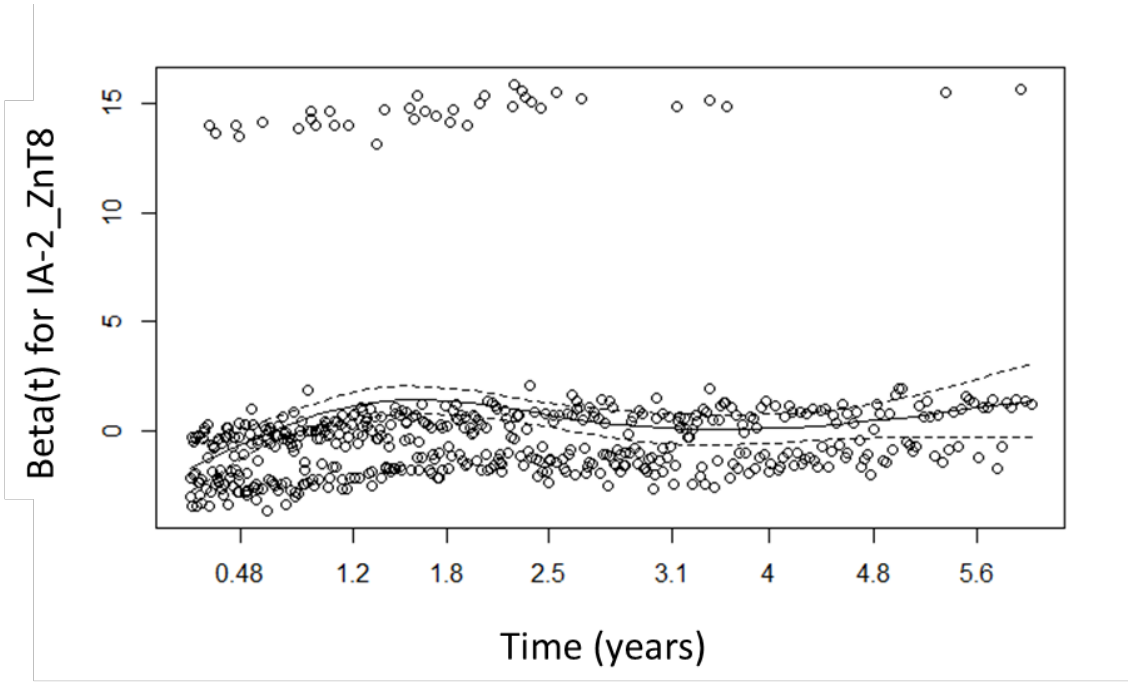

Figure 30. Graphical diagnostics with Scaled Schoenfeld residuals (Beta(t)) against survival time – selected Cox PH model IA-2_IAA_ZnT8

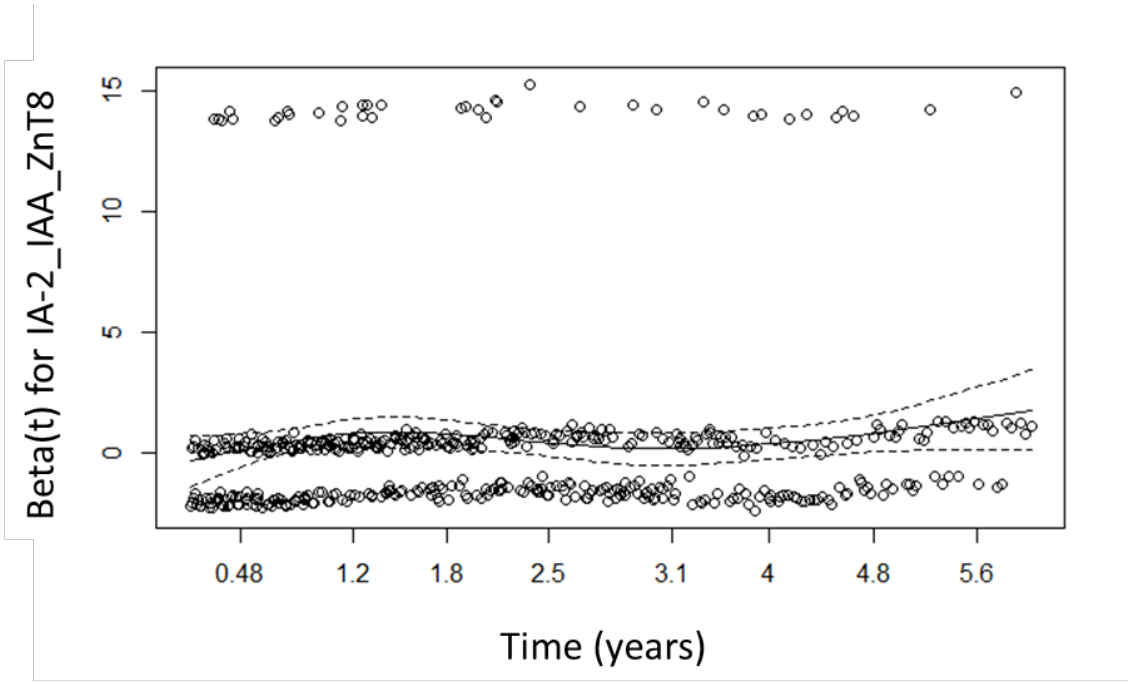

Figure 31. Graphical diagnostics with Scaled Schoenfeld residuals (Beta(t)) against survival time – selected Cox PH model GAD65_IA-2_IAA_ZnT8

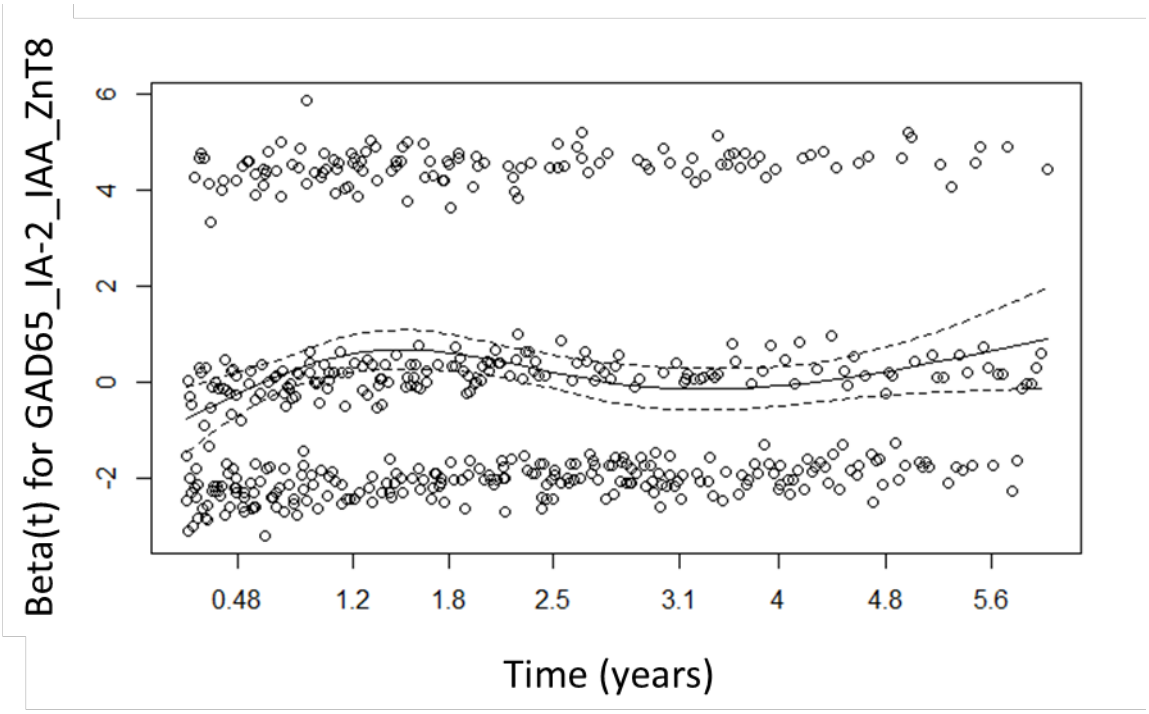

Selection of the most appropriate distribution to parameterize the form of hazard function in the AFT model analysis was conducted using 8 different distribution functions. These include exponential, Weibull, gamma, generalized gamma, generalized F, log logistic, Gompertz, and log-normal. The Weibull distribution was selected based on AIC value, survival plot, and hazard plot as discussed in Section 4.4.2.1. The cumulative hazard and hazard function plots for other distribution are shown in (Figure 32-38). As the hazard is constant in an exponential distribution, it was an inappropriate distribution to parameterize the form of hazard function for the AFT model (Figure 32). The generalized F (Figure 35), log-logistic (Figure 36), Gompertz (Figure 37), and log normal (Figure 38) distributions did not show good graphical fit. The gamma (Figure 33), and generalized gamma (Figure 34) distributions were comparable with Weibull distribution (Section 4.4.2.1 Figure 6) in terms of visual fit for the hazard function.

Figure 32. The survival and hazard function plots for exponential distributions

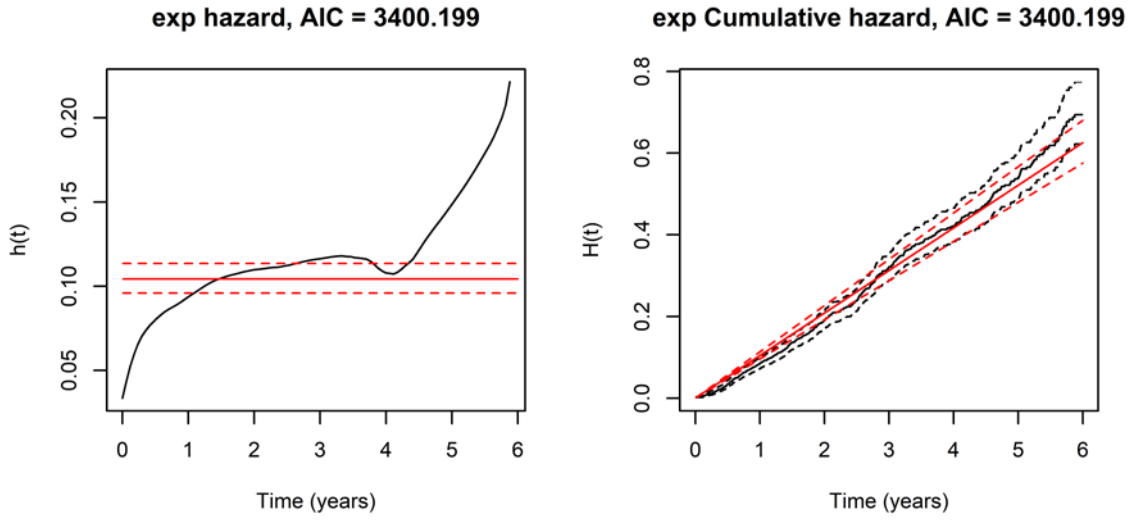

Figure 33. The survival and hazard function plots for gamma distributions

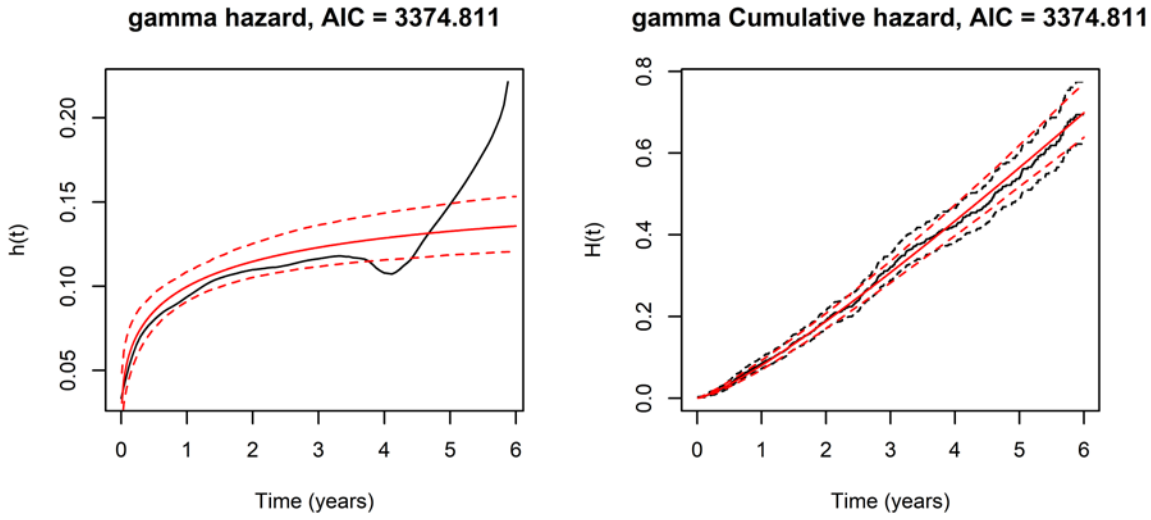

Figure 34. The survival and hazard function plots for generalized gamma distributions

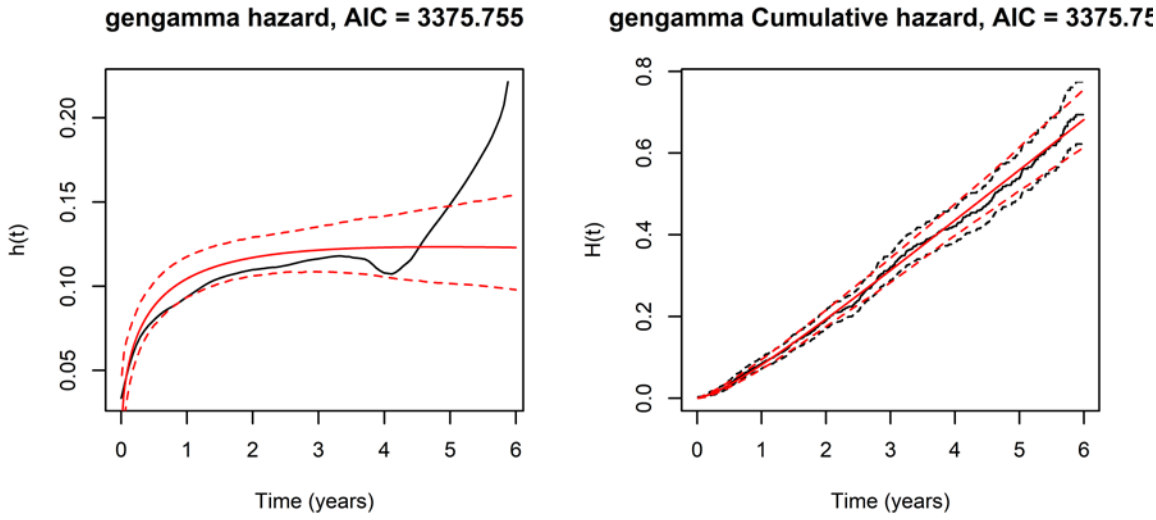

Figure 35. The survival and hazard function plots for generalized F distributions

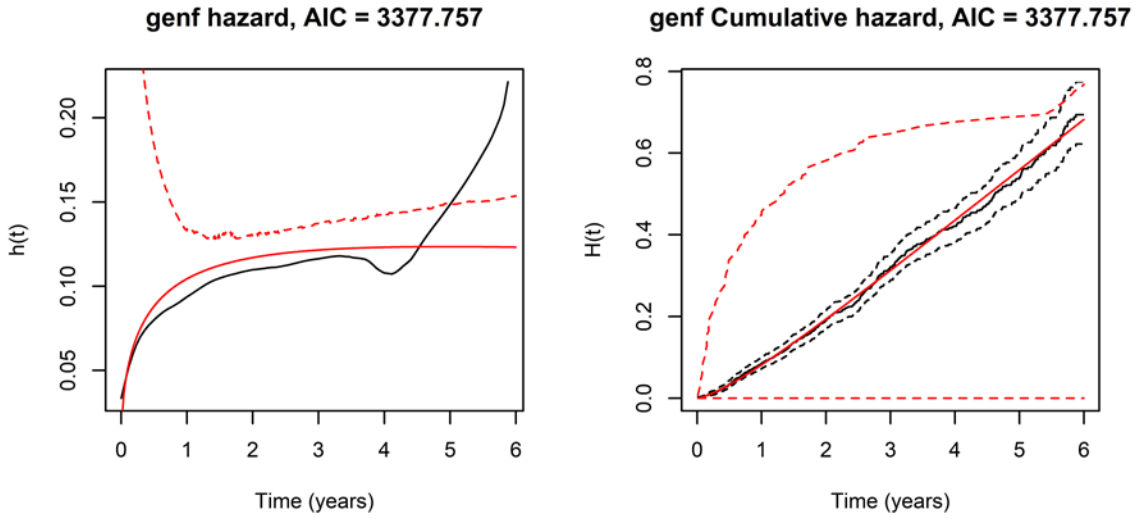

Figure 36. The survival and hazard function plots for log logistic distributions

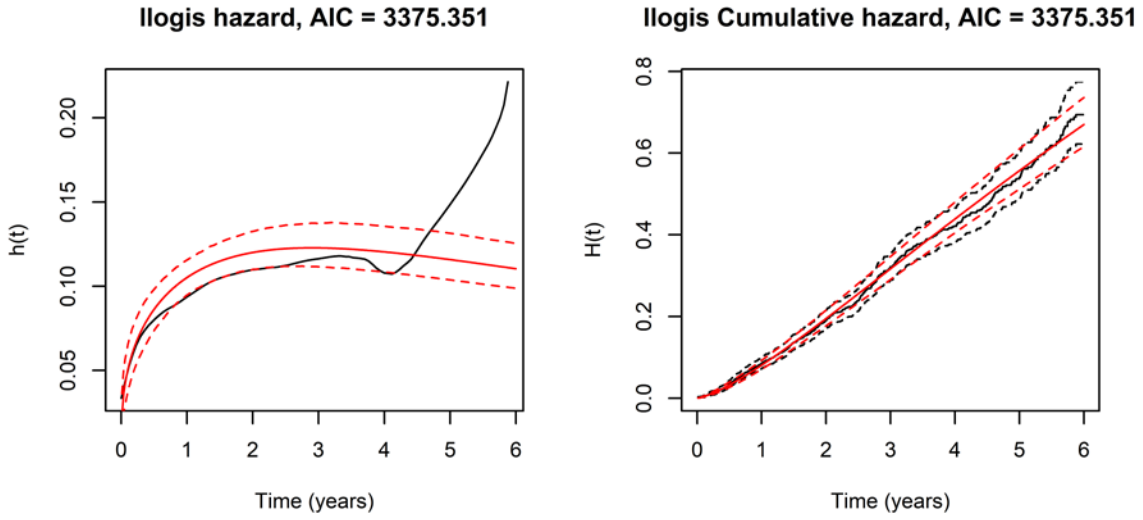

Figure 37. The survival and hazard function plots for gompertz distributions

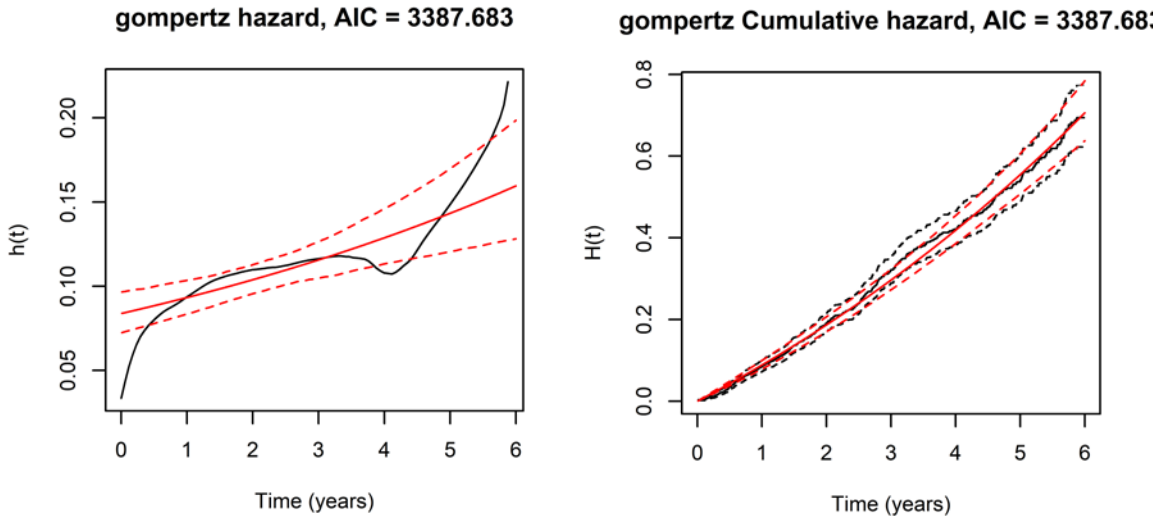

Figure 38. The survival and hazard function plots for log normal distributions

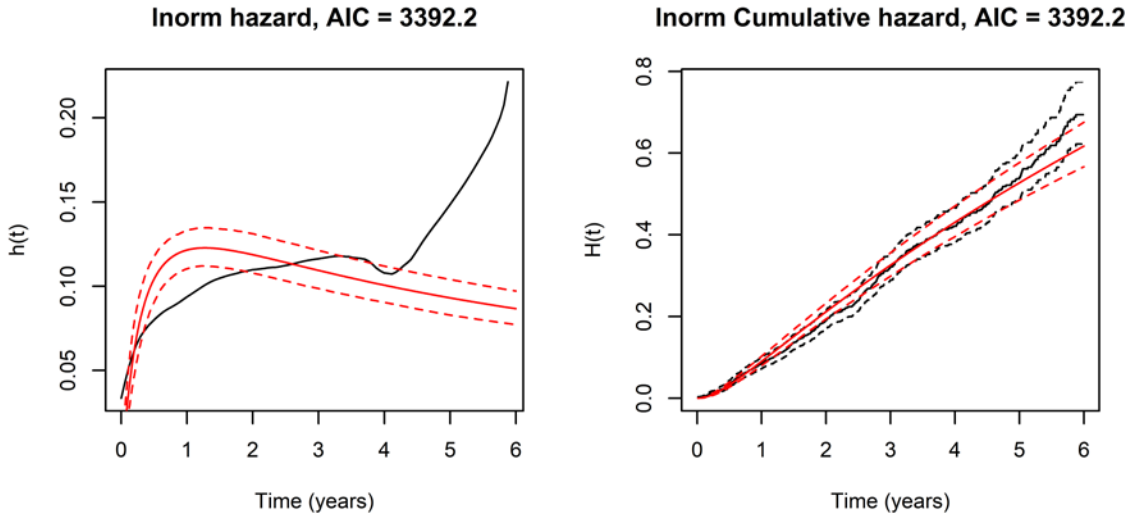

The AFT multivariate analysis produced 8 possible models as discussed in Section 4.4.2.4. Table 8 provides parameter estimates for shape and scale parameter for Weibull distribution and AA combinations (GAD65_IAA, GAD65_ZnT8, IA-2_ZnT8, IA-2_IAA_ZnT8, and GAD65_IA-2_IAA_ZnT8) for the base model. The IA-2_ZnT8 AA combination had the smallest beta coefficient value of -0.54 in the multivariate base model. Model 2 included Log_GLU0_s covariate with AA combinations from the base model. Similar to the base model IA-2_ZnT8 AA combination had the smallest beta coefficient value (Table 9). Model 3 comprised on AA combinations from the base model and HbA1c_s covariate. Among the 6 covariates IA-2_IAA_ZnT8 had the smallest beta coefficient value (Table 10). Model 4 had Log_GLU120_s covariate along with AA combination from the base model, with smallest beta coefficient value of -0.582 for Log_GLU120_s (Table 11). Model 5 had both OGTT covariates, Log_GLU120_s and Log_GLU0_s, along with AA combination from base model. Log_GLU120_s had the smallest beta coefficient value among the 7 covariates (Table 12). The parameter estimates for Model 6 is provided in Section 4.4.2.4 Table 18, which was selected as the selected AFT model. Model 7 included Log_GLU0_s and HbA1c_s covariates along with AA combinations from the base model. IA-2_IAA_ZnT8 had the smallest beta coefficient value among the 7 covariates (Table 13).Model 8 had all 8 covariates, GAD65_IAA, GAD65_ZnT8, IA-2_ZnT8, IA-2_IAA_ZnT8, GAD65_IA-2_IAA_ZnT8, Log_GLU0_s, Log_GLU120_s, and HbA1c_s, that were chosen for multivariate analysis based on univariate analysis (Section 4.4.2.2) and analysis of correlation and association between covariates (Section 4.4.2.3). Among the 8 covariates in model 8, Log_GLU120_s had the smallest beta coefficient value (Table 14).

Table 8. AFT model (Weibull distribution) parameter estimates - model 1 (base model)

Covariates	Beta	95% lower CI	95% upper CI	p-value
Shape	1.23	1.14	1.32	1.54E-173
Scale	7.62	6.77	8.57	2.86E-62
GAD65_IAA	0.539	0.292	0.786	1.93E-05
GAD65_ZnT8	0.624	0.345	0.903	1.15E-05
IA-2_ZnT8	-0.54	-0.824	-0.256	0.000196
IA-2_IAA_ZnT8	-0.514	-0.796	-0.233	0.000342

GAD65_IA-2_IAA_ZnT8	-0.253	-0.433	-0.0744	0.00553

Table 9. AFT model (Weibull distribution) parameter estimates - model 2

Covariates	Beta	95% lower CI	95% upper CI	p-value
Shape	1.24	1.15	1.33	2.50E-174
Scale	7.62	6.78	8.57	6.68E-63
GAD65_IAA	0.52	0.274	0.765	3.39E-05
GAD65_ZnT8	0.617	0.34	0.894	1.27E-05
IA-2_ZnT8	-0.528	-0.81	-0.246	0.00024
IA-2_IAA_ZnT8	-0.517	-0.796	-0.237	0.000289
GAD65_IA-2_IAA_ZnT8	-0.269	-0.447	-0.0908	0.00308
Log_GLU0_s	-0.149	-0.223	-0.0744	8.60E-05

Table 10. AFT model (Weibull distribution) parameter estimates - model 3

Covariates	Beta	95% lower CI	95% upper CI	p-value
Shape	1.25	1.17	1.34	1.35E-180
Scale	7.79	6.92	8.77	1.45E-61
GAD65_IAA	0.532	0.29	0.774	1.68E-05
GAD65_ZnT8	0.587	0.314	0.86	2.55E-05
IA-2_ZnT8	-0.473	-0.751	-0.195	0.000865
IA-2_IAA_ZnT8	-0.491	-0.767	-0.216	0.000471
GAD65_IA-2_IAA_ZnT8	-0.172	-0.348	0.00354	0.0548
HbA1c_s	-0.417	-0.494	-0.339	8.79E-26

Table 11. AFT model (Weibull distribution) parameter estimates - model 4

Covariates	Beta	95% lower CI	95% upper CI	p-value
Shape	1.32	1.24	1.41	5.92E-186
Scale	7.81	6.97	8.76	1.01E-65
GAD65_IAA	0.419	0.19	0.648	0.000339
GAD65_ZnT8	0.561	0.303	0.819	2.08E-05
IA-2_ZnT8	-0.4	-0.663	-0.137	0.00292
IA-2_IAA_ZnT8	-0.361	-0.622	-0.101	0.00656
GAD65_IA-2_IAA_ZnT8	-0.231	-0.397	-0.0645	0.0065
Log_GLU120_s	-0.582	-0.661	-0.503	9.27E-47

Table 12. AFT model (Weibull distribution) parameter estimates - model 5

Covariates	Beta	95% lower CI	95% upper CI	p-value
Shape	1.33	1.24	1.42	2.78E-186
Scale	7.8	6.96	8.74	2.25E-66

GAD65_IAA	0.408	0.18	0.636	0.000455
GAD65_ZnT8	0.546	0.289	0.803	3.16E-05
IA-2_ZnT8	-0.379	-0.641	-0.116	0.00469
IA-2_IAA_ZnT8	-0.382	-0.641	-0.122	0.00396
GAD65_IA-2_IAA_ZnT8	-0.237	-0.402	-0.072	0.0049
Log_GLU120_s	-0.573	-0.652	-0.494	1.19E-45
Log_GLU0_s	-0.0913	-0.153	-0.0293	0.00388

Table 13. AFT model (Weibull distribution) parameter estimates - model 7

Covariates	Beta	95% lower CI	95% upper CI	p-value
Shape	1.26	1.17	1.35	1.29E-180
Scale	7.78	6.91	8.75	6.03E-62
GAD65_IAA	0.522	0.28	0.763	2.36E-05
GAD65_ZnT8	0.581	0.309	0.853	2.90E-05
IA-2_ZnT8	-0.465	-0.742	-0.188	0.00101
IA-2_IAA_ZnT8	-0.493	-0.768	-0.218	0.000437
GAD65_IA-2_IAA_ZnT8	-0.183	-0.359	-0.00725	0.0413
Log_GLU0_s	-0.0635	-0.137	0.0097	0.0891
HbA1c_s	-0.4	-0.48	-0.321	3.68E-23

Table 14. AFT model (Weibull distribution) parameter estimates - model 8

Covariates	Beta	95% lower CI	95% upper CI	p-value
Shape	1.35	1.26	1.44	2.50E-191
Scale	7.71	6.89	8.62	1.52E-68
GAD65_IAA	0.43	0.206	0.655	0.000171
GAD65_ZnT8	0.535	0.282	0.788	3.41E-05
IA-2_ZnT8	-0.299	-0.559	-0.0394	0.024
IA-2_IAA_ZnT8	-0.348	-0.603	-0.0921	0.00767
GAD65_IA-2_IAA_ZnT8	-0.147	-0.311	0.0174	0.0797
Log_GLU0_s	-0.023	-0.0859	0.0399	0.473
Log_GLU120_s	-0.516	-0.593	-0.439	1.43E-39
HbA1c_s	-0.302	-0.374	-0.23	1.90E-16

The k-fold cross validation analysis with five folds was performed to assess predictive performance as discussed in Section 4.4.3.2. Additionally, a comprehensive visualization was performed by generating VPC style plots to show model predictions stratified by each of the islet AA combinations and continuous covariates using binary groups (Figure 39-73). For HbA1c, a threshold of 5.25% was selected to stratify the Kaplan-Meier curves (Figure 39-43). All five folds show good fit with fold 4 (Figure 42) performing the best. The AA combinations from the selected AFT model (alt_mod3) was also used for stratification of Kaplan-Meier curves to visualize the k-fold cross validation performance. These combinations include GAD65_IA-2_IAA_ZnT8 (Figure 44-48), GAD65_IAA (Figure 49-53), GAD65_ZnT8 (Figure 54-58), IA-2_IAA_ZnT8 (Figure 64-68), and IA-2_ZnT8 (Figure 69-73). For GLU120, threshold of 100mg/dl was selected to stratify the Kaplan-Meier curves (Figure 59-63). Model predictions in general showed good predictive performance on the stratified groups. Exceptions can be seen for groups with extremely spare data for various AA combinations. In these cases, model predictions are more robust in the first year in comparison to later years.

Figure 39. k-fold cross validation analysis stratified by HbA1c_binary threshold of 5.25% – Fold 1

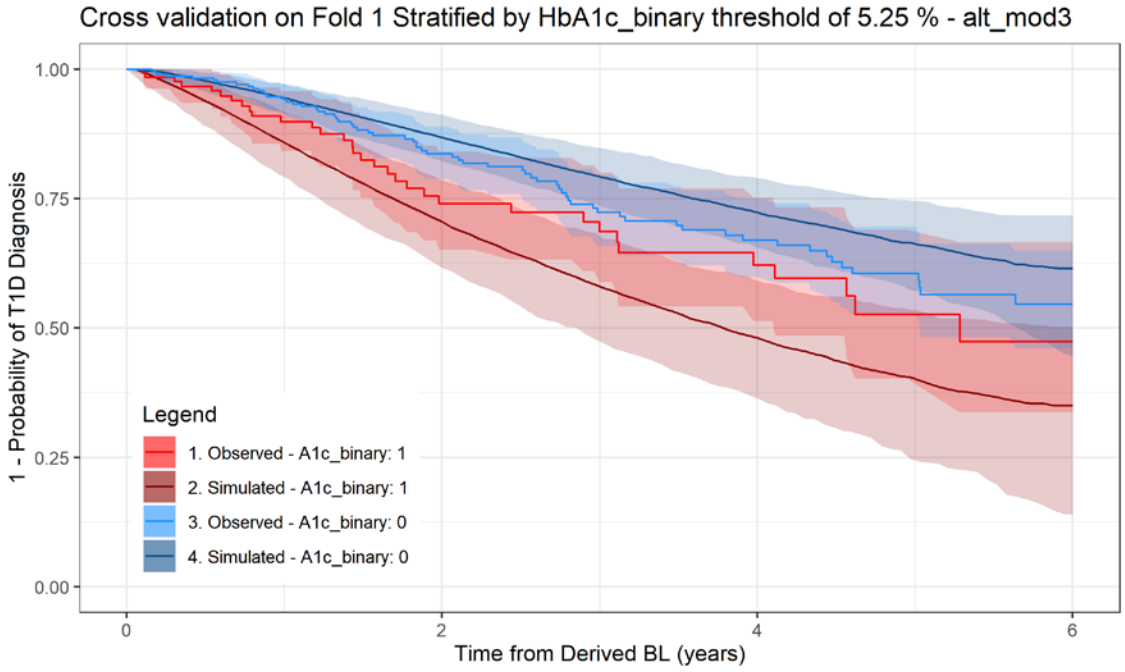

Figure 40. k-fold cross validation analysis stratified by HbA1c_binary threshold of 5.25% – Fold 2

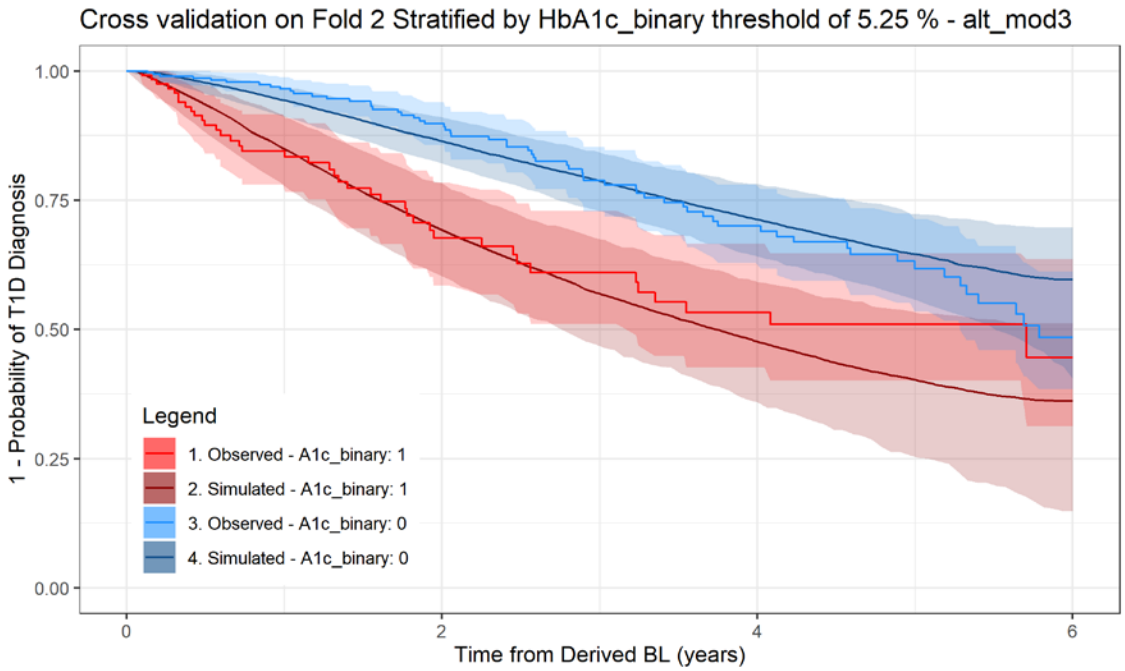

Figure 41. k-fold cross validation analysis stratified by HbA1c_binary threshold of 5.25% – Fold 3

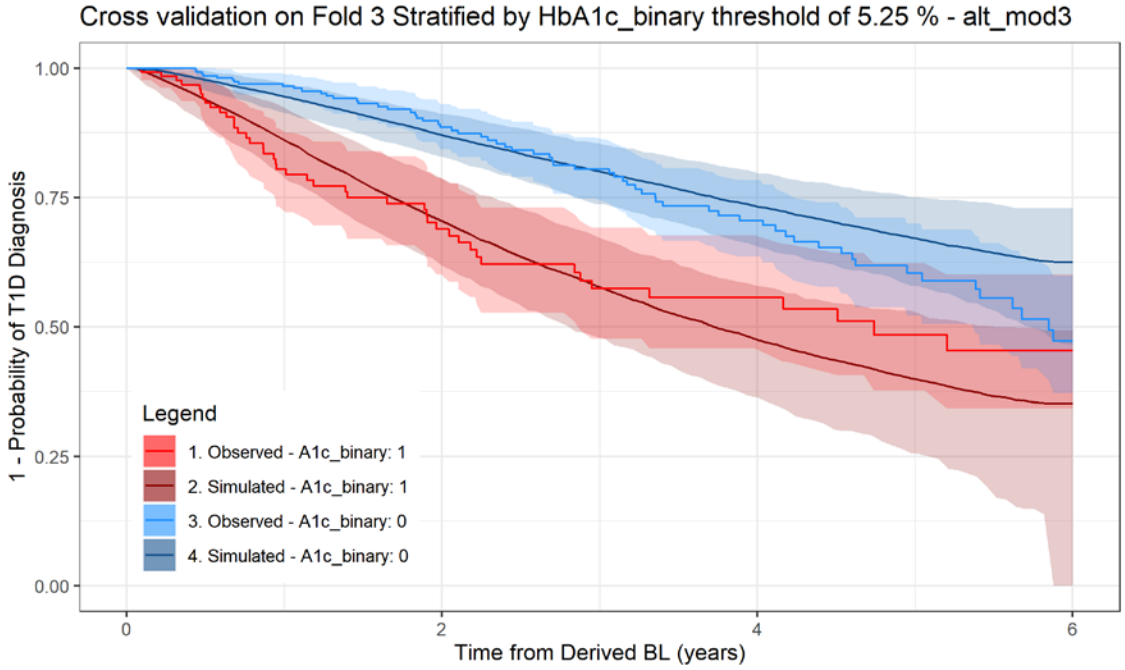

Figure 42. k-fold cross validation analysis stratified by HbA1c_binary threshold of 5.25% – Fold 4

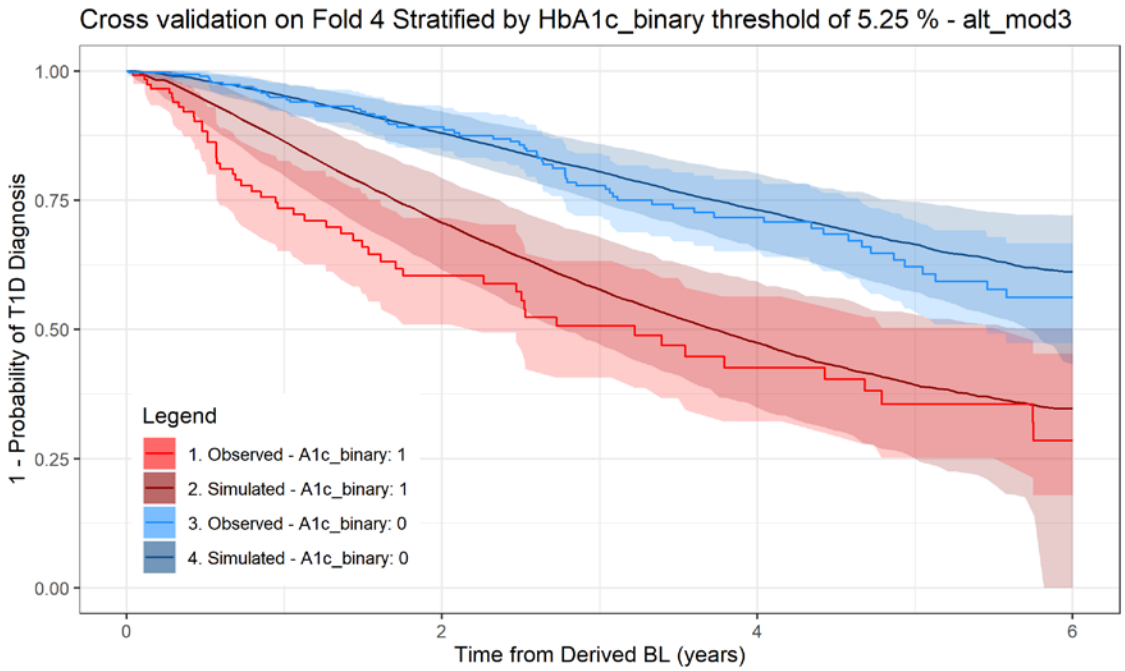

Figure 43. k-fold cross validation analysis stratified by HbA1c_binary threshold of 5.25% – Fold 5

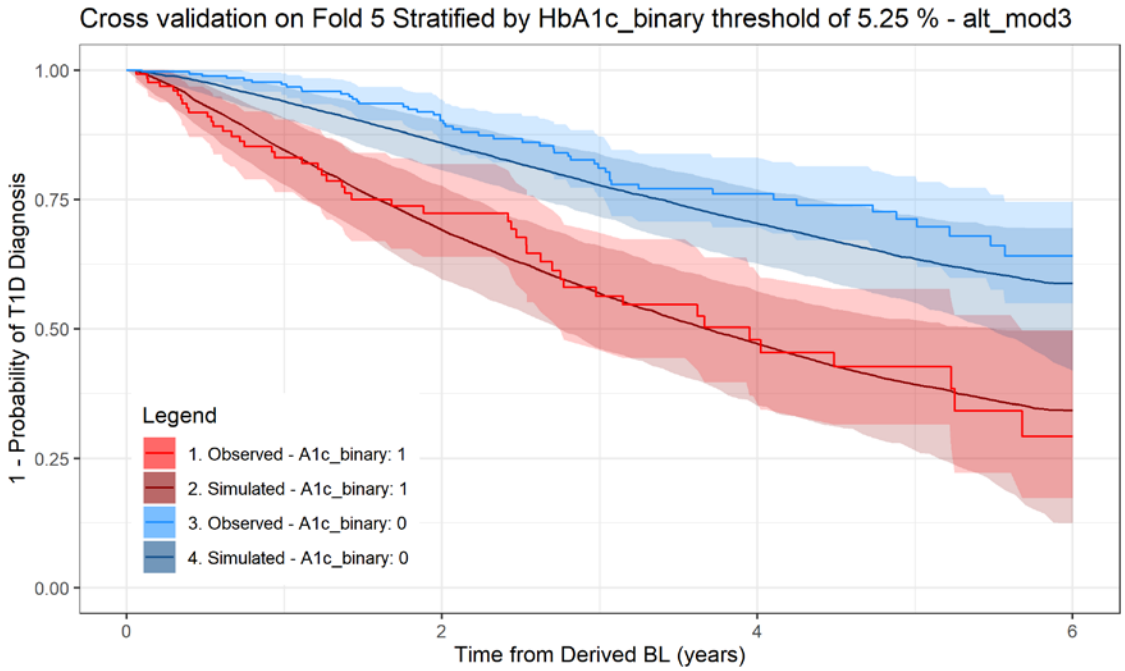

Figure 44. k-fold cross validation analysis stratified by GAD65_IA-2_IAA_ZnT8 – Fold 1

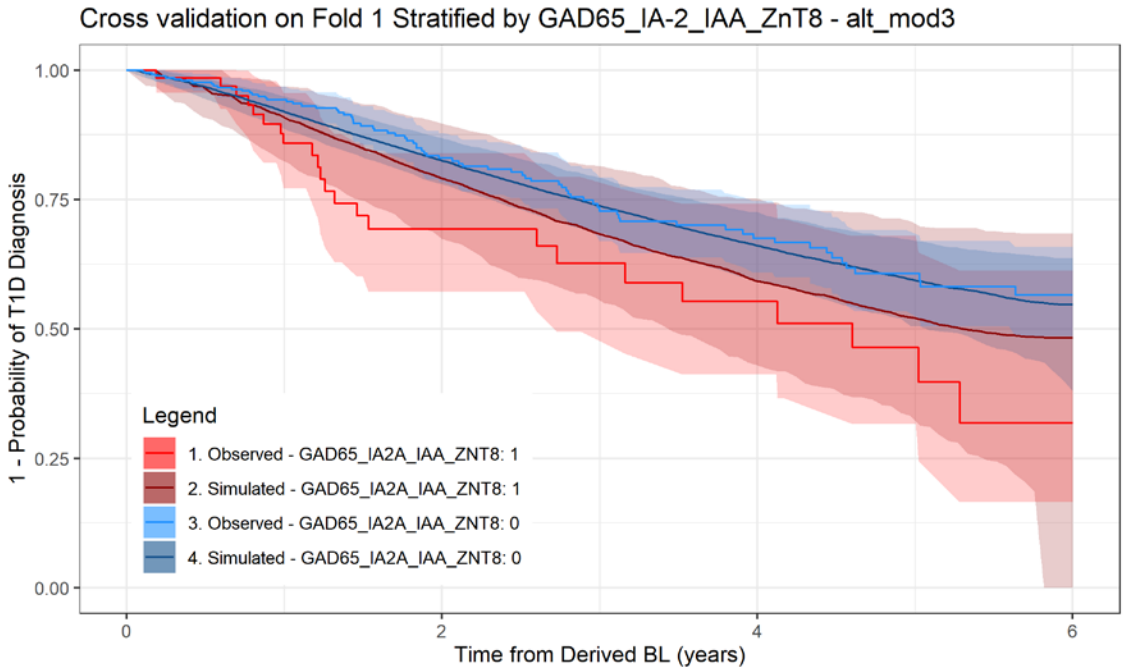

Figure 45. k-fold cross validation analysis stratified by GAD65_IA-2_IAA_ZnT8 – Fold 2

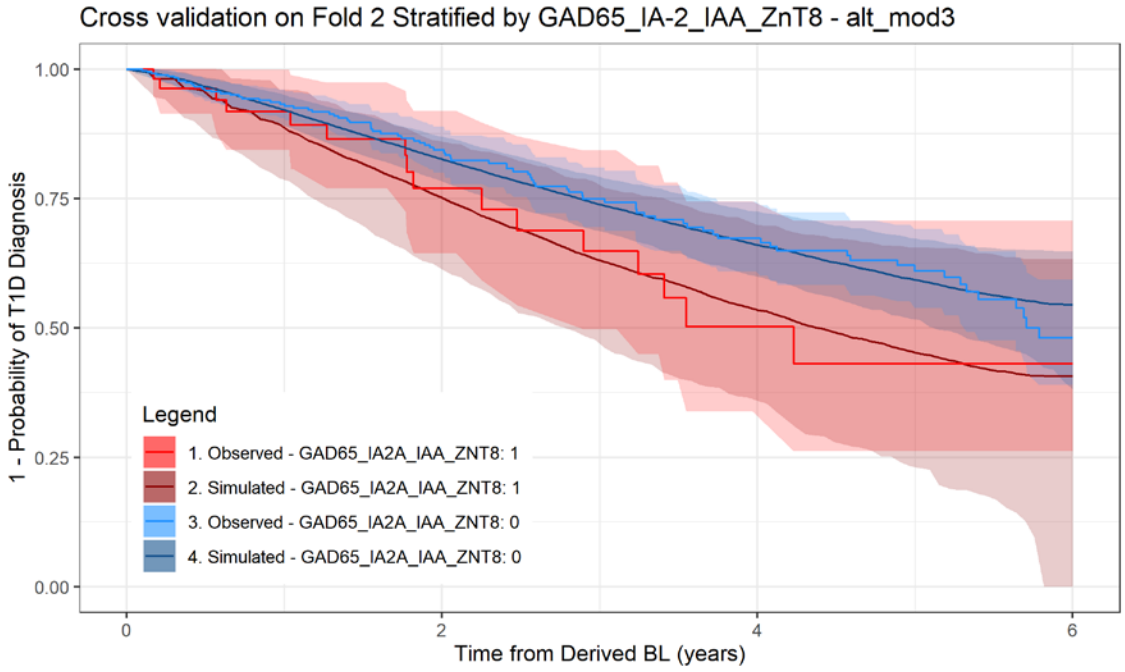

Figure 46. k-fold cross validation analysis stratified by GAD65_IA-2_IAA_ZnT8 – Fold 3

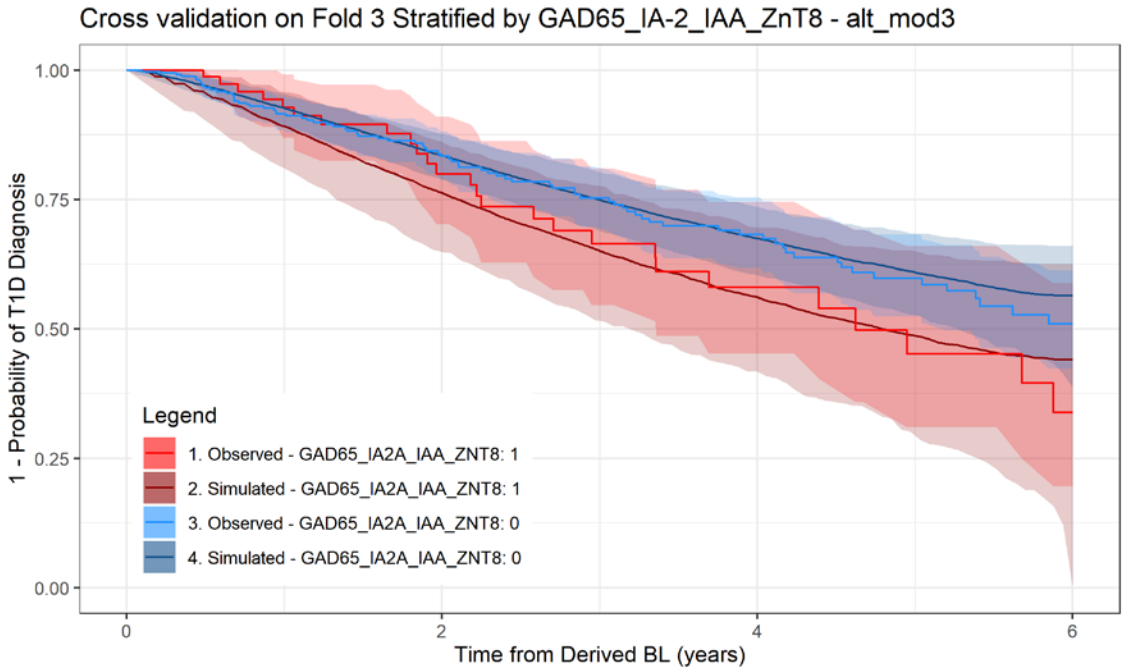

Figure 47. k-fold cross validation analysis stratified by GAD65_IA-2_IAA_ZnT8 – Fold 4

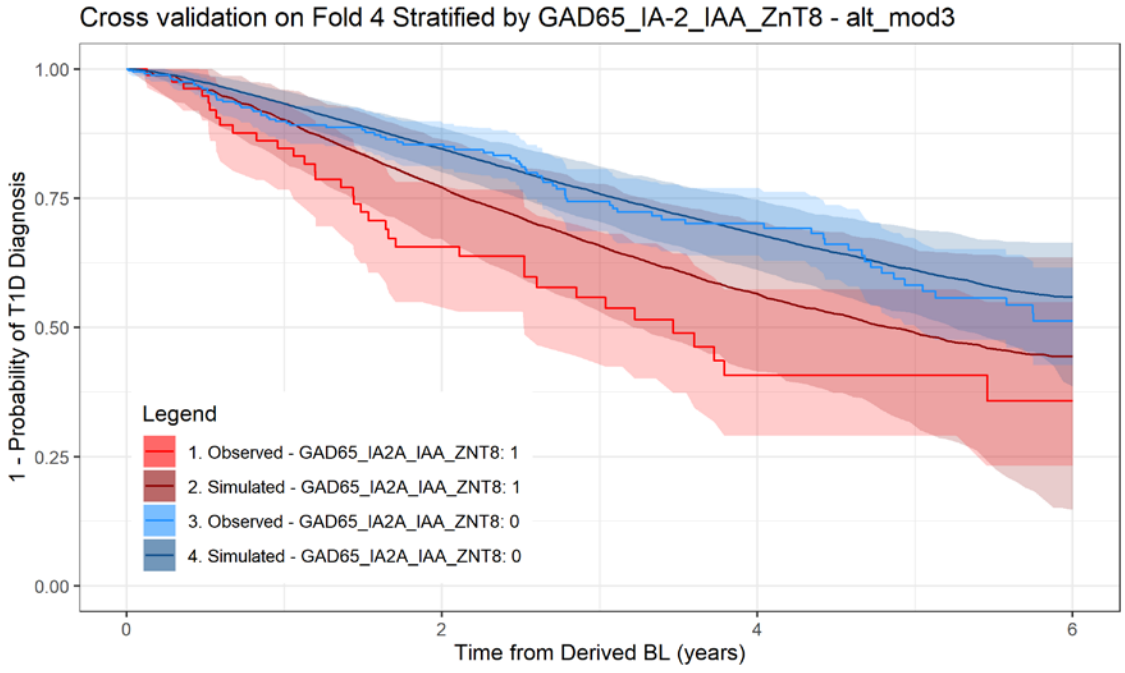

Figure 48. k-fold cross validation analysis stratified by GAD65_IA-2_IAA_ZnT8 – Fold 5

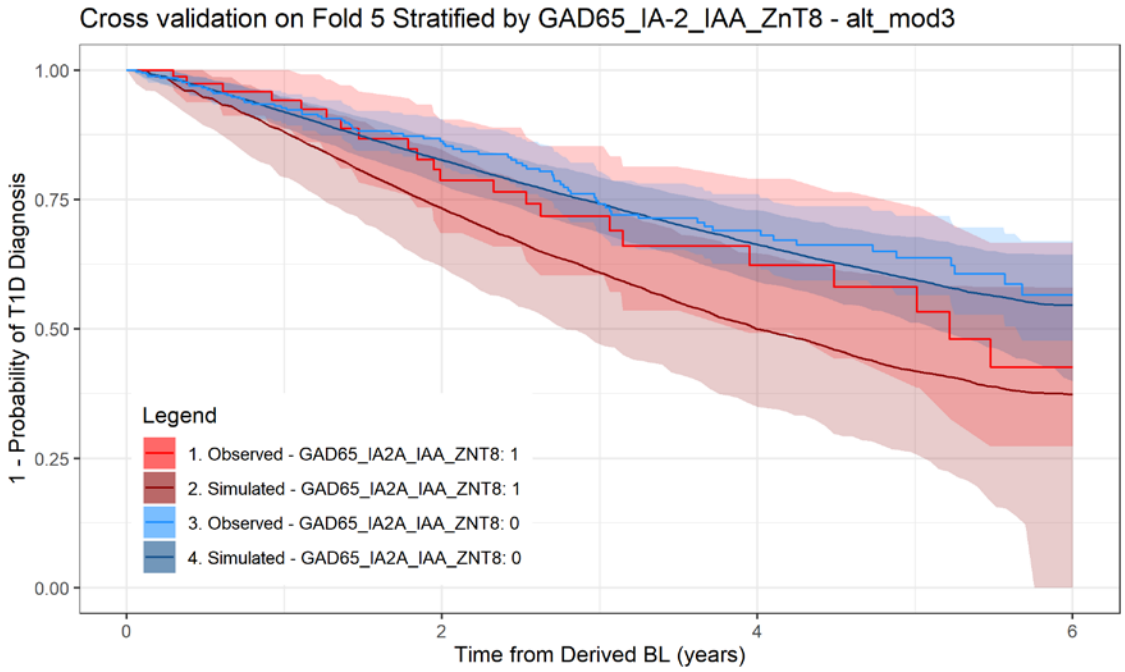

Figure 49. k-fold cross validation analysis stratified by GAD65_IAA – Fold 1

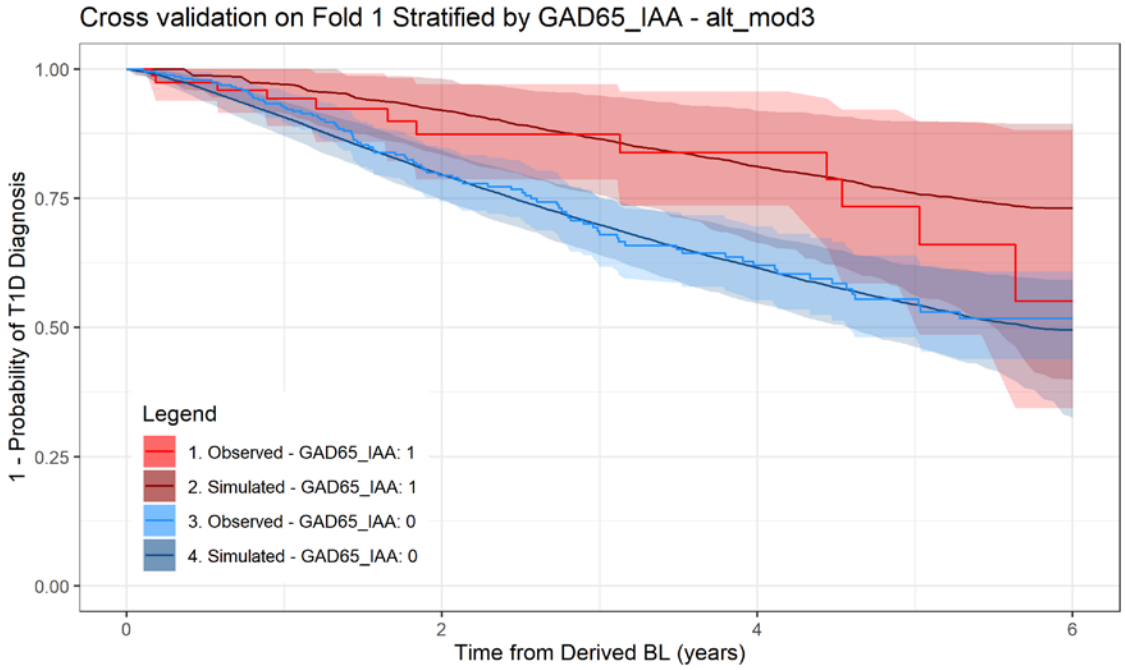

Figure 50. k-fold cross validation analysis stratified by GAD65_IAA – Fold 2

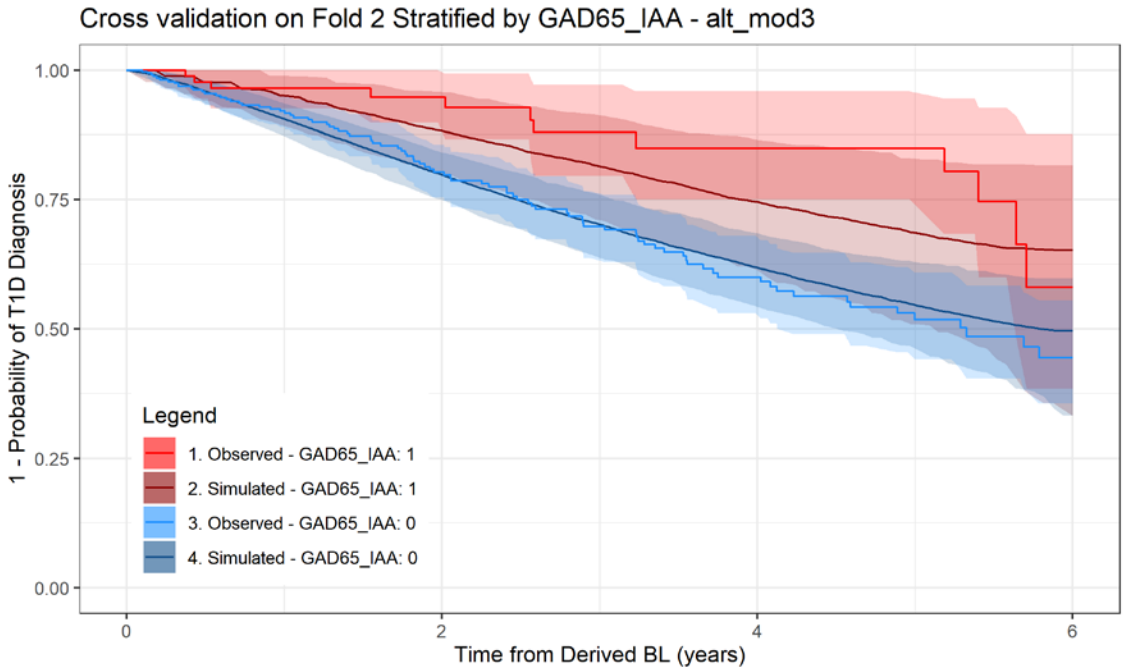

Figure 51. k-fold cross validation analysis stratified by GAD65_IAA – Fold 3

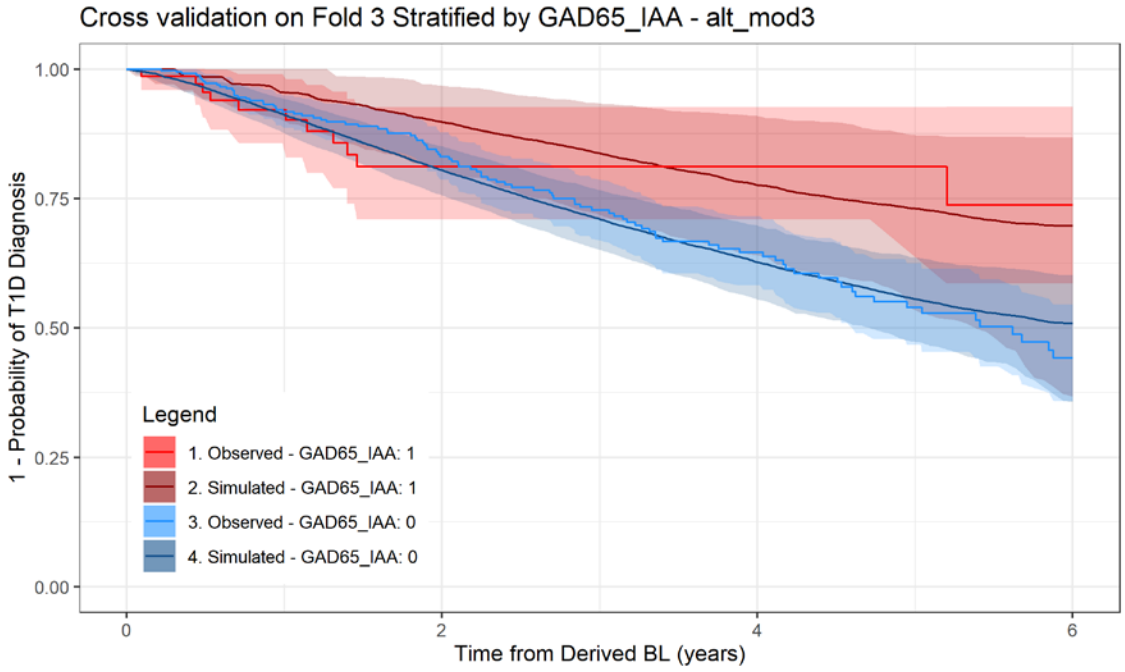

Figure 52. k-fold cross validation analysis stratified by GAD65_IAA – Fold 4

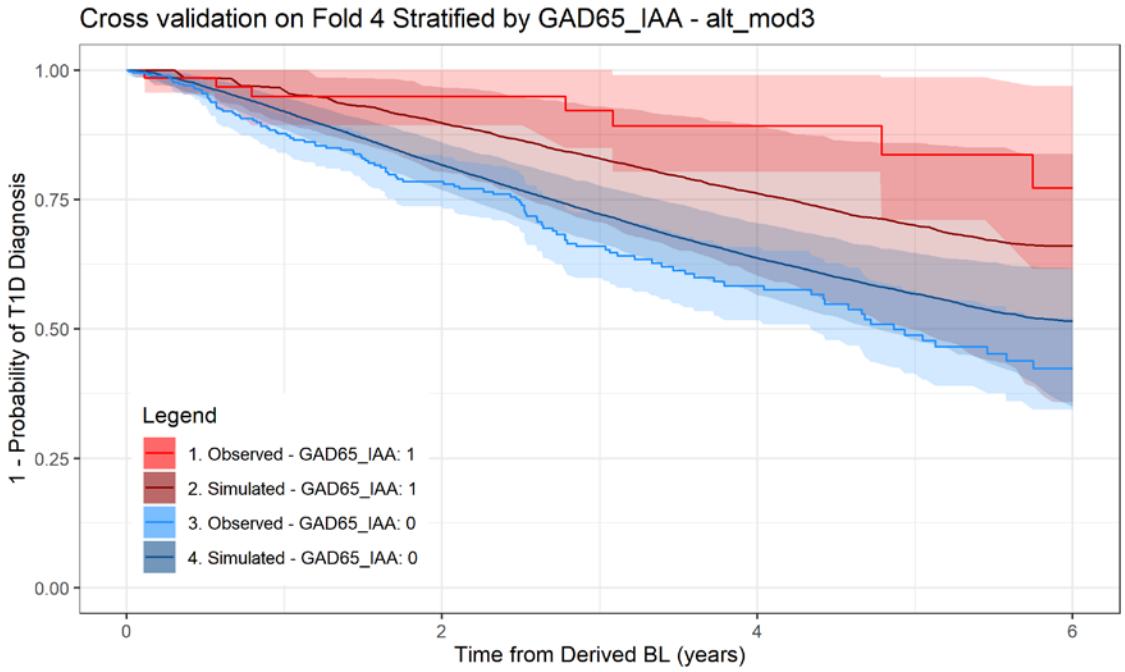

Figure 53. k-fold cross validation analysis stratified by GAD65_IAA – Fold 5

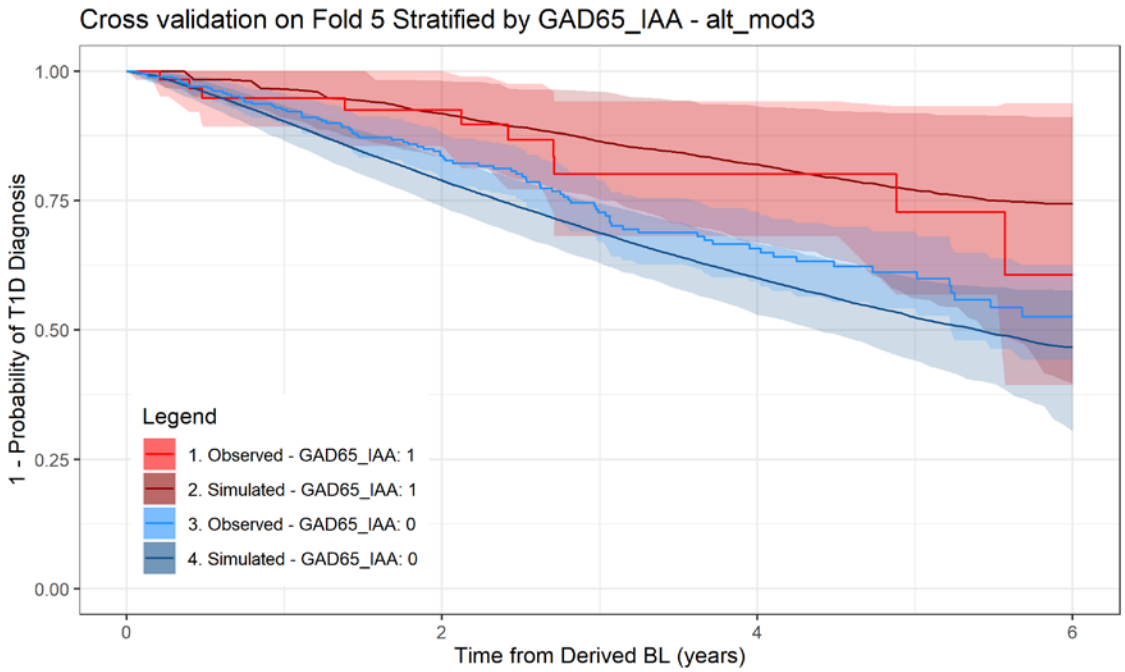

Figure 54. k-fold cross validation analysis stratified by GAD65_ZnT8 – Fold 1

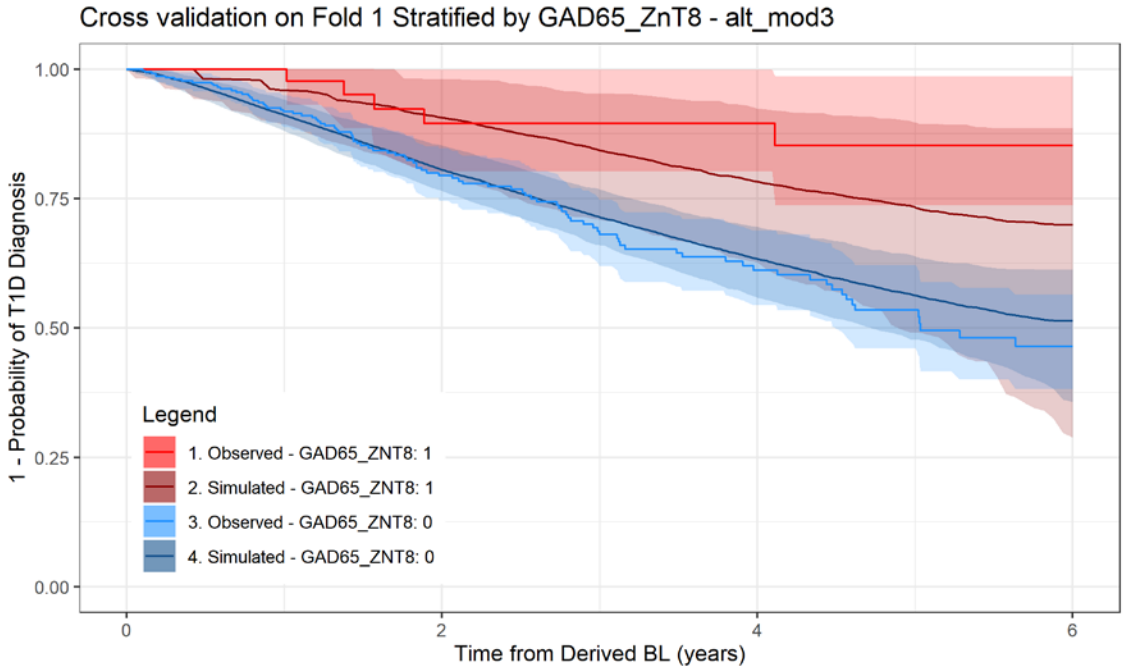

Figure 55. k-fold cross validation analysis stratified by GAD65_ZnT8 – Fold 2

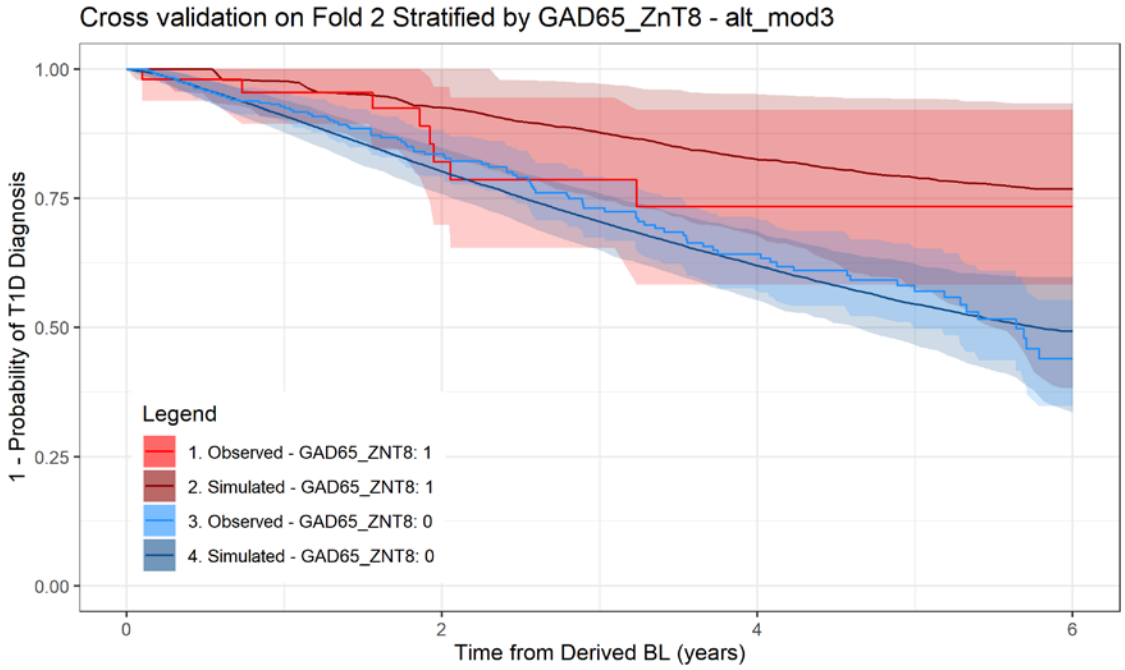

Figure 56. k-fold cross validation analysis stratified by GAD65_ZnT8 – Fold 3

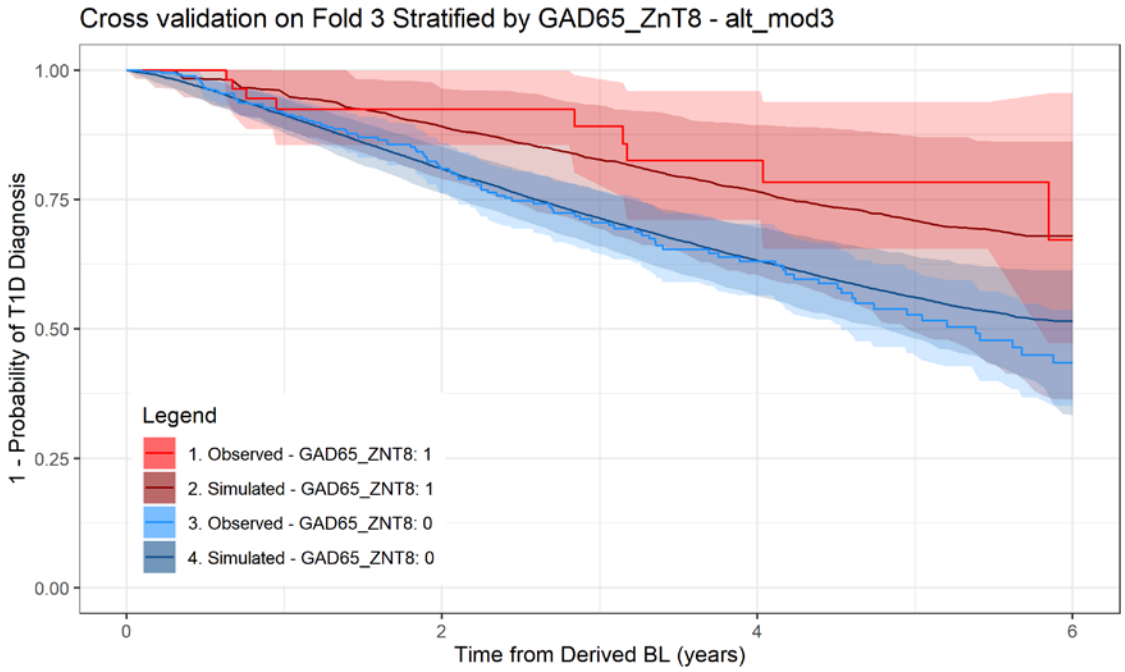

Figure 57. k-fold cross validation analysis stratified by GAD65_ZnT8 – Fold 4

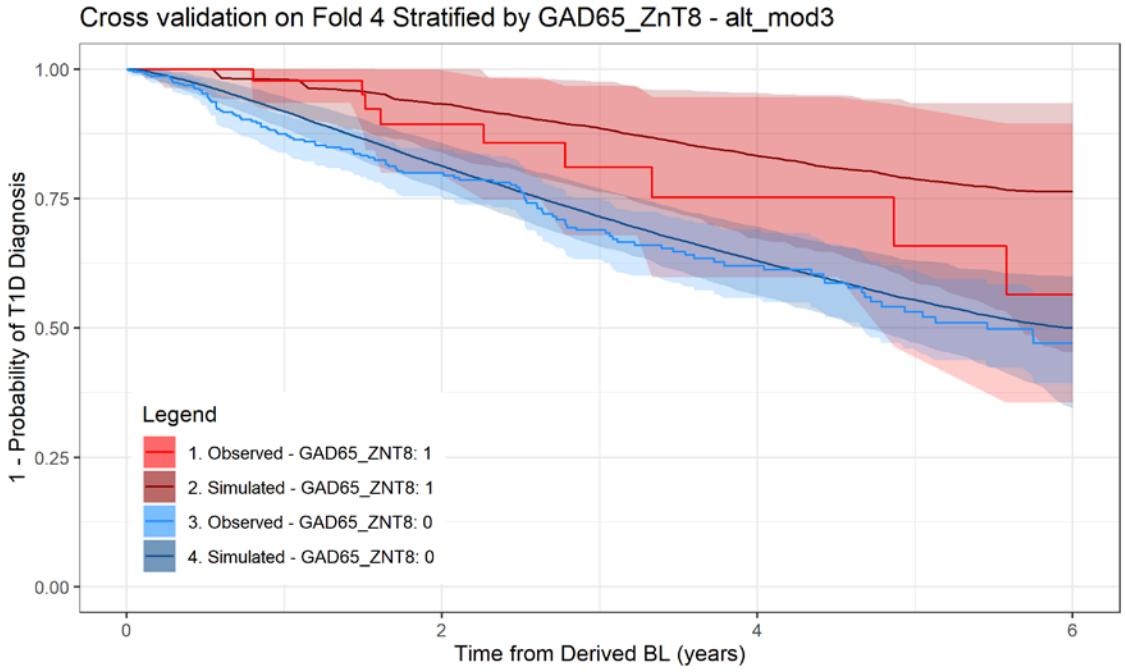

Figure 58. k-fold cross validation analysis stratified by GAD65_ZnT8 – Fold 5

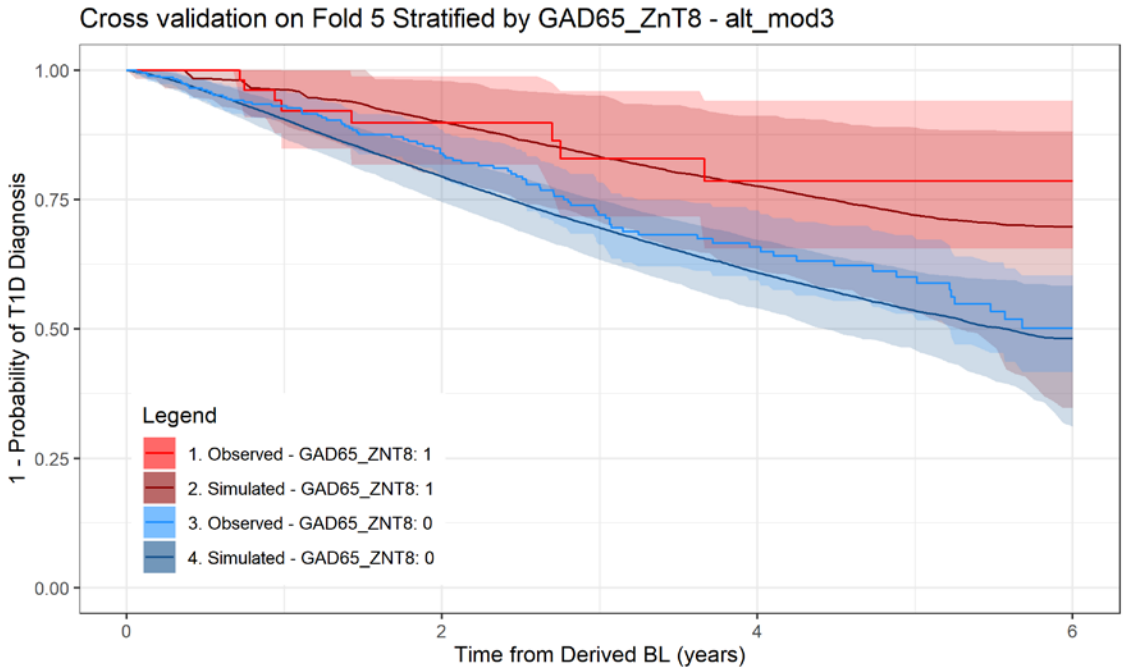

Figure 59. k-fold cross validation analysis stratified by GLU120_binary threshold of 100 mg/dl – Fold 1

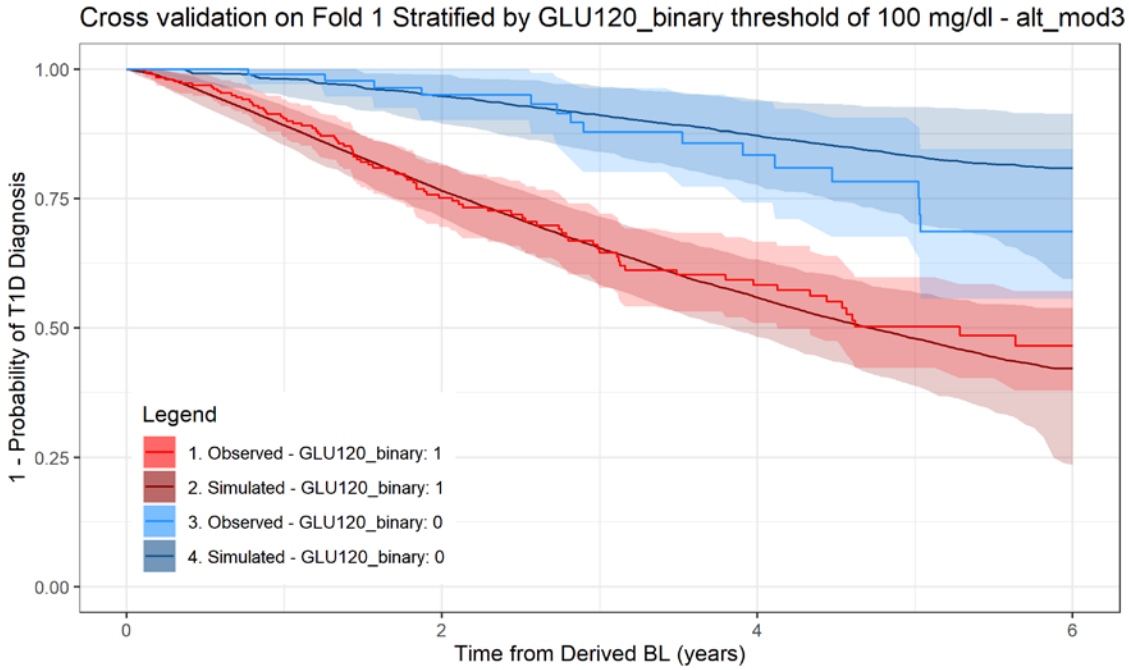

Figure 60. k-fold cross validation analysis stratified by GLU120_binary threshold of 100 mg/dl – Fold 2

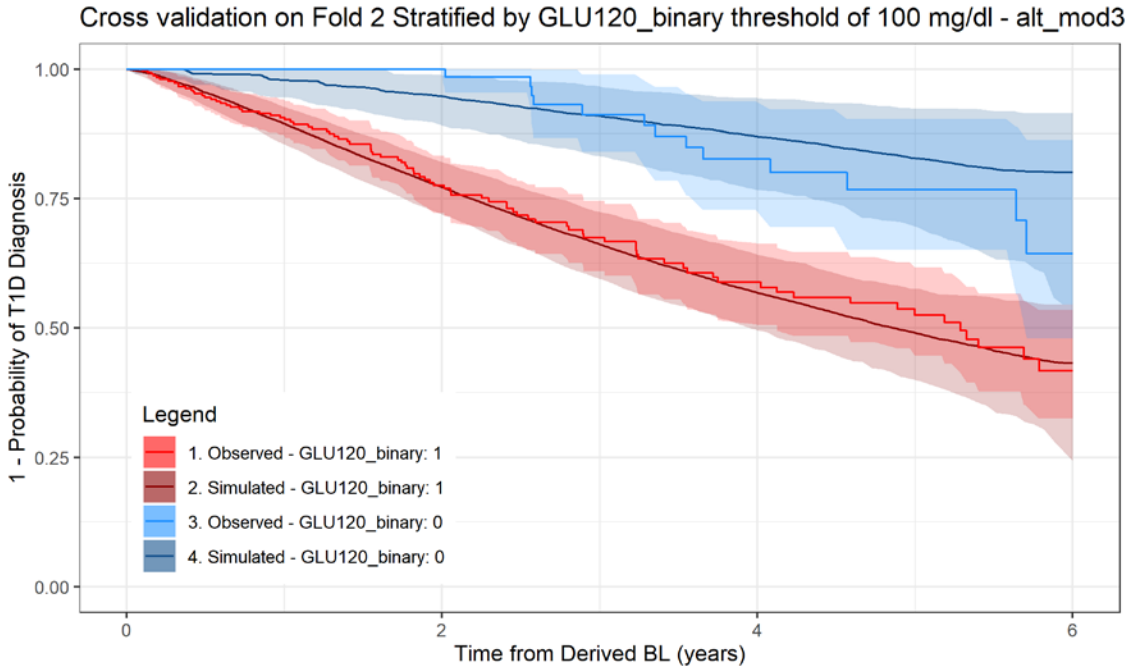

Figure 61. k-fold cross validation analysis stratified by GLU120_binary threshold of 100 mg/dl – Fold 3

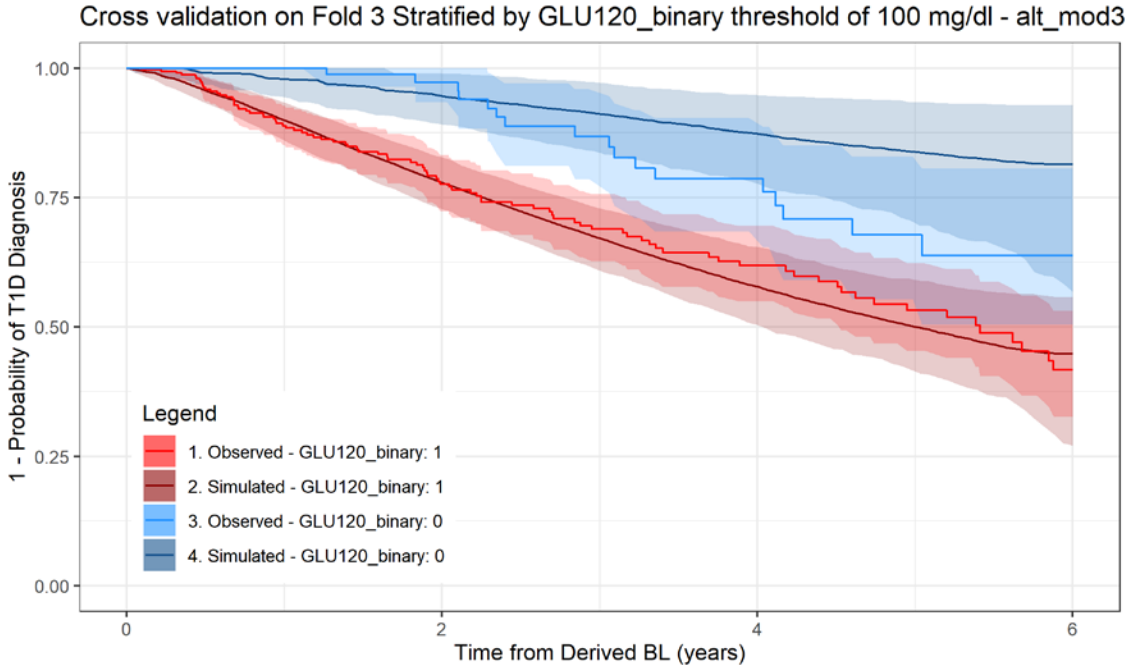

Figure 62. k-fold cross validation analysis stratified by GLU120_binary threshold of 100 mg/dl – Fold 4

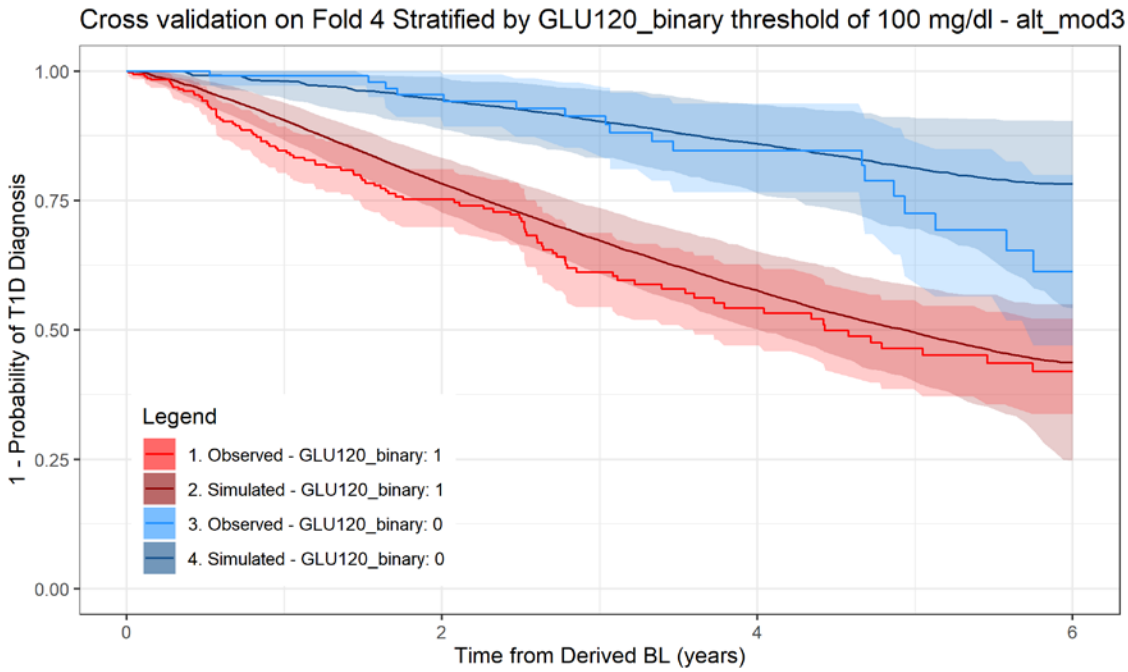

Figure 63. k-fold cross validation analysis stratified by GLU120_binary threshold of 100 mg/dl – Fold 5

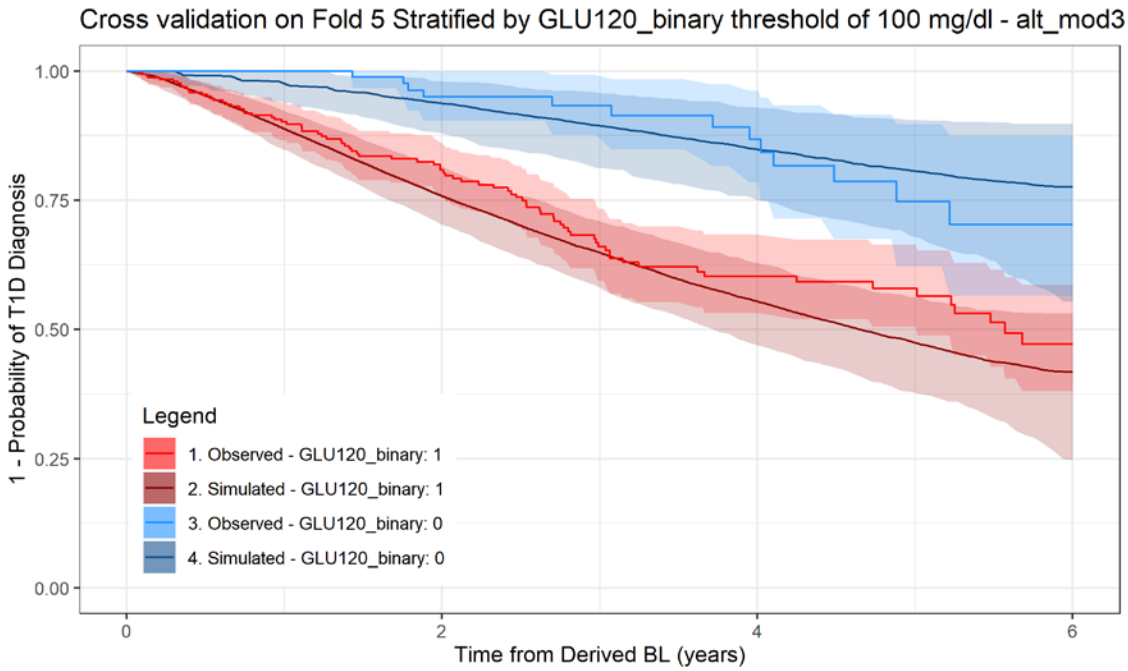

Figure 64. k-fold cross validation analysis stratified by IA-2_IAA_ZnT8 – Fold 1

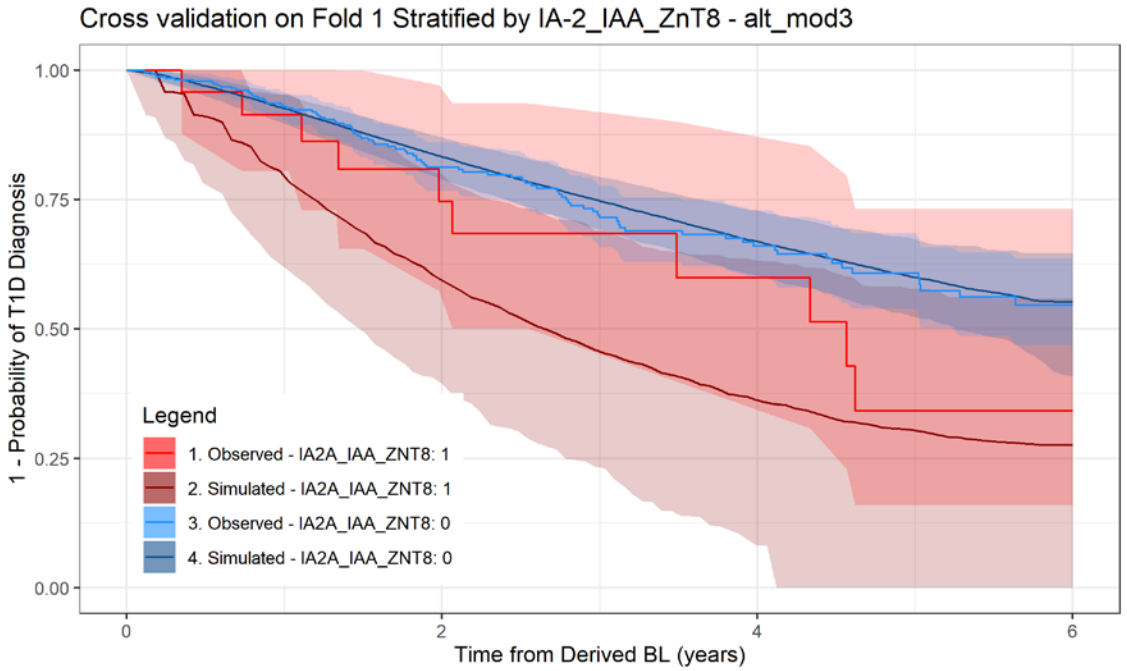

Figure 65. k-fold cross validation analysis stratified by IA-2_IAA_ZnT8 – Fold 2

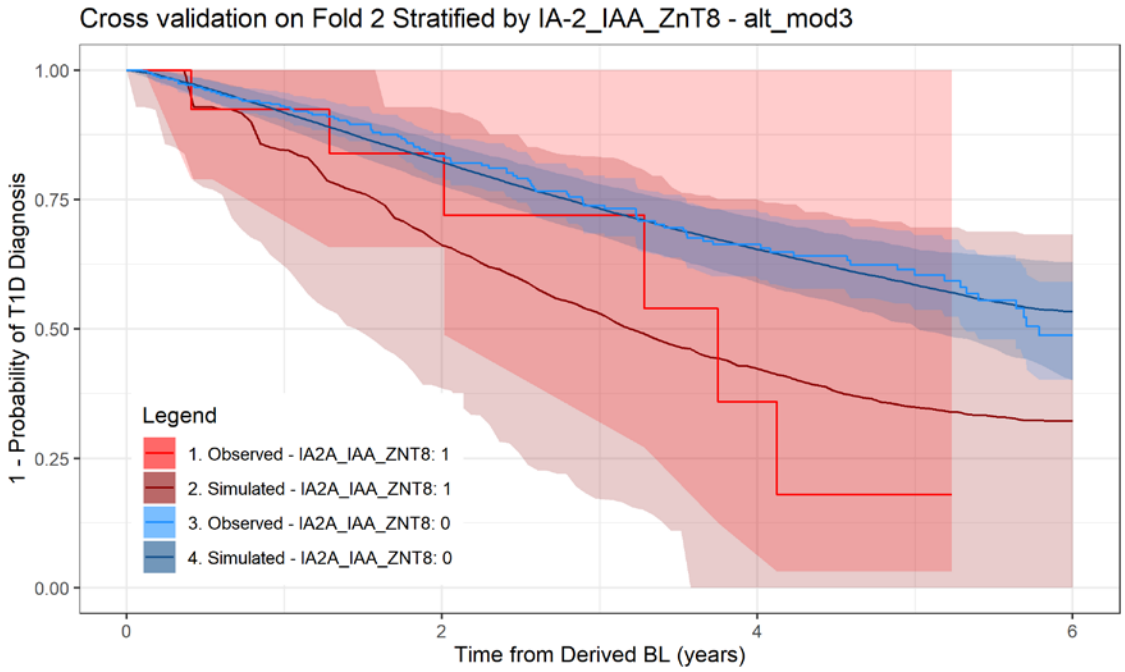

Figure 66. k-fold cross validation analysis stratified by IA-2_IAA_ZnT8 – Fold 3

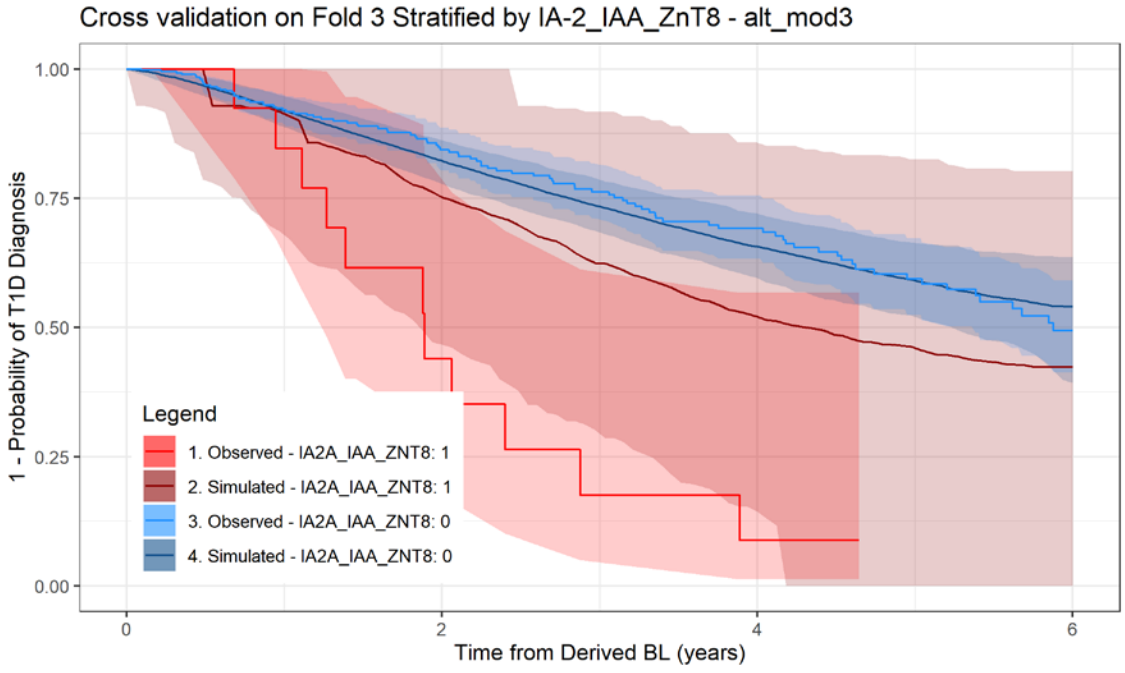

Figure 67. k-fold cross validation analysis stratified by IA-2_IAA_ZnT8 – Fold 4

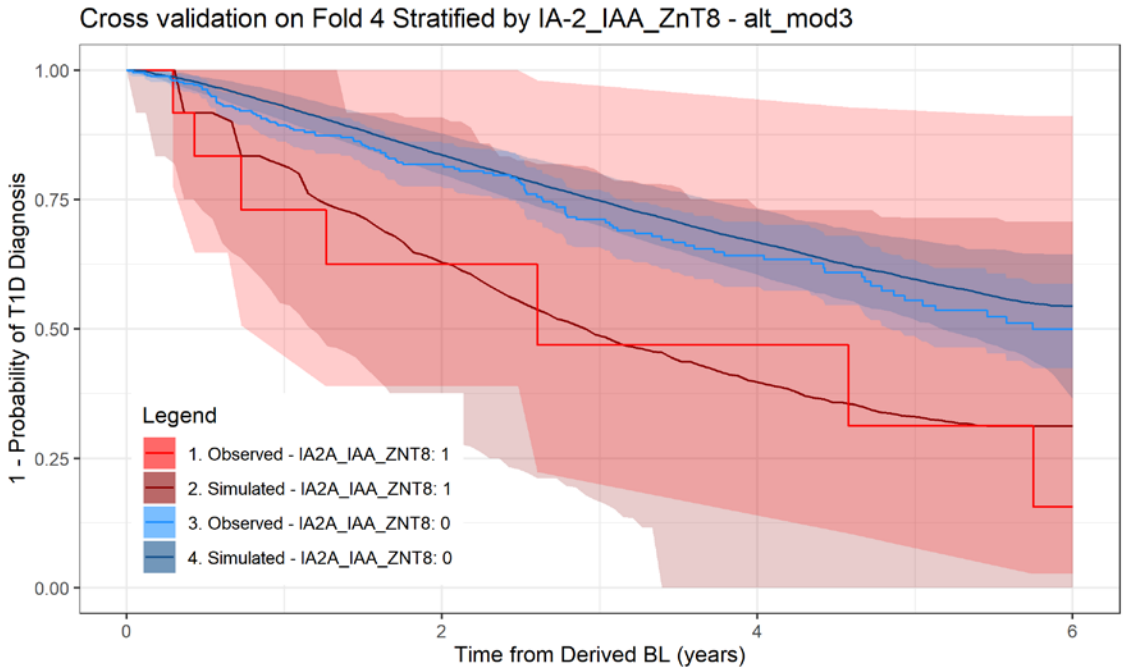

Figure 68. k-fold cross validation analysis stratified by IA-2_IAA_ZnT8 – Fold 5

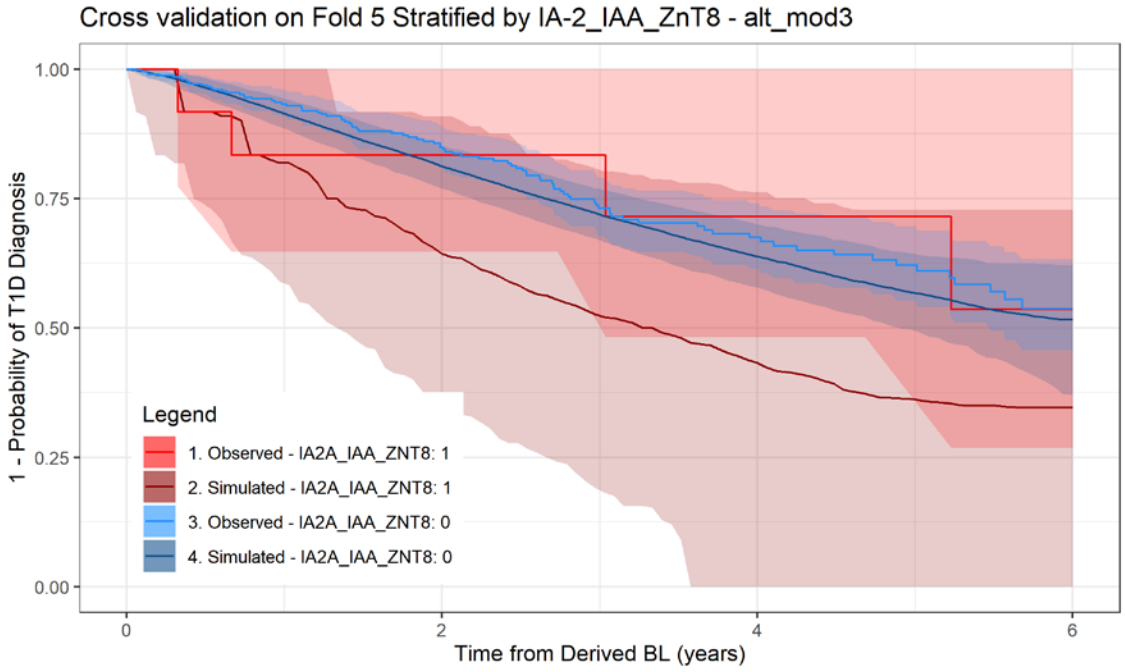

Figure 69. k-fold cross validation analysis stratified by IA-2_ZnT8 – Fold 1

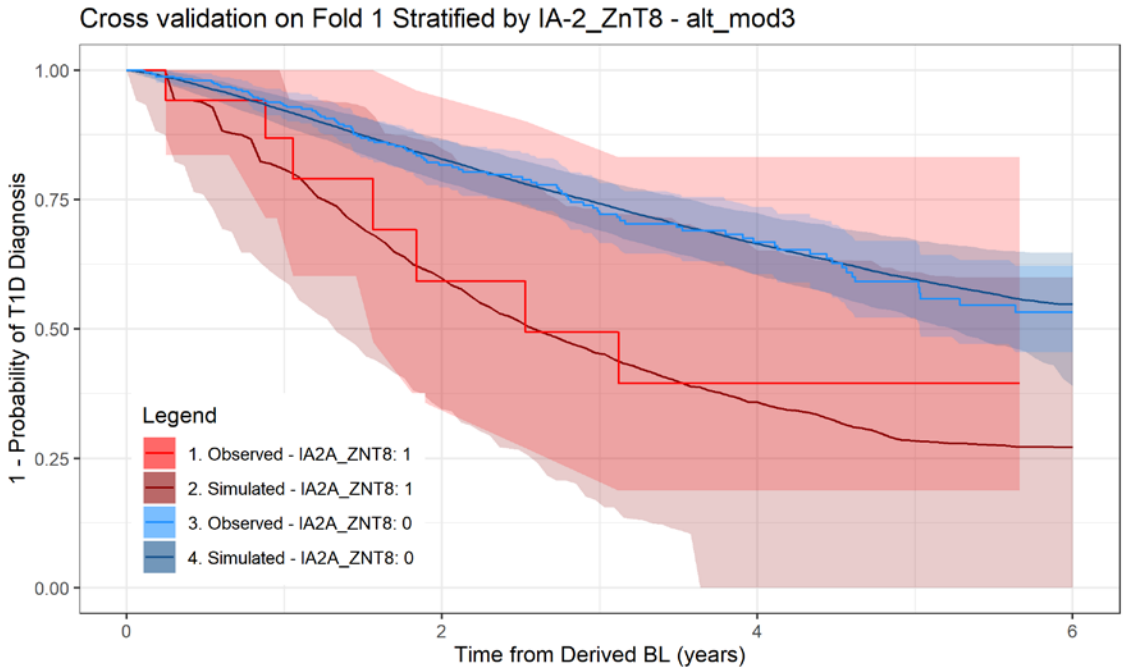

Figure 70. k-fold cross validation analysis stratified by IA-2_ZnT8 – Fold 2

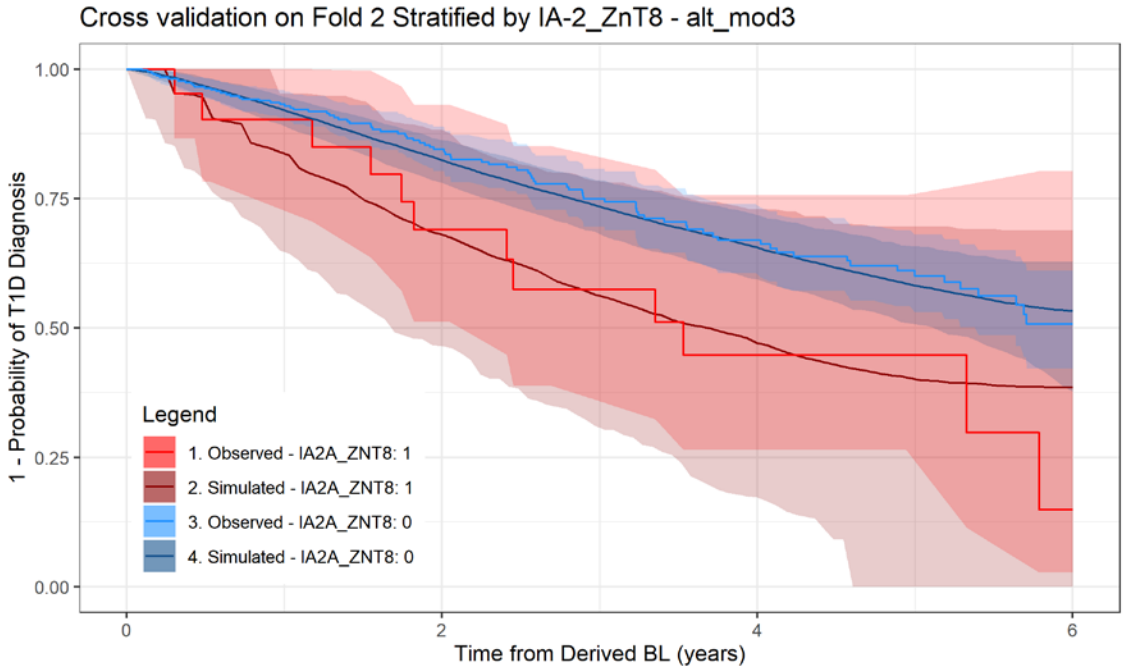

Figure 71. k-fold cross validation analysis stratified by IA-2_ZnT8 – Fold 3

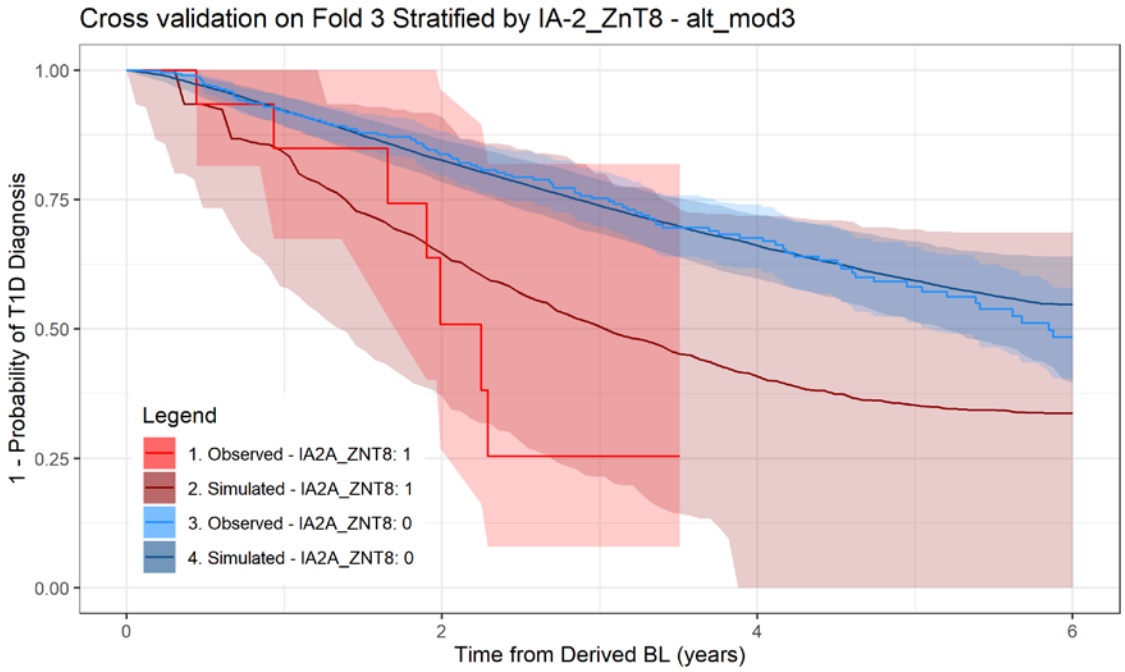

Figure 72. k-fold cross validation analysis stratified by IA-2_ZnT8 – Fold 4

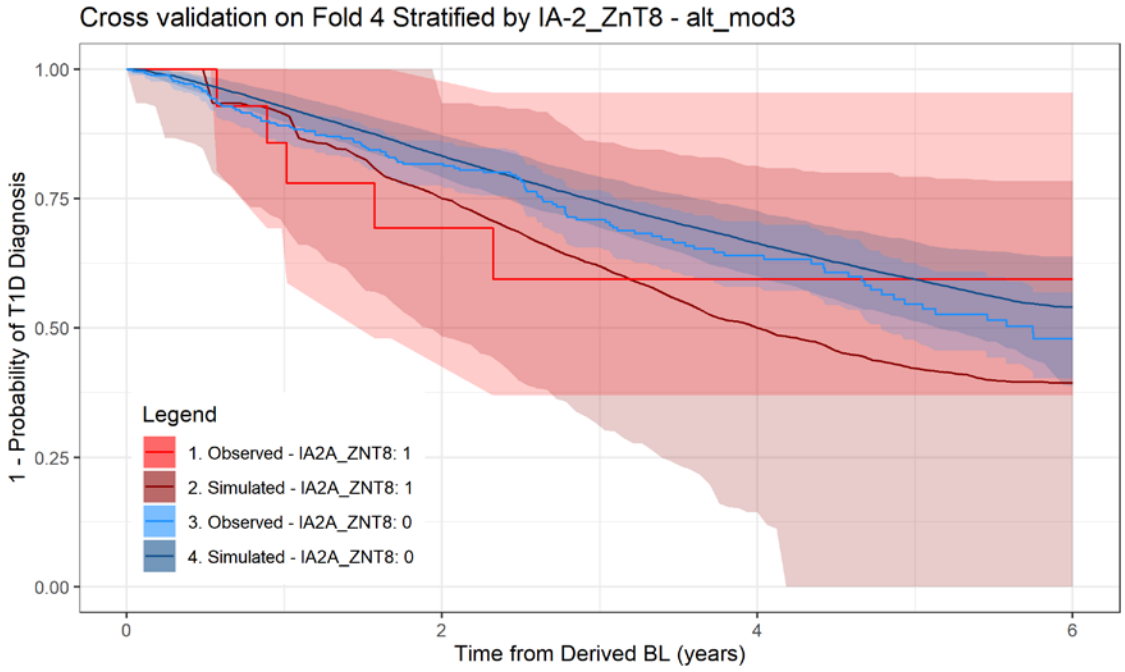

Figure 73. k-fold cross validation analysis stratified by IA-2_ZnT8 – Fold 5